NEAR EAST UNIVERSITY

INSTITUTE OF GRADUATE STUDIES

DEPARTMENT OF ANALYTICAL CHEMISTRY

MICROEXTRACTION TECHNIQUES COMBINED WITH SMARTPHONE DIGITAL IMAGE COLORIMETRY IN THE ANALYSIS OF FOOD SAMPLES

DOCTORATE THESIS

Jude Joshua Caleb

Nicosia

January 2022

NEAR EAST UNIVERSITY

INSTITUTE OF GRADUATE STUDIES

DEPARTMENT OF ANALYTICAL CHEMISTRY

MICROEXTRACTION TECHNIQUES COMBINED WITH SMARTPHONE DIGITAL IMAGE COLORIMETRY IN THE ANALYSIS OF FOOD SAMPLES

DOCTORATE THESIS

Jude Joshua Caleb

Supervisor

Assist. Prof. Dr. Usama Alshana

Nicosia

January, 2022

APPROVAL

We specify that we have read the thesis submitted by Jude Joshua Caleb titled "**Microextraction Techniques Combined with Smartphone Digital Image Colorimetry in The Analysis of Food Samples**" and that in our combined opinion it is fully adequate, in scope and in quality, as a thesis for the degree of Doctor of Philosophy of Science.

Signature

Head of Committee: Prof. Dr. Nusret Ertaş

…………..

Supervisor: Assist. Prof. Dr. Usama Alshana

…………..

Committee Member: Prof. Dr. Nusret Ertaş

…………..

Committee Member: Prof. Dr. Mustafa Soylak

…………..

Committee Member: Assist. Prof. Dr. Selin Işık

…………..

Committee Member: Assist. Prof. Dr. Hürmüs Refiker

…………..

Head of Department: Assist. Prof. Dr. Selin Işık

…………..

Approved by the Institute of Graduate Studies

/ /2022

Prof. Dr. Kemal Hüsnü Can Başer

DECLARATION

I hereby declare that all information, documents, analysis, and results in this thesis have been collected and presented according to the academic rules and ethical guidelines of Institute of Graduate Studies, Near East University. I also declare that as required by these rules and conduct, I have fully cited and referenced information and data that are not original to this study.

Jude Joshua Caleb

25/01/2022

ACKNOWLEDGEMENTS

My sincere gratitude goes to my family; my late father Mr. Joshua Caleb for his valuable contributions to my life and studies, my mother Mrs. Dinatu Caleb for being a pillar of support, my siblings Patience, Cephas and Halita. I love and appreciate you all.

I would like to thank my friends who are too numerous to mention for their moral and emotional support throughout my studies and the Forward in Faith, Cyprus family.

Finally, I would like to thank God almighty for giving me a sound mind and the ability to attain this milestone of my life.

ABSTRACT

Microextraction Techniques Combined with Smartphone Digital Image Colorimetry in The Analysis of Food Samples

Caleb, Jude Joshua
Ph.D., Department of Analytical Chemistry
Supervisor: Assist. Prof. Dr. Usama Alshana
January 2022, 122 pages

In this study, microextraction techniques including two liquid–liquid microextraction (LLME) techniques and dispersive solid-phase microextraction (DSPME) were combined with smartphone digital image colorimetry (SDIC) for the determination of ionic, molecular, and elemental analytes in food samples. In the first study, solidification of floating organic drop-dispersive liquid–liquid microextraction (SFOD-DLLME) was combined with SDIC for the determination of iodate in table salt. A colorimetric box was constructed to capture reproducible images of the colored samples. Factors affecting the performance of both SFOD-DLLME and SDIC were optimized. The optimum conditions for SFOD-DLLME include the type and volume of the extraction solvent (1-undecanol, 500 µL), the disperser solvent (ethanol, 1.5 mL), and the extraction time (20 s). The limit of detection (LOD) obtained was found as 0.10 µmol L^{-1} (0.2 µg g^{-1}) and enrichment factors ranged between 17.4 and 25.0. A good linearity, with coefficients of determination (R^2) above 0.9954 was obtained. The method was applied for the quantitation of iodate in table salt with percentage relative recovery (%RR) between 89.3 to 109.3% and percentage relative standard deviation (%RSD) below 5.6%. In the second study, supramolecular solvent liquid–liquid microextraction (SMS-LLME) was combined with SDIC for the determination of curcumin in tea and spices using a modified version of the colorimetric box used in the previous study by replacing the continuum light source with a monochromatic source. The optimum conditions for SMS-LLME were achieved using 1000 µL of tetrahydrofuran/1-undecanol (4:1, v/v) as the extraction solvent, 2.0% (w/v) of

sodium chloride for adjusting the ionic strength, an extraction time of 60 min and pH of the sample solution at 7.0. LOD was found to range between 0.2 to 0.9 $\mu g\ mL^{-1}$ (0.04 to 0.18% w/w). Linear calibration graphs were obtained with R^2 values above 0.9965. The method was applied for the quantitation of curcumin in tea and spices with %RSD below 8.5% and %RR between 94.0 to 104.0%. In the third study, DSPME was combined with SDIC for the determination of boron in nuts using a monochromatic light source similar to the second study. Optimum DSPME conditions were obtained with zirconium nanoparticles (30 mg) as the adsorbent, acetone (100 µL) as the eluent, pH of the sample solution adjusted to 2.5 with phosphate buffer (25.0 mmol L^{-1}), at adsorption and desorption times of 2.0 and 1.0 min, respectively. Under optimum conditions, LOD values ranged between 0.05 and 0.11 µg mL^{-1} (1.27 to 2.83 µg g^{-1}) and calibration graphs showed a good linearity with R^2 above 0.9954. The method was applied for the quantitation of boron in nuts with %RR between 91.0 and 105.6% and %RSD below 6.77%. The three studies demonstrated the potential of SDIC, when combined with a suitable microextraction technique, to replace more sophisticated analytical techniques for the determination of ionic, molecular, and elemental analytes in complicated food matrices.

Keywords: Dispersive liquid–liquid microextraction, Dispersive solid-phase microextraction, Food, Smartphone digital image colorimetry, Supramolecular solvent.

ÖZ

Gıda Örneklerinin Analizinde Mikro Ekstraksiyon Teknikleri ile Dijital Görüntü Kolorimetrisi

Caleb, Jude Joshua

Doktora, Analitik Kimya Anabilim Dalı

Danışman: Yrd. Doç. Dr. Usama Alshana

Ocak, 2022, 122 sayfa

Bu çalışmada, gıda örneklerinde iyonik, moleküler ve elementel analitlerin tayini için iki sıvı–sıvı mikroekstraksiyon (LLME) ve dispersif katı-faz mikroekstraksiyon (DSPME) yöntemleri akıllı telefon dijital görüntü kolorimetrisi (SDIC) ile birleştirildi. İlk çalışmada, sofra tuzunda iyodat tayini için katılaşan-yüzen organik damla-dispersif sıvı–sıvı mikroekstraksiyonu (SFOD-DLLME) ile SDIC birleştirildi. Renkli örneklerin tekrarlanabilir görüntülerini yakalamak için kolorimetrik bir ölçüm hücresi oluşturuldu. SFOD-DLLME için optimum koşullar, ekstraksiyon solventi (1-undekanol, 500 µL), dağıtıcı solventin (etanol, 1.5 mL) türü ve hacmini, ekstraksiyon süresini (20 s) kapsamaktadır. Optimum koşullarda teşhis sınırı (LOD) 0.1 µmol L^{-1} (0.2 µg/g) ve zenginleştirme faktörü 17,4 ila 25.0 arasındadır. Yöntemde kalibrasyon grafikleri (R^2) 0.9954'ten büyük belirleme katsayıları ile doğrusal davranmaktadır. Yöntem sofra tuzu numunesinde iyodat tayinine uygulanmış, yüzde bağıl geri kazanım (%RR) %89.3 ile %109.3 arasında ve yüzde bağıl standart sapma (%RSD) %5,6'dan küçük bulunmuştur. İkinci çalışmada, supramoleküler çözücü sıvı-sıvı mikroekstraksiyon (SMS-LLME), SDIC ile birleştirilerek çay ve baharatlarda kurkumin tayini gerçekleştirildi. Bu çalışmada kullanılan kolorimetrik hücre modifiye edilerek sürekli ışık kaynağı yerine monokromatik bir ışık kaynağı kullanıldı. SMS-LLME için optimum koşullar, ekstraksiyon çözücüsü olarak 1000 µL tetrahidrofuran/1-undekanol (4:1 h/h), iyonik şiddeti ayarlamak için %2.0 (a/h) sodyum klorür, 60 dakika ekstraksiyon süresi ve numune çözeltisinin pH'sı 7.0 seçildiğinde sağlandı. LOD 0,2 - 0,9 $\mu g \ mL^{-1}$ (0,04 ila 0,18 a/a) arasında bulundu. Kalibrasyon grafikleri, 0.9965'dan büyük R^2 değerleri ile doğrusaldır. Yöntem, çay ve

baharatlardaki kurkumin miktarının tayini için uygulandığında bağıl standart sapma %8.5'ten küçük, bağıl geri kazanım (%RR) değerleri ise %94.0 - %104.0 arasında bulundu. Üçüncü ve son çalışmada, kuruyemişlerde bor tayini için dispersif katı faz mikroekstraksiyon (DSPME) yöntemi, ikinci çalışmaya benzer monokromatik bir ışık kaynağı kullanılan SDIC ile birleştirilmiştir. Adsorban olarak 30 mg zirkonyum nanoparçacık, eluent olarak aseton (100 µL), numune çözeltisinin pH'ı fosfat tamponu (25.0 mmol L^{-1}) ile 2.5'e ayarlanmış ve sırasıyla 2.0 ve 1.0 dakika adsorpsiyon ve desorpsiyon sürelerinde optimum DSPME koşulları sağlanmıştır. Optimum koşullarda LOD değerleri 0,05 ila 0,11 $\mu g\ mL^{-1}$ (1,27 ila 2,83 µg g^{-1}) arasındadır ve kalibrasyon grafiklerinin R^2'si 0.9954'ten büyüktür. Yöntem, kuruyemişlerde bor miktarının tayinine uygulandığında bağıl geri kazanım (%RR) değerleri %91.0- %105.6 arasında, bağıl standart sapma ise %6.77'den küçüktür. Bu üç çalışma, SDIC'in uygun mikroekstraksiyon yöntemleri ile birleştirildiğinde, karmaşık gıda matrislerinde iyonik, moleküler ve elemental analitlerin tayini için, sofistike analitik tekniklerin yerini alma potansiyelini göstermektedir.

Anahtar kelimeler: Akıllı telefon dijital görüntü kolorimetresi, Dispersif katı-faz mikro ekstraksiyonu, Dispersif sıvı–sıvı mikro ekstraksiyonu, Gıda, Supramoleküler sıvı.

TABLE OF CONTENTS

LIST OF TABLES

LIST OF FIGURES

LIST OF ABBREVIATIONS

Abbreviation	Definition
%RR	Percentage relative recovery
%RSD	Percentage relative standard deviation
1-DO	1-Dodecanol
1-UN	1-Undecanol
5-ME-TAR	5-Methyl-4-(2-thiazolylazo) resorcinol
AD	Amperometric detection
APDC	Ammonium pyrrolidine dithiocarbamate
CD	Conductivity detection
CE	Capillary electrophoresis
CF	Chloroform
CPE	Cloud-point extraction
CZE	Capillary zone electrophoresis
D-µSPE	Dispersive micro solid-phase extraction
DAD	Diode-array detector
DCM	Dichloromethane
DDTC	Diethyldithiocarbamate
DES-LLME	Deep eutectic solvent liquid–liquid microextraction
DPC	Diphenylcarbazide
DPE	Diphenyl ether
DPT	2,9-Dimethyl-1,10-phenanothroline
EF	Enrichment factor
EME	Electromembrane extraction
ETAAS	Electrothermal-atomic absorption spectrometry
FAAS	Flame-atomic absorption spectrometry
FDA	Food and Drug Administration
FLD	Fluorescence detection

GC-FID	Gas chromatography-flame ionization detection
GFAAS	Graphite-furnace atomic absorption spectrometry
HF-LPME	Hollow fiber-liquid-phase microextraction
HPLC	High-performance liquid chromatography
IC	Ion chromatography
IDDs	Iodine deficiency disorders
IL	Ionic liquid
LDR	Linear dynamic range
LED	Light-emitting diode
LLE	Liquid–liquid extraction
LOD	Limit of detection
LOQ	Limit of quantitation
LPME	Liquid-phase microextraction
MOF	Metal organic framework
MRL	Maximum residual limit
MS	Mass spectrometry
MS-IL-DLLME	Magnetic stirrer-induced dispersive ionic-liquid microextraction
OES	Optical emission spectrometry
PAR	4-(2-Pyridylazo) resorcinol
PCA	Popping candy-assisted
PTFE	Polytetrafluoroethylene
RGB	Red-green-blue
SDIC	Smartphone digital image colorimetry
SDME	Single-drop microextraction
SDS	Sodium dodecyl sulfate
SFOD	Solidification of floating organic drop
SMS	Supramolecular solvent
SPE	Solid-phase extraction
SPME	Solid-phase microextraction

TBABr	Tetrabutylammonium bromide
TCD	Thermal conductivity detection
TCM	Tetrachloromethane
THF	Tetrahydrofuran
TSIL	Task-specific ionic liquid
UA	Ultrasound-assisted
UPLC	Ultra-performance liquid chromatography
UV/Vis	Ultraviolet/visible spectrophotometry
WHO	World Health Organization

CHAPTER I
INTRODUCTION

Sample preparation has repeatedly been shown to be the most challenging, time consuming and critical step in the entire analytical process even with the introduction of sophisticated and costly instruments (Burato et al., 2020). It is critical to ensure that the analyte's integrity is maintained during sample preparation without jeopardizing the method's sensitivity, accuracy, or precision (Plotka-Wasylka et al., 2015). Traditional sample preparation techniques, such as liquid–liquid extraction (LLE) and solid-phase extraction (SPE), have been replaced by miniaturized versions because of the latter's superior properties such as low consumption of organic solvents, short analysis time, high enrichment factors (EF), simplicity of procedure, small sample volume, and the potential for automation. These miniaturized methods are broadly classified as liquid–liquid microextraction (LLME) and solid-phase microextraction (SPME) (Maciel et al., 2018).

Food samples are considered as complex matrices due to the presence of numerous constituents with a wide range of physical and chemical properties, posing an interesting challenge for the extraction of analytes from such media prior to their determination (Paiva et al., 2021). The determination of inorganic and organic species in food samples is necessary in many cases because these species can serve as both essential ingredients and toxic contaminants for living organisms. In both cases, the importance of either cannot be overstated because, even for essential compounds, different regulatory agencies such as the World Health Organization (WHO), European Commission (EC), and United States Food and Drug Administration (FDA) which have recommended some limits to ensure that food quality is maintained (Cacciola et al., 2017). Similarly, these agencies establish a maximum residue limit (MRL) for undesirable compounds in order to control the exposure to these constituents (Maciel et al., 2018). As a result, developing efficient, robust, fast, and easy to use analytical methods for their determination in food samples becomes crucial.

Various instrumental techniques have been proposed for the determination of different analytes in food samples in the literature such as ultraviolet-visible spectrophotometry (UV/Vis) (Hassan et al., 2021), high-performance liquid chromatography (HPLC) with diode array detection (DAD) (Al-Nidawi et al.), mass spectrometry (MS) detection (MacMahon et al., 2014), and fluorescence detection (FLD) (Campmajo et al., 2021). Ultra-performance liquid chromatography (UPLC) with DAD (Xie et al.), MS (Manful et al., 2019), and FLD detection (Ritota & Manzi, 2020). Capillary electrophoresis (CE) with DAD (Alshana et al., 2015), amperometric (AD) (Sun et al., 2002), MS (Daniel et al., 2018), conductivity (CD) (Klampfl & Katzmayr, 1998) and FLD detection (Tezcan & Erim, 2018). Flame-atomic absorption spectrometry (FAAS) (Hassan et al., 2020), electrothermal-atomic absorption spectrometry (ETAAS) (Xing et al., 2021), inductively coupled plasma-optical emission spectrometry (ICP-OES) (Bozorgzadeh et al., 2021), and ICP-MS (Liu et al., 2021). Although these techniques provide excellent analytical performance, they require significant capital, analysis, and maintenance costs, as well as high expertise to operate and maintain them. As a result, there is a need to develop alternative complementary analytical techniques that are simple, readily available, and have low acquisition and maintenance costs, that can especially benefit small low-income laboratories and people in developing countries.

Due to the fast progress in mobile technology and software, application of mobile phones to chemical analysis is now possible. Recently, smartphone digital image colorimetry (SDIC) has evolved as an alternative miniaturized analytical technique with the sole purpose of reducing the analysis cost, making the analytical process simple, and offering portability with the potential for on-site analysis (Caleb & Alshana, 2021). SDIC's basic principle entails placing a colored solution in a colorimetric box and exposing it to light, typically from a light-emitting diode (LED) (Barreto et al., 2020). The images are captured with a smartphone camera and processed with a suitable software by splitting the images into their red-green-blue components (RGB) based on a standard scale by assigning a whole number value from 0 to 255 for each of the channels. The number [0,0,0] represents an absolute black, while [255, 255, 255] represents an absolute white (Quesada-Gonzalez

& Merkoci, 2017). The implication is that as the color intensity increases, the mean histogram value of the most intense RGB channel linearly decreases, whereas it may slightly increase or remain constant for the other two channels (Lopez-Molinero et al., 2013). Absorbance or reflectance can then be measured to obtain a linear response between the concentration of the colored analyte and intensity of a specific channel, which can be used to plot a calibration graph for quantifying the analyte in genuine samples.

SDIC has recently been used for the determination of several organic and inorganic analytes in food samples (Masawat et al., 2015; Peng et al., 2017; Song et al., 2019; Urapen & Masawat, 2015; Wongthanyakram et al., 2019). The low cost and simplicity of the technique is accompanied by some drawbacks such as poor sensitivity and low selectivity, especially when applied to complex matrices, which is to be expected given that a continuum light source is used in the absence of a wavelength selector, i.e., a monochromator. To overcome these limitations, SDIC must then be combined with a preconcentration technique and/or an analyte-specific derivatization reaction, allowing the technique to be used for ultra-trace analysis with better selectivity and sensitivity. Furthermore, white LED's, generally applied in SDIC as a continuum illumination source, can be replaced with a monochromatic light source to maintain the main benefits of SDIC, namely low cost and simplicity.

Some miniaturized microextraction techniques have been combined with SDIC for the determination of a few organic and inorganic analytes in food samples such as dispersive liquid–liquid microextraction (DLLME) (Barreto et al., 2020; Jain et al., 2021), on-chip electro-membrane extraction (EME) (Zarghampour et al., 2020), reversed-phase switchable-hydrophilicity solvent liquid–liquid microextraction (RP-SHS-LLME) (Al-Nidawi & Alshana, 2021), and effervescence-assisted liquid-phase microextraction based on solidification of switchable hydrophilicity solvent (Xu Jing et al., 2021).

In this study, two LLME methods and dispersive solid-phase microextraction (DSPME) were combined with SDIC for the determination of iodate, curcumin and boron

in food samples. In the first study, solidification of floating organic drop-dispersive liquid–liquid microextraction (SFOD-DLLME) was combined with SDIC for the determination of iodate ions in table salt. In the second study, supramolecular solvent liquid–liquid microextraction (SMS-LLME), combined with SDIC, was used to determine curcumin in tea and spices. In the third study, DSPME-SDIC was applied for the determination of boron in nuts.

Statement of the Problem

Sample preparation has remained the most difficult and important step in the entire analytical process, particularly for complex matrices such as food. Conventional extraction methods, such as LLE and SPE, have several drawbacks, including the use of large amounts of organic solvents, a long analysis time, low EFs, and excessive chemical waste that is harmful to living organisms and the environment. As a result, there is a need to focus on developing alternative miniaturized extraction techniques to overcome these obstacles. Furthermore, the high cost of analytical instruments is a significant impediment for researchers working in low-income laboratories, necessitating the development of low-cost alternatives.

Aim of the Study

The aim of this study is to combine two LLME techniques and DSPME with SDIC for the determination of ionic, molecular, and elemental analytes in food samples.

The objectives include but are not limited to:

- Developing an SFOD-DLLME-SDIC method for the preconcentration and determination of iodate in table salt.
- Developing an SMS-LLME-SDIC method for the preconcentration and determination of curcumin in tea and spices.

- Developing an DSPME-SDIC method for the sample clean-up and determination of boron in nuts.
- Using microextraction techniques and replacing continuum sources with monochromatic light sources as tools for improving the sensitivity and selectivity of SDIC.
- Proving the accuracy of the developed methods through addition-recovery tests and analysis with well-established analytical techniques, e.g., UV/Vis and HPLC-DAD.

Research Questions and Hypothesis

Some research questions considered include.
- Are microextraction techniques capable of replacing traditional extraction techniques for complex matrices such as food?
- Are there alternative detection techniques that provide comparable results to those obtained with sophisticated instrumental techniques but at a lower cost?
- Will the sensitivity of SDIC be enough for trace and ultra-trace analysis?
- Will microextraction and use of monochromatic light sources improve the sensitivity and selectivity of SDIC?
- Will the combination of microextraction and SDIC be efficient enough to detect analytes in complex food samples?

Significance of the Study

Combining microextraction techniques with SDIC as an alternative detection technique that can provide comparable performance to expensive and complicated instrumental techniques at a lower cost and with less reliance on electricity, with the potential for on-site analysis, will be extremely beneficial to low-income laboratories and people in developing countries.

CHAPTER II
LITERATURE REVIEW

Theoretical Framework

The need to miniaturize analytical methodologies drove the development of microextraction techniques. Miniaturization decreases the amount of solvents and reagents used per sample, resulting in less chemical waste, among other benefits over traditional extraction techniques (Pena-Pereira et al., 2021). In a nutshell, microextraction is an extraction technique in which the volume of the extraction phase (extraction solvent) is very small (µL volume) as compared to the sample volume and the analyte extraction is not exhaustive. (Lord & Pawliszyn, 2000). In 1990, Arthur and Pawliszyn coined the term "microextraction" in an article in which they described a method derived from conventional SPE involving a small diameter fiber coated with a stationary phase placed in an aqueous solution. The analytes were partitioned into the stationary phase and thermally desorbed on column and injected into a gas chromatograph. The technique was called as SPME (Arthur & Pawliszyn, 1990). Later, in 1996, Jeannot and Cantwell coined the term "solvent microextraction" to describe a method they developed that employed 8 µL of an organic solvent suspended on the cavity at the end of a polytetrafluoroethylene (PTFE) rod immersed in the sample (Jeannot & Cantwell, 1996). This method was later known as single drop microextraction (SDME). The development of SPME and SDME resulted in a series of variations to these techniques, which can be divided into two categories: LLME and sorbent-based microextraction (SBME).

Liquid–liquid microextraction

The theoretical principle of LLME is based on the partition coefficient of a given analyte between an extraction solvent (octanol) and water, commonly known as log$P$, which is described in Equation 1 and takes kinetics and equilibrium into account. This is

based on the general principle that like dissolves like. An ideal extraction solvent is expected to be immiscible with water while having a high affinity for the analyte, allowing the analyte to transfer voluntarily from the aqueous (donor) phase to the extraction (acceptor) phase, resulting in a high EF.

$$logP = \frac{[Analyte]_{octanol}}{[Analyte]_{water}} \qquad \text{(Equation 1)}$$

where, $[Analyte]_{octanol}$ and $[Analyte]_{water}$ are the equilibrium concentrations of the analyte in octanol and water, respectively.

Before developing an LLME method, it is recommended that the $logP$ value of a given analyte be known. A high $logP$ value for a given analyte indicates that it is hydrophobic, whereas a low $logP$ value indicates that it is hydrophilic (Burato et al., 2020). The appropriate extraction solvent for a given problem can be chosen based on this value. However, the transfer of the analyte from the sample to the solvent is not a straightforward process. The equilibrium and kinetics of the process need to be put into consideration. These can be affected by various parameters that require optimization such as sample pH, temperature, ionic strength, mechanical agitation and duration, solvent type, solvent volume, and ratio, etc.

There are detailed reviews in the scientific literature that cover the basic principles of various LLME and their application to various matrices such as SDME (Kailasa et al., 2021; Tegladza et al., 2020), hollow-fiber liquid-phase microextraction (HF-LPME) (Gjelstad, 2019; Khan et al., 2020; Madikizela et al., 2020), dispersive liquid–liquid microextraction (DLLME) (Campillo et al., 2017; Dmitrienko et al., 2020; Zgola-Grzeskowiak & Grzeskowiak, 2011), switchable-hydrophilicity solvent liquid–liquid microextraction (SHS-LLME) (Alshana et al., 2020; Musarurwa & Tavengwa, 2021c), SMS-LLME (Moradi et al., 2021; Musarurwa & Tavengwa, 2021b), deep eutectic solvent-liquid–liquid microextraction (DES-LLME) (Dwamena, 2019; Musarurwa & Tavengwa,

2021a), solidification of floating organic drop-based liquid-phase microextraction (LPME-SFOD) (Ghambarian et al., 2013; Wang et al., 2010), and cloud-point extraction (CPE) (Bezerra et al.; Kori, 2021). Because DLLME, SMS-LLME and DSPME were used in this study, a few details will be provided below.

Dispersive liquid-liquid microextraction

DLLME is a LLME technique developed by Assadi and colleagues in 2006 (Rezaee et al., 2006). The method is as simple as injecting an appropriate mixture of an extraction solvent and a disperser solvent into an aqueous sample containing the analyte, resulting in the formation of a cloudy solution due to the extraction solvent microdroplets dispersed entirely in the aqueous sample. For phase separation, a centrifugation step is used, in which the extraction solvent, containing the analyte, settles down at the bottom of the centrifuge tube. If the solvent is compatible with the instrument, the final extract can be injected directly into it. Otherwise, the solvent can be evaporated to dryness and reconstituted into a suitable solvent or, if the analyte is ionizable, it can be back-extracted into another compatible solvent (Caleb et al., 2021).

Some conditions are required for DLLME to be successful. Both the extraction solvent and the aqueous solution must be miscible with the disperser solvent. The extraction solvent must be capable of extracting the analyte and be miscible with the disperser solvent while remaining immiscible with the aqueous solution or should have a low miscibility. Finally, there must be a substantial difference in density between the extraction solvent and the aqueous phase. To achieve a high EF, both solvents must be carefully chosen (Zgola-Grzeskowiak & Grzeskowiak, 2011). DLLME has a number of advantages, including high speed due to the infinitely large surface area of the extraction solvent dispersed in the aqueous sample, low sample volume, simplicity, low solvent and energy consumption, and high EF, among others.

Despite the obvious benefits of DLLME, there are some drawbacks, the most significant of which being the use of toxic chlorinated solvents as extraction solvents in conventional DLLME, such as chloroform (CF), tetrachloromethane (TCM), dichloromethane (DCM). To address these issues, Leong and Huang proposed a greener alternative in 2008 (Leong & Huang, 2009) via replacing toxic high-density chlorinated solvents with low-density ones such as long-chain alcohols including 1-undecanol (1-UN), 1-dodecanol (1-DO), etc. that can be easily solidified near room temperature for easy collection of the analyte-rich microdrop of the extraction solvent suspended at the surface of the aqueous phase. Other efforts to improve DLLME are known as auxiliary DLLME techniques, and they involve a variety of strategies such as using some form of energy to eliminate centrifugation to increase extraction efficiency and decrease extraction time, such as ultrasound, which is known as ultrasound assisted microextraction. (UA-DLLME) (Ghoraba et al., 2018), the use of a popping candy for mechanical agitation termed "popping candy-assisted dispersive liquid–liquid microextraction (PCA-DLLME-SFOD)" (X. Jing et al., 2021), the use of cyclodextrins as a disperser (Xu et al., 2021), as well as the use of magnetic stirrer termed "magnetic stirrer induced dispersive ionic-liquid microextraction (MS-IL-DLLME)" (Naeemullah et al., 2015). Green alternative extraction solvents, such as ionic liquids, have also been proposed, dubbed "ionic liquid-based dispersive liquid–liquid microextraction (IL-DLLME)" (Zhao et al., 2021). The use of DES in combination with ultrasound was termed as "hydrophobic deep eutectic solvent based on ultrasonic-assisted dispersive liquid–liquid microextraction (DES-UA-DLLME)" (Ji et al., 2021) and the use of supramolecular solvents as extractant termed supramolecular solvent dispersive liquid–liquid microextraction based on solidification of floating drop (SS-DLLME-SFOD) (Liang et al., 2014). Some studies carried out involving auxiliary DLLME techniques in food matrices are summarized in Table 1 for molecular analysis and Table 2 for elemental analysis.

Table 1.

Studies involving auxiliary DLLME methods in molecular analysis.

DLLME Method[a]	Matrix	Analytes	Detection[b]	LOD ($ng\ mL^{-1}$)	Ref.
UA-DLLME	Water, soil, food and beverage samples	Bendiocarb, azinphos-ethyl	IMS	1.04 - 1.31	(Ghoraba et al., 2018)
DLLME-SFOD	Vegetables and food samples	Quercetin	HPLC-UV	0.15–0.17	(Arabi et al., 2018)
PCA-DLLME-SFOD	Water, beer, Baijiu, and vinegar samples	Prothioconazole and its chiral metabolite prothioconazole-desthio	HPLC-DAD	8.10–11.20	(X. Jing et al., 2021)
DLLME	Food packaging	Bisphenols	HPLC-UV	0.44 to 1.60	(Xu et al., 2021)
DLLME	Drink and food paraphernalia	Benzodiazepines	HPLC-HRMS/MS	1.00-14.00 pg	(Vincenti et al., 2021)
IL-DLLME	Wheat	Aflatoxins	HPLC-FD	0.015–0.20 µg kg^{-1}	(Zhao et al., 2021)

[a]UA-DLLME: Ultrasound-assisted-dispersive liquid–liquid microextraction; PCA-DLLME: Popping candy-assisted dispersive liquid–liquid microextraction; IL-DLLME: Ionic liquid-based dispersive liquid–liquid microextraction.

[b]IMS: Ion mobility spectrometry; HPLC-HRMS/MS: High-performance liquid chromatography-high resolution mass spectrometry/mass spectrometry; HPLC-FD: High-performance liquid chromatography-fluorescence detection.

Table 2.

Studies involving auxiliary DLLME methods in elemental analysis.

DLLME Method[a]	Matrix	Analytes	Complexing agent[b]	Detection	LOD ($ng\ L^{-1}$)	Ref.
MS-IL-DLLME	Food	Vanadium	PAR	GFAAS	125.0 and 18.0	(Naeemullah et al., 2015)
SS-DLLME-SFOD	Food and water	Lead	DDTC	GFAAS	27.0	(Liang et al., 2014)
DLLME	Cereals, vegetable and food samples	Copper	DPT	FAAS	50.0	(Shrivas & Jaiswal, 2013)
TSILs-DLLME	Water, rice and urine samples	Arsenic species	APDC	ETAAS	10.0	(Ashouri et al., 2021)
UA-SUPRAS-DLLME	Water, beverages, and vegetables	Cr (VI) and total chromium	Azorubine	FAAS	30.0	(Tuzen et al., 2021)
DES-UA-DLLME	Wine	Cadmium and arsenic	Ligandless	FAAS	80.0 and 300.0	(Ji et al., 2021)

[a]MS-IL-DLLME: dispersive liquid–liquid microextraction, magnetic stirrer induced dispersive ionic-liquid microextraction; SS-DLLME-SFOD: Supramolecular solvent dispersive liquid–liquid microextraction based on solidification of floating drop; TSILs-DLLME: Task-specific ionic liquids-dispersive liquid–liquid microextraction; UA-SUPRAS-DLLME: ultrasound assisted supramolecular solvent dispersive liquid–liquid microextraction; DES-UA-DLLME: Hydrophobic deep eutectic solvent based on ultrasonic-assisted dispersive liquid–liquid microextraction.

[b]PAR: 4-(2-Pyridylazo) resorcinol; DDTC: Diethyldithiocarbamate; DPT: 2,9-dimethyl-1,10-phenanothroline; APDC: Ammonium pyrrolidine dithiocarbamate.

Supramolecular solvent liquid-liquid microextraction

SMS, also known as SUPRAS, are green solvents made up of water-immiscible amphiphile aggregates (Salamat et al., 2018). Because of the non-covalent interaction between SMS and the self-assembly process that allows them to form, the term supramolecular is frequently used to distinguish their properties from those of traditional molecular and ionic solvents (Ballesteros-Gomez et al., 2010). The amphiphiles are generated through the sequential self-assembly of amphiphile molecules caused by changes in external stimuli such as pH, temperature, or ionic strength (Gouda et al., 2018; Menghwar et al., 2018). The process involves the following two steps:

- The first step is for the amphiphile molecules to self-aggregate at a concentration greater than the critical aggregate concentration required for the formation of micelles or vesicles (Ezoddin et al., 2015).
- As a result of changing the external stimuli, the second step involves further aggregation of the nano-structured aggregates formed in the first step to form a water-immiscible phase (Faraji et al., 2017).

The self-assembly process causes the spontaneous separation (coacervation) of a liquid-phase (SMS phase) from an amphiphile-rich bulk solution. Several interactions occur between the SMS and the analyte, such as ionic bonding, hydrogen bonding, and hydrophobic interaction, which improves extraction efficiency (Zohrabi et al., 2016). SMS have unique physio-chemical properties that are easily tunable, making them ideal substitutes for organic solvents, and they are easily accessible due to the abundance of amphiphiles in nature and synthetic chemistry (Ballesteros-Gomez et al., 2010). There are different ways of forming SMS. However, the most widely used SMS for analytical applications is the reversed micelle, which is frequently formed by tetrahydrofuran (THF) and medium-chained alcohols and carboxylic acids (Ballesteros-Gomez et al., 2010). SMS-LLME has been applied to a wide range of food matrices for elemental and molecular analysis, as shown in Table 3. For elemental, total metal (Kashanaki et al., 2018; Ozkantar

et al., 2019) and speciation analysis has been carried out (Abadi et al., 2013). In general, the SMS used is a mixture of THF and 1-UN, 1-octanol, and 1-DO. Because complexation is frequently required for metal ion extraction, a suitable complexing agent is used. The detection systems often employed include FAAS and GFAAS, which are generally more suited for elemental analysis although molecular techniques such as UV/Vis has also been used (Abadi et al., 2013). SMS-LLME has been hyphenated with another microextraction methods in some applications to improve the EF. For example, dispersive micro solid-phase extraction (D-SPE) with metal organic framework (MOF) as sorbent was hyphenated with SMS-LLME for the determination of copper in various beverages prior to GFAAS using ammonium pyrrolidine dithiocarbamate (APDC) as the complexation agent (Kashanaki et al., 2018). In a similar study involving molecular analysis, magnetic D-SPE was hyphenated with SMS-LLME to determine diazinon and metalaxyl in fruit juices using gas chromatography-flame ionization detection (GC-FID) (Adlnasab et al., 2019). These studies show the wide range of applicability of SMS-LLME.

Table 3.

Application of SMS-LLME for elemental and molecular analysis of food samples.

SMS Component[a]	Matrix	Analytes	Complexation agent[b]	Detection	LOD ($ng\ mL^{-1}$)	Ref.
1-UN/THF	Food and water	Cu	5-ME-TAR	FAAS	1.4	(Ozkantar et al., 2019)
1-OC/THF, D-µSPE	Beverages and water	Cu	APDC	GFAAS	0.2	(Kashanaki et al., 2018)
DA/THF	Water	Cr (III) and Cr (VI)	DPC and SDS	UV/Vis	0.2	(Abadi et al., 2013)
SDS and (TBABr)	Rice and water	Six phenoxy acid herbicides	-	HPLC-DAD	1.0-2.0	(Seebunrueng et al., 2020)
DA/THF	Beverages	Bisphenol A (BPA), ochratoxin A (OTA) and benzo(a)pyrene (BaPy)	-	LC-FLD-MS	0.0013-0.18	(Ballesteros-Gomez et al., 2009)
1-DO/THF, D-µSPE	Fruit juices	diazinon and metalaxyl	-	GC-FID	0.2	(Adlnasab et al., 2019)

[a]1-UN: 1-Undecanol; 1-OC: 1-Octanol; D-µSPE: Dispersive micro solid-phase extraction; DA: Decanoic acid; THF: Tetrahydrofuran; SDS: Sodium dodecyl sulfate; TBABr: Tetrabutylammonium bromide.
[b]5-ME-TAR: 5-methyl-4-(2-thiazolylazo) resorcinol; APDC: Ammonium pyrrolidine dithiocarbamate; DPC: Diphenylcarbazide.

Sorbent-based microextraction

The theoretical principle of SBME is based on the adsorption of the analyte(s) in the sample to a solid sorbent before desorption of the analyte from the surface of the sorbent into a suitable solvent prior to analysis (Er et al.). The amount of the analyte extracted depends on the distribution coefficient of the analyte between the sample matrix and the sorbent, as well as the amount of the sorbent and sample. Hence, the chemical properties of the sorbent material is critical to the extraction efficiency (Duan et al., 2011). SPME was the first SBME proposed with the goal of eliminating the use of organic solvents by coating a fused silica fiber with a stationary phase and exposing the fiber to an aqueous or gaseous

sample until equilibrium was achieved between the analyte present in the sample and the fiber. The analyte was thermally desorbed from the fiber into GC for analysis (Prosen & Zupancic-Kralj, 1999). SPME has been applied to a wide range of samples including food (Castro et al., 2008; Li et al., 2015; Xu et al., 2016). However, DSPME, a mode of SBME, was proposed as an alternative to conventional SPME.

Dispersive solid-phase microextraction

DSPME is a type of SBME in which the adsorbent is introduced directly into the sample solution to extract the analyte, rather than through a fiber. This is followed by dispersion od the adsorbent into the sample solution in order to increase the surface area of contact between them, which significantly reduces the extraction time. The analyte is then desorbed into a suitable solvent before introducing it into the analytical instrument (Tsai et al., 2009). DSPME has a number of advantages, including high speed, simplicity, affordability, broad applicability, low sample volume, high extraction efficiency, and high EF (Khezeli & Daneshfar, 2017). The main limitation of DSPME is the difficulty of separating the adsorbent from the sample solution after extraction, as well as difficulty of automation (Ghorbani et al., 2019). Because of their high extraction efficiencies and large surface area/volume ratio, nanoparticles have emerged as indispensable sorbents for DSPME. (Karlidag, Toprak, et al., 2020).

Smartphone digital image colorimetry

Colorimetry is the science and technology used to measure and describe what the human eye physically perceives, and it is traditionally divided into visual colorimetry and photoelectric colorimetry (Fan et al., 2021). The former is used to measure concentration by observing color changes with the naked eye, whereas the latter employs measurement apparatus such as a photoelectric colorimeter and spectrophotometer, which is more accurate in both resolution and quantitation (Clydesdale & Ahmed, 1978). Hence, photoelectric colorimetry is more commonly used for colorimetric measurements.

DIC is a subfield of colorimetry that digitalizes images captured by image acquisition devices such as mobile phones, digital cameras, webcams, scanners, and so on (Firdaus et al., 2014). Due to the needs of modern society to acquire and share data in a timely and on-site manner, DIC has gained significant traction in recent years. Because of their portability, lightness, and advancement in camera technologies and applications, smartphones and digital cameras have become the most widely used image acquisition tools in this regard (Coskun et al., 2013). The use of a smartphone as an image acquisition tool for DIC will be the focus of subsequent discussions. As a result, the term SDIC will be used for smartphone-based digital image colorimetry. SDIC consists of two fundamental steps:

- Image acquisition by a smartphone.
- Image quantification by some image processing software such as Adobe Photoshop, ImageJ, Matlab, Pantone Studio, etc.

In this regard, there is a need to construct a suitable colorimetric box that will enable reproducible image acquisition free of interferences from daylight, taking into consideration the basic components of optical instruments.

Basic components of optical instruments

Optical instruments are those that operate in the X-ray, ultraviolet, visible, and infrared regions of the electromagnetic spectrum. The human eye works only in the visible region of the spectrum, which is what SDIC uses. In this regard, the basic optical instrument components will serve as a guide for building the colorimetric box that will be used as a detector in SDIC. Optical instruments, in general, have similar basic components (Figure 1), though their configuration may vary to some extent depending on the region of the spectrum it is applied for. (Skoog et al., 2017). The basic components of an optical instrument include:

- A stable light source that produces radiant energy.

- A transparent sample holder.

- A wavelength selector that isolates a specific region of the electromagnetic spectrum for measurement.

- A detector that converts radiant energy to usable electric signal.

- A signal processor that displays the signal on a scale.

Figure 1.

Basic Components of an Optical Instrument.

Source   Wavelength   Sample   Detector   Signal
          selector   holder   processor
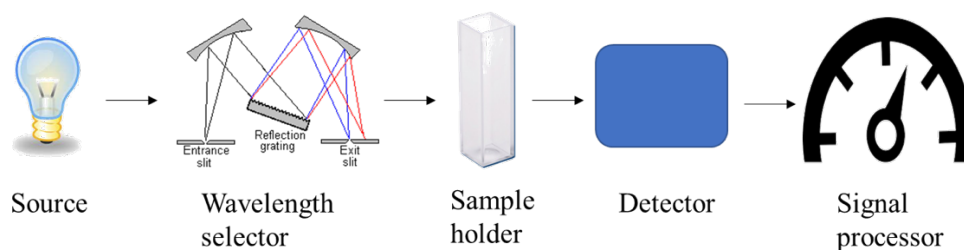
Construction of the colorimetric box

The colorimetric box that was built so that it can resemble a simple standard optical instrument. The box is made of aluminum and measures $25 \times 18 \times 9$ cm. In this study, two designs were proposed (Figure 2). The interior of one design is black, while the interior of the other is white. In one design, the light source was the screen of a smartphone camera, which served as a monochromatic light source as well as a wavelength selector by emitting a specific wavelength of radiant energy (Figure 2A) A battery-powered light emitting diode (LED) lamp was used as a continuum light source in the second design Figure 2.B). The sample holder in both designs was a quartz UV/Vis microcuvette. The detector was a smartphone, and the signal processor was the freely available ImageJ software for personal computers.

Figure 2.

Components of the colorimetric box as an optical detector: A). Monochromatic light source used to emit radiant energy; B). Continuum light source used to emit radiant energy.
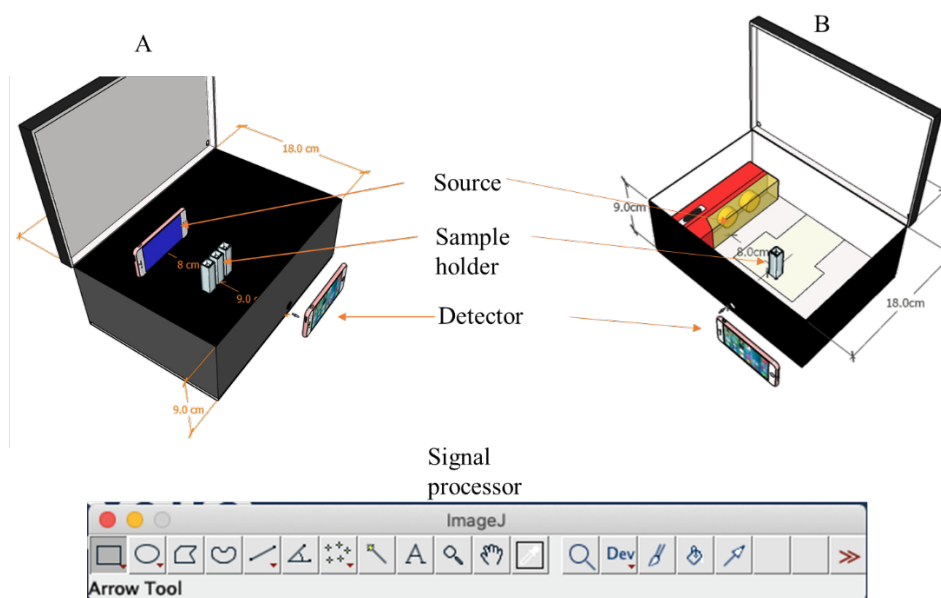
Optimization of SDIC parameters

To obtain maximum response from SDIC, some important parameters need to be optimized such as.

- Selection of the RGB channel.
- The region of interest (ROI).
- Data processing or converting signal into concentration.
- Distance of the sample solution to the detection camera.
- Wavelength of the monochromatic light source.

Selection of the RGB channel

Color spaces have been developed to standardize the specifications of colorimetric measurements. RGB, CMYK, XYZ, L*a*b*, HSV, Gray model, and other color spaces are examples (Capitan-Vallvey et al., 2015). The pixel intensity is converted into a numerical value that can be used as analytical information for each color space. The color space is visualized as a unit cube in the red-green-blue (RGB) model used for computer-based display systems. In the 3D space, each color is assigned to one of three orthogonal coordinate axes. Each R, G, and B component contributes to varying degrees along each axis of the color cube. At each point (color) within the cube, three numbers are specified, represented as R, G, B triples ranging from absolute black (0, 0, 0) to absolute white (255, 255, 255) (Fan et al., 2021). As a result, for each channel, a number between 0 and 255 is generated, with 0, 0, 0 representing absolute black and 255, 255, 255 representing absolute white. In comparison to the other channels, one of the R, G, B channels provides the most intense response for a specific analyte characterized by a specific color. As a result, a digital image must be divided into three channels and the most intense one is chosen. To accomplish this with ImageJ software, click 'file,' then 'open' (or Ctrl O). Open the folder that contains the JPG image. Next, select 'image,' then 'color,' and finally 'split channels' from the drop-down menu. The image will be divided into three RGB channels. For analysis, the most intense channel can be chosen. The B channel is the most intense in this illustration (Figure 3).

Figure 3.

Selection of the RGB channels: (a) Image before splitting; (b) Image after splitting.
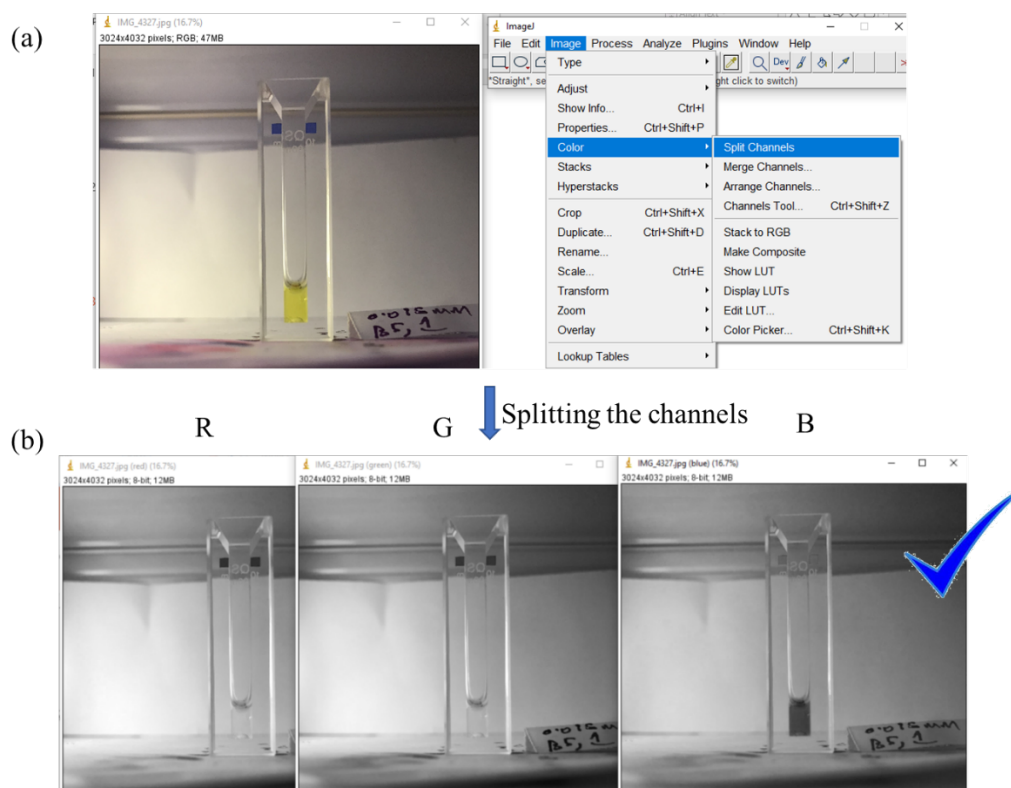
Region of interest

The region of interest (ROI) is the cropped area chosen by the software to convert the pixel intensity into a number that can be correlated to the analyte concentration for quantitation. Go to 'edit' to select the ROI. Click 'selection' and then 'specify' in the drop-down menu. A pop-up menu will appear, allowing you to choose the shape and orientation of the ROI; in this case, a square is selected and centered (Figure 4). The X and Y coordinate of the sample solution should be adjusted and finally the width and height of the ROI should be written. the selected value was 80×80 which is equivalent to 6400 px^2, which is the ROI. for subsequent analysis, a shortcut can be used to place the ROI with the

selected properties by selecting Ctrl + shift + E from the keyboard. The ROI will automatically appear.

Figure 4.

Selection of ROI.
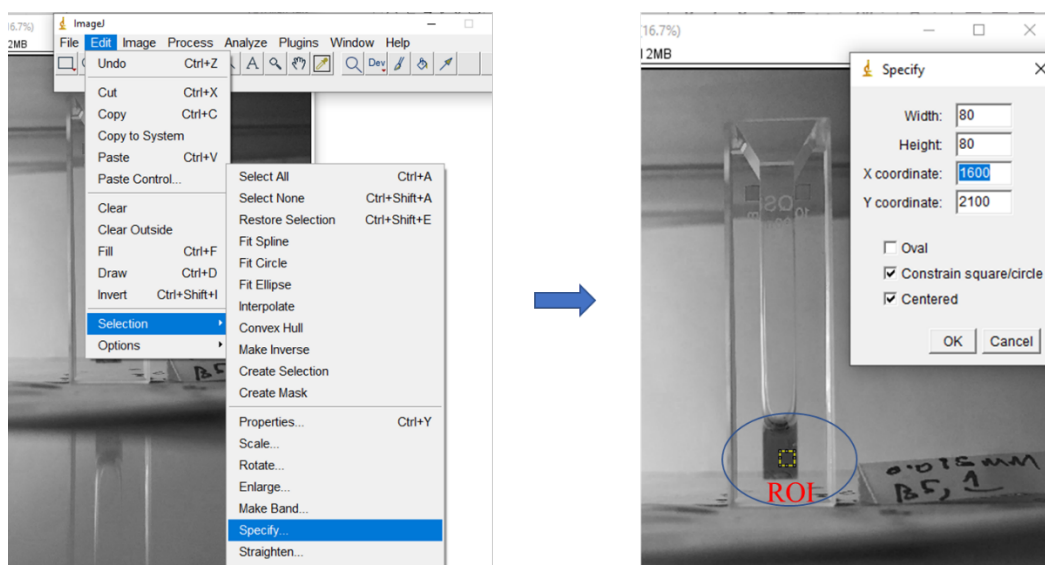
Data processing or converting signal into concentration

The ROI of the most intense channel can be converted to a histogram by selecting 'Analyze' and then 'Histogram' from the drop-down menu (or Ctrl H). Quantitation is done using the histogram's mean value. However, unlike other optical instruments where the response is directly proportional to the analyte concentration, SDIC has an inverse relationship. As a result, as the concentration of the analyte increases, as indicated by an increased color intensity, the mean value of the histogram decreases. Therefore, different formulas have been proposed to obtain a positive slope in the calibration graphs for quantitation, depending on the phenomenon measured, whether it is absorbance or reflectance. Figure 5 depicts the most commonly used formulas (Porto et al., 2019).

Figure 5.

Data processing.
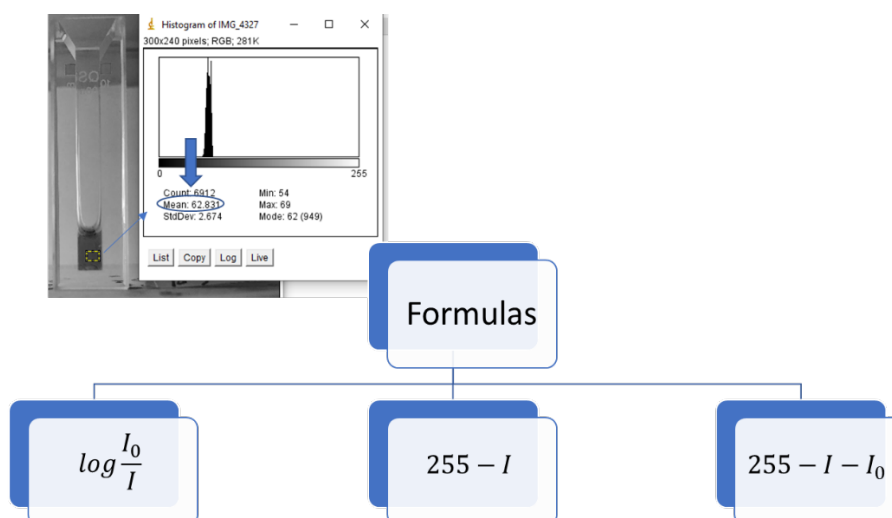
I_0 is the response obtained from the histogram of a blank solution in a particular channel and *I* is the response obtained from the analyte solution in the same channel as the blank. The number 255 is often used because the number generated from the histogram of the channels is between 0 and 255. With 255 representing the number that will be obtained from an ideal blank.

Distance of the sample solution to the detection camera

The distance between the sample solution and analyte is optimized because efficiency of the detection camera's autofocus is affected by the distance between the detection camera and the target (i.e., sample solution) if other factors such as lenses, light intensity, focus settings, size, contrast, and camera motion are held constant (Zhang et al., 2018).

Wavelength of the monochromatic light source

The wavelength of the monochromatic light source is an important parameter because, as with optical instruments operating in the UV/Vis region of the spectrum, the maximum absorption wavelength for each analyte varies. Similarly, in the RGB model, the background color of the monochromatic light source is varied to find the color that provides the best response for a specific analyte. This is accomplished by using the online free wavelength-to-color converter, which may be found the following link (https://www.wolframalpha.com/widgets/view.jsp?id=5072e9b72faacd73c9a4e4cb36ad08d). The color equivalent of a specific wavelength within the visible region of the spectrum is generated in the Microsoft Paint software, transferred to the smartphone via a cloud and is used as the monochromatic light source for analysis. Within the complementary color of the analyte, different wavelengths are investigated and the wavelength that results in the greatest response is chosen.

The Analytes

Iodate

Iodine is essential for the normal development of the thyroid gland, which oversees cell growth. It is responsible for producing triiodothyronine (T3) and thyroxine (T4) hormones that regulate the body temperature and metabolism in both adults and children (Bhagat et al., 2009). The WHO recommends a daily iodine intake range of 90 to 250 μg. The lower limit is for children and the upper one is for pregnant women (Chandra et al., 2019). Iodine deficiency disorders (IDDs) are the consequences of iodine deficiency in the body, which include goiter, infant mortality, miscarriage, infertility, and dwarfism (Eckhoff & Maage, 1997). One the other hand, an excess of iodine in the body can have negative health consequences such as hypothyroidism and hyperthyroidism (Leung &

Braverman, 2014). As a result, it is advised to adhere to the WHO iodine consumption limit.

Iodized table salt is the primary source of iodine for humans, with milk, cereals, eggs, and vegetables serving as secondary sources (Kulkarni et al., 2013). Table salt was previously iodized with potassium iodide. However, in recent years, it has been replaced with potassium iodate to prevent iodine deficiency (Mortazavi & Farmany, 2014). The iodometric redox titrimetric analysis method is the standardized method for determining iodate in table salt. It involves reacting iodate with iodide in the presence of an acid to liberate iodine, which is then reacted with a thiosulphate standard solution in the presence of a starch indicator (https://www.canterbury.ac.nz/media/documents/science-outreach/salt_iodate.pdf). Other methods for determining iodate in table salt have been proposed, such as using cadmium sulphide quantum dots as fluorescence probes (Tan et al., 2010), ion chromatography with ultraviolet detection (IC-UV) (Huang et al., 2013), ion chromatography with conductivity detection (Kumar et al., 2001), ion chromatography with amperometric detection (Rebary et al., 2010), gas chromatography with thermal conductivity detection (GC-TCD) (Xie et al., 2019), UV/Vis (Pena-Pereira et al., 2010) and capillary zone electrophoresis (CZE) (Wang et al., 2009).

Curcumin

Curcumin belongs to a class of compounds known as polyphenols, and it is primarily found in turmeric (Curcumin longa), an Indian spice. Curcumin is a yellow pigment that is the primary constituent of turmeric. This compound is highly valued and is often referred to as "Indian solid gold" (Aggarwal et al., 2007). The bright color of curcumin has made it very useful in the food coloring industry for many centuries. Recent studies have revealed several pharmacological effects associated with curcumin such as anti-cancer properties (Tamddoni et al., 2020), antioxidant (Noon et al., 2020), anti-ageing (Zheng et al., 2020), anti-inflammatory (Zhou et al., 2020), anti-diabetes (Pivari et al.,

2019), anti-bacterial, anti-viral, and anti-fungal (Moghadamtousi et al.) making it very popular in the pharmaceutical industry.

Several well established techniques have been proposed in the literature for the determination of curcumin with various instruments such as UV/Vis (Afkhami et al., 2017), HPLC-UV (Khorshidi et al., 2020), HPLC-FLD (Schiborr et al., 2010), LC-MS/MS (Song et al., 2019), ultrahigh-performance liquid chromatography-tandem mass spectrometry (UHPLC-MS/MS) (Yu et al., 2019), CE-AD (Sun et al., 2002) and electrochemical sensors (Raril et al., 2020).

Boron

Boron is a trace mineral that functions as a micronutrient and plays several important roles in metabolism, making it essential for plant, animal, and human health. Some of the advantages to human health include bone growth and maintenance, wound healing speed, increased oestrogen, testosterone, and vitamin D levels in the body, antioxidant activity, and preventive and therapeutic effects against certain cancer cells (Pizzorno, 2015). However, excessive boron consumption can cause nausea, diarrhoea, breathing difficulties, and even death at high concentrations, necessitating the establishment of a tolerable threshold for adults ranging from 1 to 20 mg per day.

For elemental analysis, AAS is the method of choice. However, because boron is a metalloid, its sensitivity suffers significantly due to poor atomization efficiency, rendering the readily available FAAS insufficient for detecting boron in genuine samples (Luguera et al., 1991). While ETAAS has sufficient sensitivity for detecting boron, several modifiers such as zirconium and citric acid are required (Burguera et al., 2001). Plasma-based atomic techniques such as ICP-OES and ICP-MS provide adequate sensitivity for determining boron in genuine samples, but they are extremely expensive instruments that necessitate a high level of technical expertise making it out of reach for most laboratories (Sah & Brown, 1997).

To address these issues, the curcumin method for boron colorimetric determination was developed, which involves forming a complex (i.e., rosocyanin) between boron and curcumin in an acidic medium (curcumin reagent) prior to spectrophotometric detection (Toida & Watanabe, 1993). The curcumin reagent's high selectivity for boron in the formation of rosocyanin eliminates potential interferences (Wimmer & Goldbach, 1999). Besides, rosocyanin can be formed even at relatively low boron concentrations, providing adequate sensitivity for quantifying trace amounts of the element in genuine samples (Qin, 2013). Moreover, the intense red color of rosocyanin, which is easily distinguished from the yellow color of the curcumin reagent, suggests that the spectrophotometric detection technique could be replaced with a relatively simple and inexpensive colorimetric method such as SDIC.

CHAPTER III
MATERIALS AND METHODS

Chemicals and Reagents

Unless otherwise specified, all chemicals and reagents used in the study were of analytical grade. 1-DO (log$P$ 4.36, density, d: 0.83 g mL^{-1}; melting point, m. p.: 22–26 °C), 1-UN (log$P$ 3.92, d: 0.83 g mL^{-1}; m. p.: 11 °C), acetone (ACT), curcumin (log$P$ 4.85, pK_{a1} 8.8), HPLC-grade acetonitrile (ACN), methanol (MeOH) THF (log$P$ 0.34), CF (log$P$ 1.83, d: 1.48 g mL^{-1}), diphenyl ether (DPE, log$P$ 3.47, d: 1.08 g mL^{-1}), ethanol (EtOH), hydrochloric acid (HCl), phosphoric acid, sodium phosphate monobasic, oxalic acid and potassium iodide (KI) were obtained from Sigma-Aldrich (Germany). Potassium iodate was purchased from Merck (USA). Zirconium nanoparticles were kindly provided by Prof. Dr. Sezgin Bakırdere from Yıldız Technical University (Istanbul, Turkey). Deionized (DI) water, used for the preparation of all aqueous solutions, was prepared with Purelab Ultra Analytic (ELGA LabWater, UK).

Apparatus

A homemade colorimetric box made of aluminum with the dimensions 25 × 18 × 9 cm was designed to capture reproducible images of the sample solution. A hole was drilled in the box's side to allow the camera's lens to capture images of the sample solution. The colorimetric box was modified based on the requirements of the specific application described in the Results and Discussion section.

The images were captured with an iPhone 7 smartphone (model number MN972VC/A). The specifications of the smartphone included a 12 MP rear camera, aperture of f/1.8. The screen is a 4.70-inch touch screen display with a resolution of 750 × 1334 pixels. The internal memory was 254 GB, with a 2.34 GHz quad-core Apple A10

Fusion processor and 2.0 GB RAM. In the boron study, images were taken with an iPad mini tablet (5th generation, 2019) equipped with an 8 MP rear camera with focal aperture of f/2.4. The screen is a 7.40-inch touch screen display with a resolution of 1536 × 2048 pixels. The built-in memory was 65-GB, 3.0 GB RAM, and an Apple A12 Bionic chip processor. A second smartphone (iPhone 6s) was used as a monochromatic light source. The specification of the smartphone included a 4.7-inch touch screen display with a resolution of 750 × 1334 pixels. The rear camera is 12 MP with f/2.2 and 2.0 GB RAM. The processor is a 1.8 GHz quard-core Apple A9 processor with a 64 GB built-in memory. For image processing, the ImageJ software for PC was used (version 1.52a, Java 1.8.0-211, 64 bit) designed by the National Institute of Health (NIH), USA (Rueden et al., 2017). MavinSketch (Rev. 20.11.0, ChemAxon Ltd., USA) was employed for the calculation of $logP$ and pK_a values.

Sonication was carried out with an ultrasonic bath (Isolab, Germany). Vortex was carried out with an MS 3 digital vortex (IKA, Germany) whereas, centrifugation was performed with an EBA20 Portable Centrifuge C2002 (Hettich, Germany). For transferring accurate volumes of the solutions, a 2-20 µL Eppendorf micropipette (Sigma-Aldrich, USA), 20-200 µL, 100-1000 µL and 1000-5000 µL micropipettes (Isolab, Germany) were used. Weighing of samples and standards was performed with an electronic balance (Mettler-Toledo, Switzerland). Hot-water extraction and evaporation-to-dryness was carried out with a Heidolph MR HEI-Standard hotplate (Schwabach, Germany). A pH meter, equipped with a glass electrode, (Mettler-Toledo, Greifensee, Switzerland) was used for measuring the pH of solutions. Accuracy check was performed by independent studies with a single beam 1240 UV/Vis spectrophotometer (Shimadzu, Japan) at wavelengths of 352.0 nm for iodate, 428 nm for curcumin, and 540 nm for boron.

Statistical Analysis

All statistical analyses were performed using the single-factor analysis of variance (ANOVA) test in Microsoft Office Excel 2016 for Windows (Microsoft Corporation, USA). At $P < 0.05$ the variable was considered to have a statistical significance.

Solidification of Floating Organic Drop-Dispersive Liquid-Liquid Microextraction Combined with Smartphone Digital Image Colorimetry for the Determination of Iodate in Table Salt

The section that follows is devoted to the first study that was conducted to determine the concentration of iodate ion in table salt.

Iodate standard solutions

By dissolving an appropriate mass of potassium iodate in DI water, a 50.0 mmol L^{-1} standard stock solution of iodate ion was prepared. An intermediate stock solution was prepared from the stock solution at 1.0 mmol L^{-1} of iodate ions. From this intermediate stock, working solutions were prepared in DI water for calibration within the concentration ranges of 10.0 to 300.0 µmol L^{-1} for SDIC and 0.5 to 20.0 µmol L^{-1} for SFOD-DLLME-SDIC and UV/Vis.

Sample preparation

Iodized and non-iodized salt samples were obtained from local markets in Nicosia, TRNC. The samples were then stored in a dry, dark place until analyzed. To conduct the experiment, a 2.0 ± 0.01 g portion of table salt was weighed into a 25.0 mL volumetric flask. This was followed by the addition of DI water below the mark and sonication for 5.0

min at 25 °C and 60 kHz to completely dissolve the salt. Next, the solution was made up to the mark with DI water.

Redox reaction

For detection by SDIC to be possible, iodate must be derivatized into iodine, being yellow, via the well-known redox reaction of iodate with iodide ions in an acidic medium. A portion of the sample solution (5.0 mL), which could be iodate standard or salt solution, was transferred to a 15.0 mL capped conical graduated polypropylene centrifuge tube (Isolab, Germany). This was followed by the addition of an excess of HCl (0.5 mL, 1.0 M) and KI (0.5 mL, 0.6 M) to the solution, which immediately turned yellow, indicating the formation of iodine (Figure 6). The color intensity was proportional to the concentration of iodate ions in the solution. The redox reaction is shown below.

$$IO_{3(aq)}^- + 5I^-_{(aq)} + 6H^+_{(aq)} \rightarrow 3I_{2(aq)} + 3H_2O_{(l)}$$
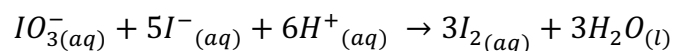
Figure 6.

Schematic diagram of the redox reaction.
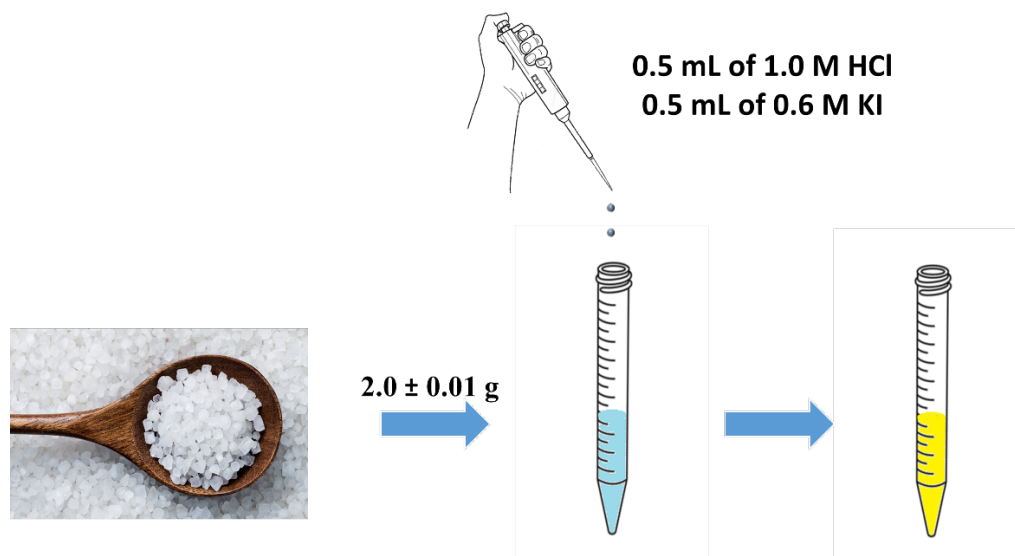
Solidification of Floating Organic Drop-Dispersive Liquid-Liquid Microextraction

A 2.0 mL mixture of the extraction and disperser solvent (1-UN/EtOH at a 1:3, v/v ratio) were injected rapidly into the reaction mixture which caused the solution to form an emulsion after mechanical agitation by vortex for 20 s. Phase separation was achieved by centrifugation for 1 min at 6000 rpm. The solution was solidified within a duration of 5.0 min. The solidified organic drop was transferred into a microvial with a spatula. A portion of this drop (100 µL) was transferred into a UV/Vis microcuvette after melting and placed into the colorimetric box for detection with the smartphone camera. A schematic diagram of the SFOD-DLLME procedure is given in Figure 7.

Figure 7.

Schematic diagram of SFOD-DLLME procedure.
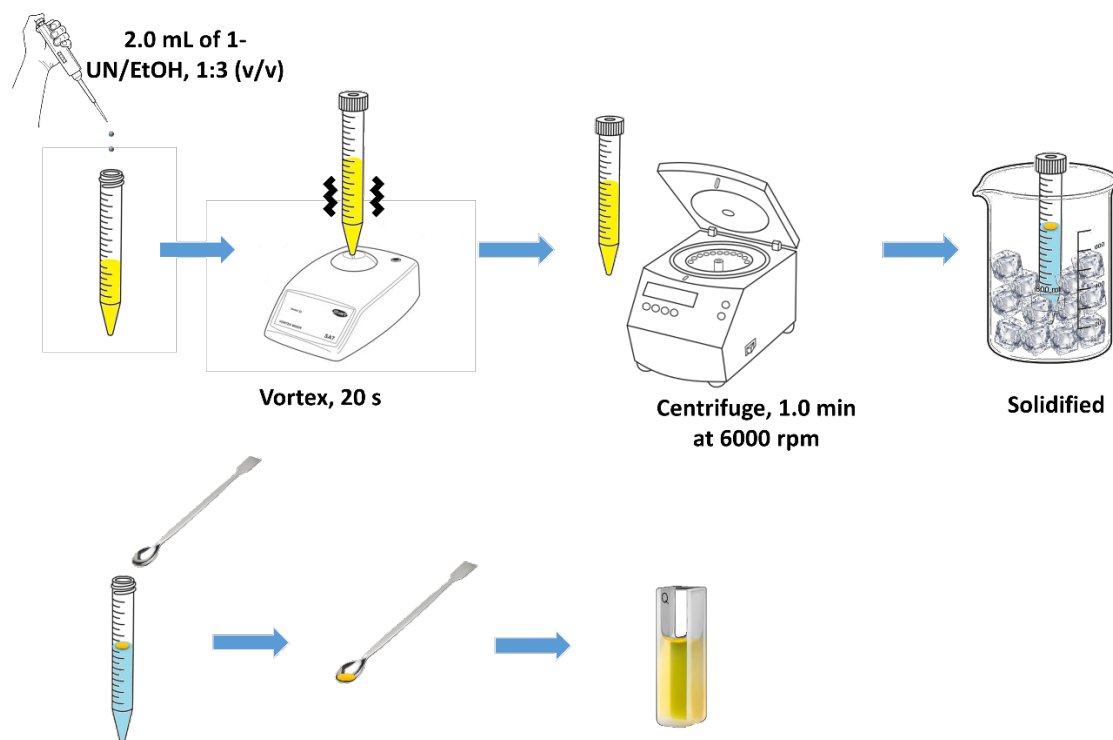
Data processing

The captured images were saved in JPG format and uploaded to Google Drive for retrieval from a personal computer for processing with ImageJ software. The images were split into their respective RGB channels by the software, and the B channel provided the best response and was used for all analysis. A schematic diagram of the proposed SDIC system is provided (Figure 8). The equation below is used to calculate the response (R).

$$R = I_0 - I_s \qquad \text{(Equation 2)}$$

where, I_0 and I_s are the mean intensity obtained from the histogram of the blue channel of the blank and sample solution, respectively.

Figure 8.

The proposed SDIC system with continuum light source. (a) Table salt solution spiked with increasing concentrations of iodate ions; (b) The colorimetric box; (c) Image of the extract containing the analyte is processed; (d) Image is split into the RGB channels; (e) Histogram of the B channel; and (f) Standard-addition calibration graph for iodate ions in the table salt
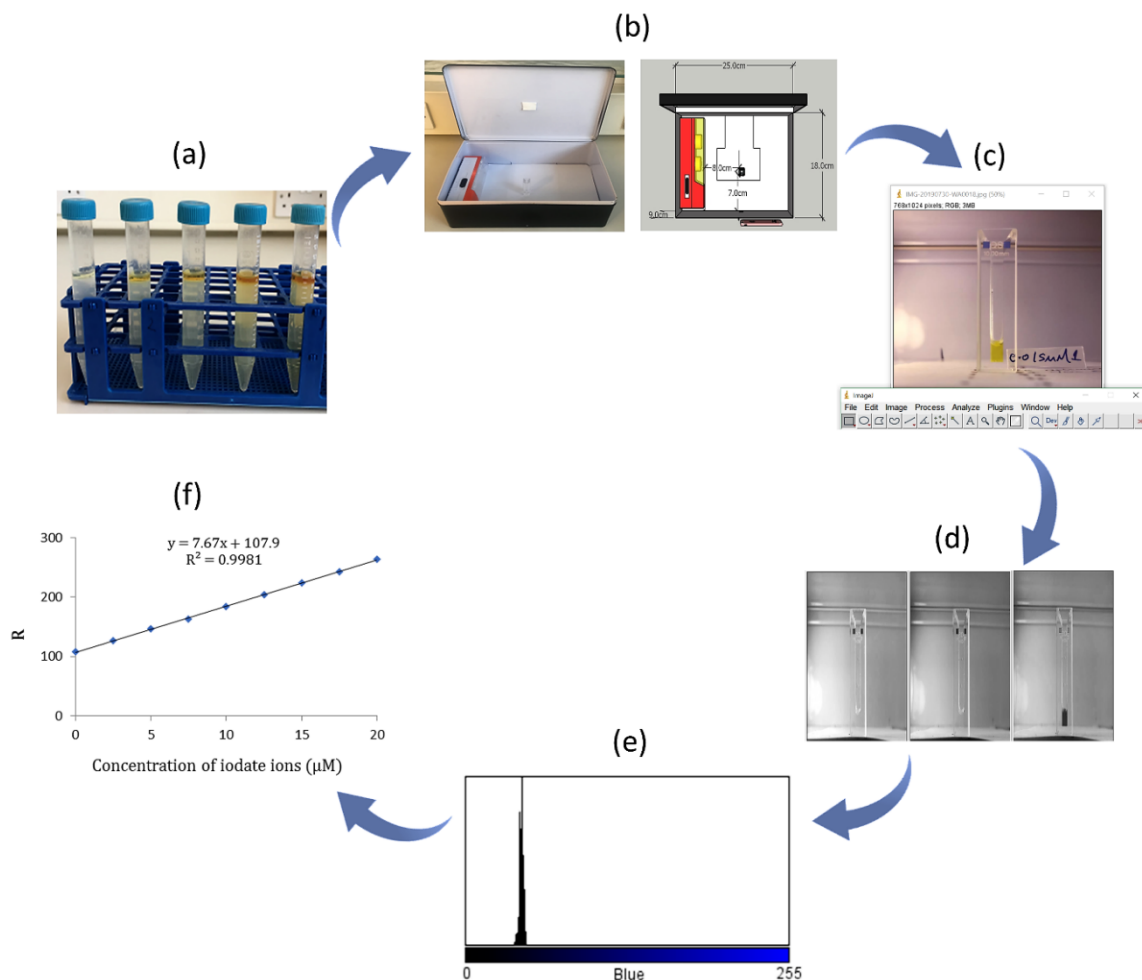
Supramolecular Solvent Liquid-Liquid Microextraction Combined with Smartphone Digital Image Colorimetry for The Determination of Curcumin in Food Samples

The section that follows is specific to the second study for determining curcumin in food samples.

Curcumin standard solutions

A 1000 $\mu g\ mL^{-1}$ standard stock solution of curcumin was prepared in ACN and SMS (THF:1-UN, 4:1, v/v) separately by weighing the required mass of curcumin standard. The standard prepared in ACN was used for accuracy check with UV/Vis whereas the one prepared in SMS was used for the proposed SMS-LLME-SDIC method.

Supramolecular Solvent Liquid-Liquid Microextraction procedure

Tea and turmeric samples were obtained from local markets in Nicosia, TRNC. The samples were ground into fine powder in a glass mortar before being stored in dry glass bottles in a dark environment before analysis. A 5.0±0.1 mg portion of the sample was weighed into a 15.0 mL of a capped polypropylene graduated conical centrifuge tube. A 1000 μL volume of SMS was added directly into the solid before adding DI water up to 10.0 mL mark. The solution was mechanically agitated for 1 min with a vortex before centrifugation for 1 min at 6000 rpm to separate the phases. A representative 100 μL portion of the curcumin-rich supernatant solution was collected and transferred into the quartz microcuvette for SDIC detection. When necessary, SMS was used to dilute the extract. The SMS-LLME schematic diagram is provided in Figure 9.

Figure 9.

Schematic diagram of SMS-LLME experimental procedure.
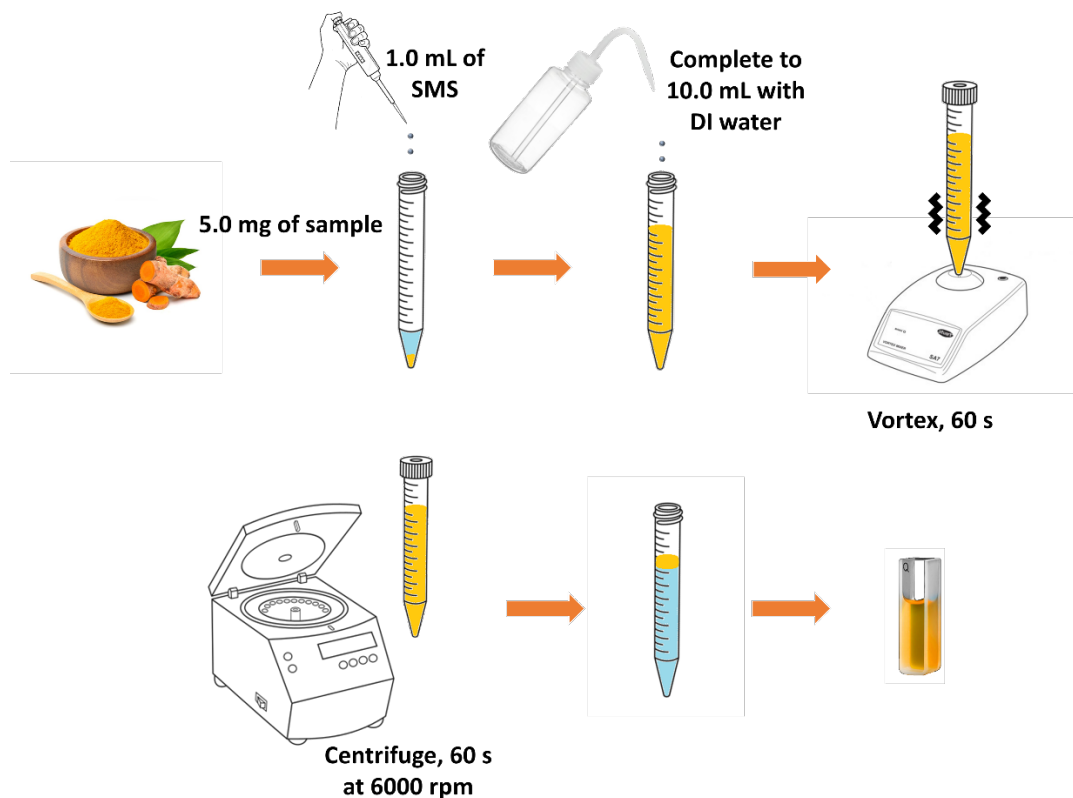
Data processing

The captured images were saved in JPG format and transferred to the cloud via Google Drive for retrieval from a personal computer for processing with ImageJ software. The software split the images to their respective RGB channels, and the B channel gave the highest response and was used for all analysis. A schematic diagram of the proposed SDIC system is given in Figure 10. Absorbance was calculated from the mean values obtained from the histogram of the B channel for the blank and analyte solution in the equation below.

$$R_B = -A = log\frac{I_0}{I}$$ **(Equation 3)**

where, R_B is the response calculated using the mean values from the histogram, I_0 and I are the intensities of the signals obtained for the blank and the analyte solution at the same channel, respectively.

Figure 10.

Proposed SDIC system with monochromatic light source. (a) Schematic diagram of the colorimetric box; (b) Image of the sample from the colorimetric box processed: The three cells contain blank and two replicates of analyte respectively; (c) Image split into RGB channels; and (d) A calibration graph plotted using the B channel.
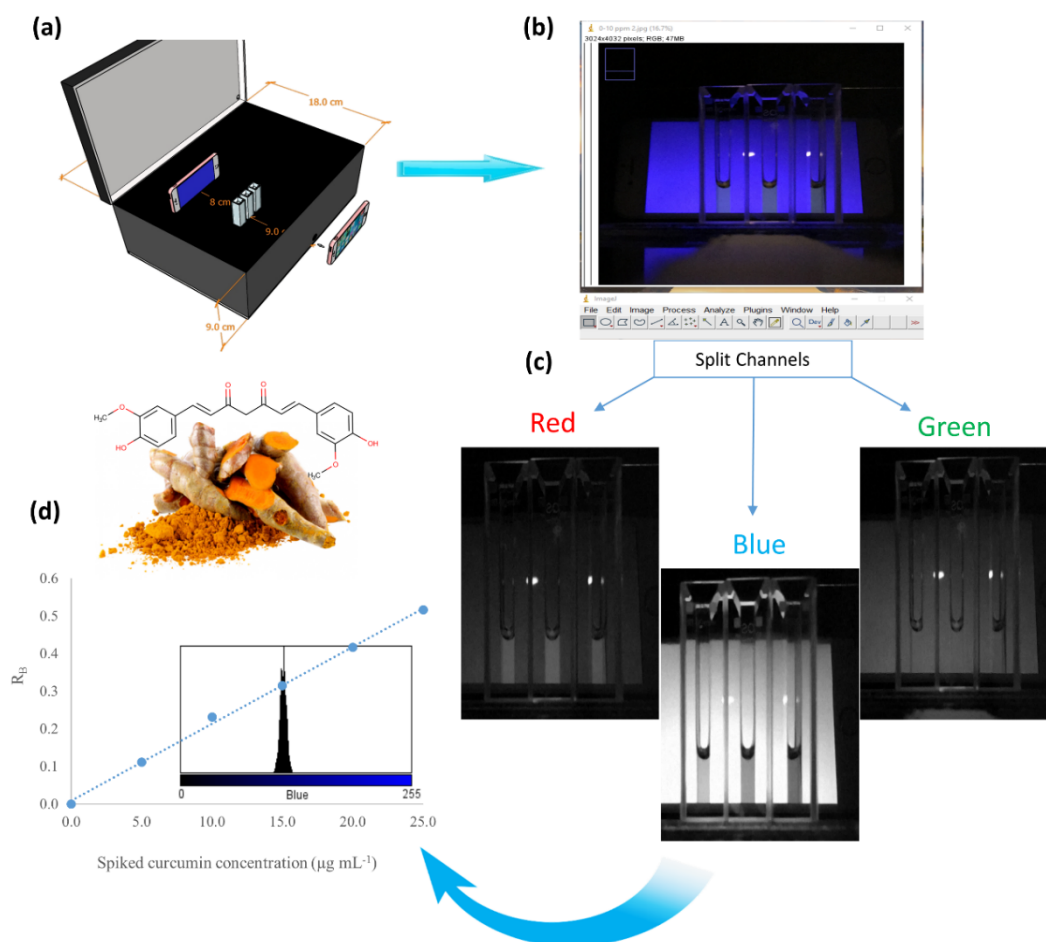
Dispersive Solid-Phase Microextraction Combined with Smartphone Digital Image Colorimetry for the Determination of Boron in Nuts

The section that follows is specific to the third study, which was conducted to determine the boron concentration in various types of nuts.

Boron standard solutions

To prepare a standard stock solution containing 1000 µg mL^{-1} of boron, an appropriate mass of boric acid was transferred into a 50 mL volumetric flask, dissolved, and completed to the mark with DI water. Working standard solutions were prepared by diluting them with DI water.

Sample preparation

Different nut samples (i.e., almond, hazelnut, ivory, peanut, and walnut) were purchased from local markets in Nicosia, TRNC. The samples were kept in the oven at 40 °C until they were dried. A glass mortar and pestle were used to grind the samples to a fine powder before storing them in a dry place until analysis. A 1.0±0.01 g portion of each sample was weighed into a beaker for hot water extraction with DI water at 150 °C on a hot plate. The samples were filtered while hot with a 0.45 µm Whatman syringe filter paper into a 25 mL volumetric flask and filled to the mark with DI water (Figure 11.). This was referred to as the sample solution.

Figure 11.

Procedure of sample preparation
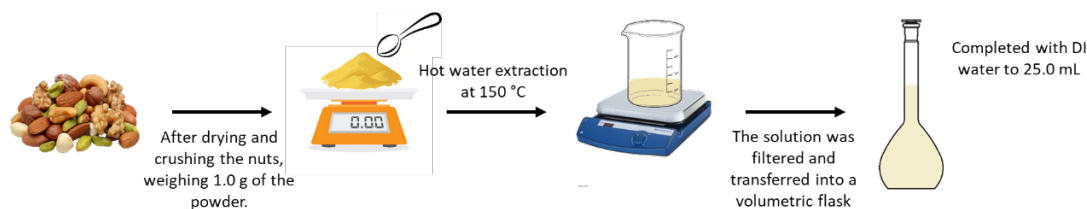
Complexation of boron by the curcumin method

The procedure proposed previously for the preparation of the curcumin reagent (Qin, 2013) was adopted in this study by collecting 40 mg of curcumin and 5 g of oxalic acid into a 100 mL volumetric flask and dissolved with appropriate volume of absolute EtOH below the mark. Concentrated HCl (4.2 mL) was added before completing to the mark with absolute EtOH. For the complexation, 100 µL of the sample solution was taken into a porcelain evaporation dish and 400 µL of the curcumin reagent was added. The solution was evaporated to dryness on a hot plate at 55 °C and re-dissolved with 1.0 mL of MeOH and transferred to a 15.0 mL closed cap centrifuge tube for DSPME (Figure 12.**Error! Reference source not found.**). The structure of the rosocyanin complex formed as given in a previous study (John et al., 2018) is shown in Figure 13.

Figure 12.

Schematic diagram of the complexation of boron by the curcumin method.
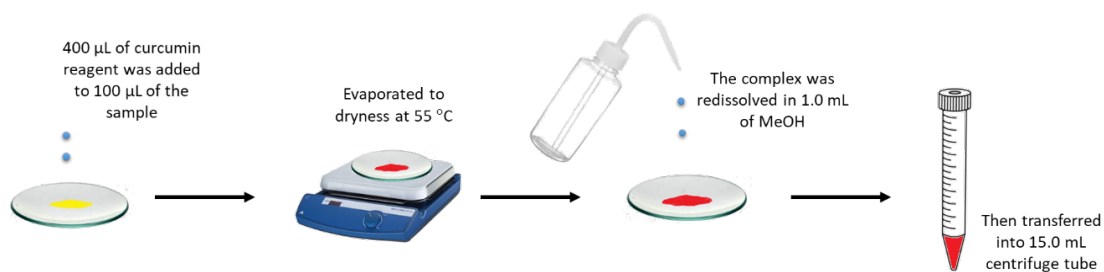
Figure 13.

Structure of rosocyanin.
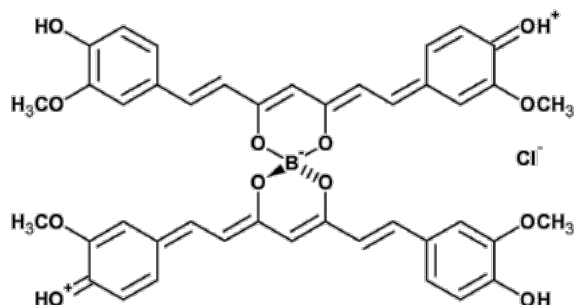
Dispersive Solid-Phase Microextraction

In a 15 mL closed cap centrifuge tube, preconditioned ZrNPs (30.0 mg) was used as the adsorbent for DSPME. A 25 mM Phosphate buffer solution, pH 2.5 was added followed by DI water to 10 mL. The solution was vortexed for 2 min and centrifuged for 1 min at 6000 rpm. After discarding the supernatant, the analyte was eluted with 100 μL of acetone for SDIC (Figure 14). The same procedure was followed for a DI water blank solution.

Figure 14.

Schematic diagram of the DSPME procedure.
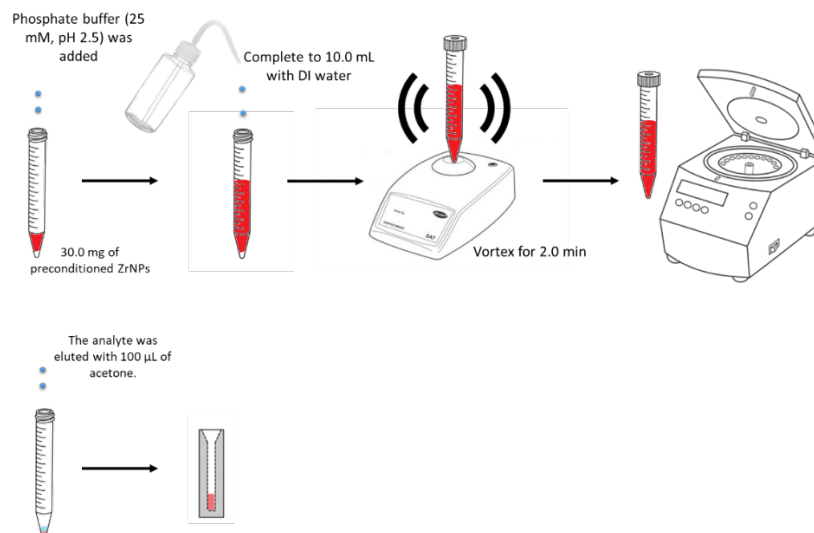
Data processing

The sample solution and blank were transferred into a quartz microcuvette for SDIC, and their digital images were captured in JPG format and saved in the cloud via Google Drive for retrieval in a PC for ImageJ processing. The images were divided into RGB channels, and the G channel produced the highest response, as calculated in equation 3 below.

$$R_G = -A = log\frac{I_0}{I} \hspace{3cm} \textbf{(Equation 4)}$$

where, R_G represents the response based on the mean values gotten from the histogram of the G channel of the blank signal (I_0) and analyte signal (I). Figure 15 depicts a schematic diagram of the SDIC procedure.

Figure 15.

Schematic diagram of the SDIC procedure. (a) The colorimetric box; (b) Image of the blank and analyte solutions; (c) Image split into RGB channels; (d) Standard-addition calibration graph for boron using the G channel.
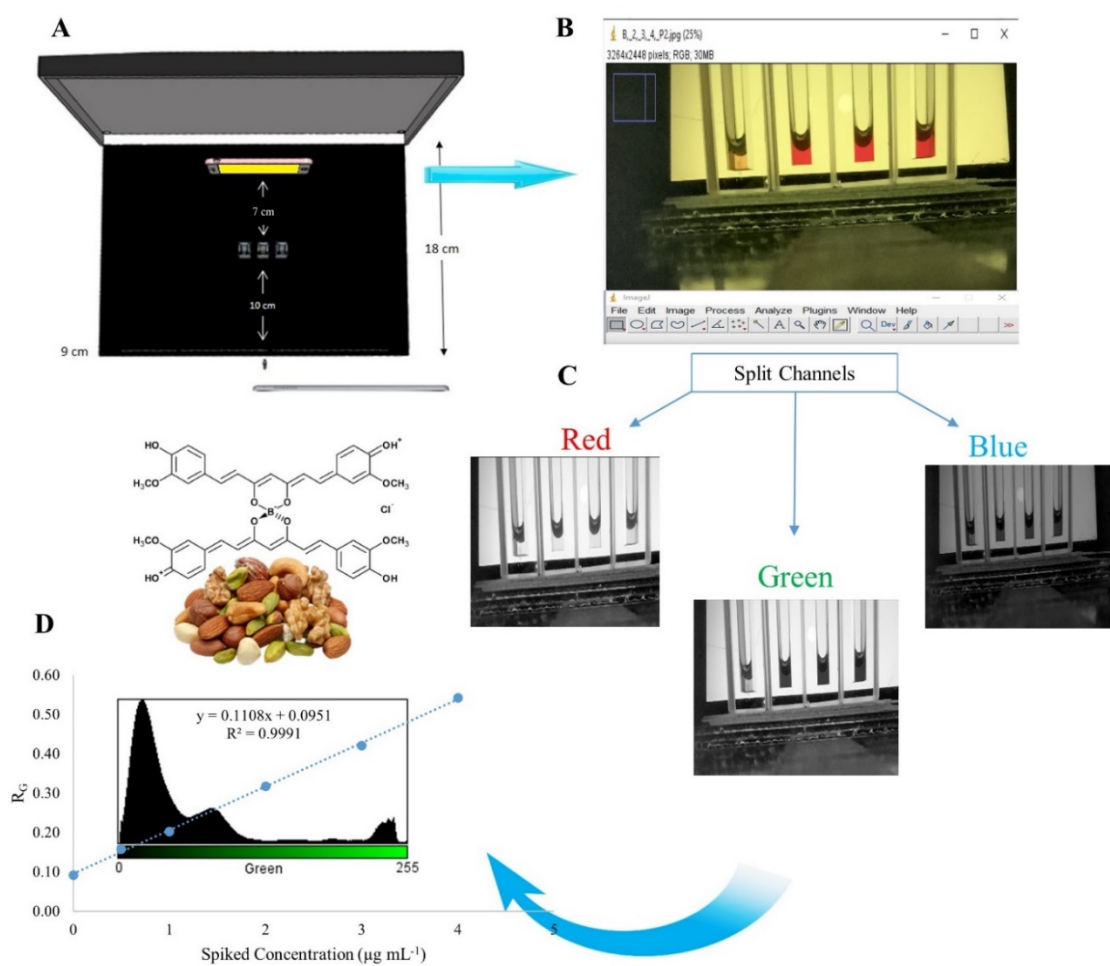
CHAPTER IV
RESULTS AND DISCUSSION

Solidification of Floating Organic Drop-Dispersive Liquid-Liquid Microextraction Combined with Smartphone Digital Image Colorimetry for the Determination of Iodate in Table Salt

Optimization of Smartphone Digital Image Colorimetry conditions

Construction of the colorimetric box

To capture reproducible images of the sample solution, a rectangular colorimetric box was built using an aluminum box with dimensions of 25 × 18 × 9 cm. The interior was painted white to ensure minimal reflection and a homogeneous surface, and a small hole was punched in the side of the box to allow the smartphone camera lens to capture reproducible images of the sample solution placed in a quartz UV/Vis microcuvette (Hellma, Belgium) at 7 cm from the camera. To prevent saturation of the camera lens if placed directly in front of the camera, a continuum light source in the form of a 1.2 V/ 1300 mA battery-powered white light-emitting diode (LED) was positioned perpendicular to the lens. Images of the sample were taken with the rear camera and the flash turned off. The colorimetric box's schematic diagram is shown in Figure 16.

Figure 16.

The Colorimetric box.
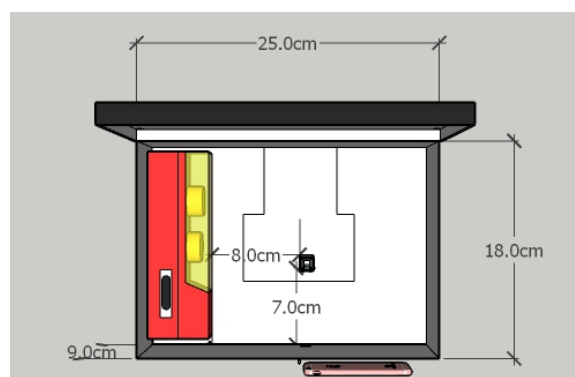
Selection of the RGB channel and data processing method

The ability of the ImageJ software to split the image of the sample solution into its respective R, G, and B components is one of its features. The most intense channel, as defined by the lowest mean value of the histogram, is chosen as the best, in this case the B channel. Because using the mean value of the histogram directly will result in a negative slope in calibration, the number must be converted to a form that will result in a positive slope. For this purpose, several formulas have been proposed in the literature. For example, R=255-I (Porto et al., 2019). Nonetheless, this formula assumes that the blank is ideal, such as pure white, resulting in a mean value of 255. However, because the blank produces a signal less than the ideal 255, a high intercept will be obtained in calibration graphs even when the analyte is present in the sample solution below the method's LOD. Taking this into account, the response (R) is calculated as follows.

$$R = I_0 - I_s$$

Type of smartphone camera

The overall quality of an image obtained with a smartphone is affected by several factors, including but not limited to the resolution (in MP), aperture, size, and type of light

sensor, as well as the image processing algorithm used. The aperture, for example, which allows light into the camera's sensor, is important because the degree to which the sensor is exposed to light affects the overall picture quality. In conventional digital cameras, the aperture can be adjusted to achieve the desired exposure by opening the camera's iris, which is measured in f-stops ($f/$). The aperture, on the other hand, is fixed in smartphone cameras. Nonetheless, a small f/ is preferred for smartphone cameras due to brighter exposure, while a large sensor is preferred for better light control. To investigate the overall effect of smartphone camera type on response, four smartphones labelled phone1, phone2, phone3, and phone4 were used. Except for the phone 2, which has a 16 MP rear camera, all smartphones have a 12 MP resolution. The apertures of smartphones 1–4 was $f/1.8$, $f/1.9$, $f/1.7$, and $f/2.2$, respectively. Phone 1 provided the highest response and was used in all studies (Figure 17).

Figure 17.

Type of smartphone camera.
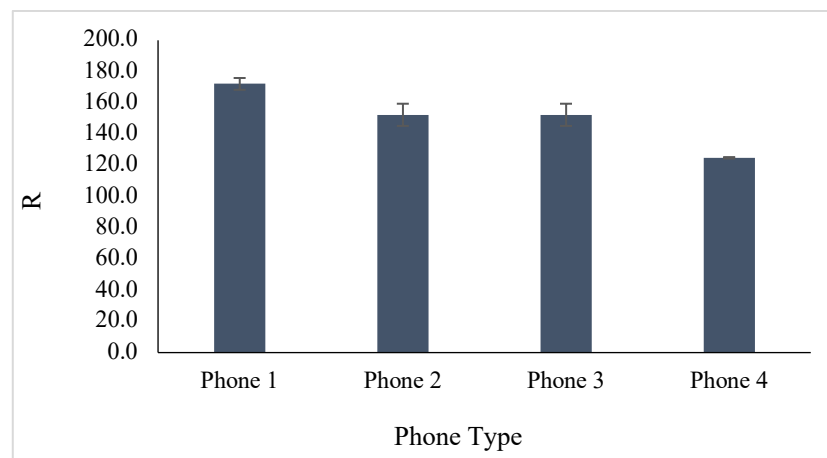
Region of interest

The region of interest (ROI) which is the cropped area selected using the software in px^2 while ignoring other areas was studied by varying the area between the range of 400

to 14400 px^2. A constant response was observed to show that the ROI has no effect due to the homogeneity of the sample solution hence, any ROI can be used (Figure 18.). A ROI of 1600 px^2 was selected as optimum and used for further experiments.

Figure 18.

Region of interest.
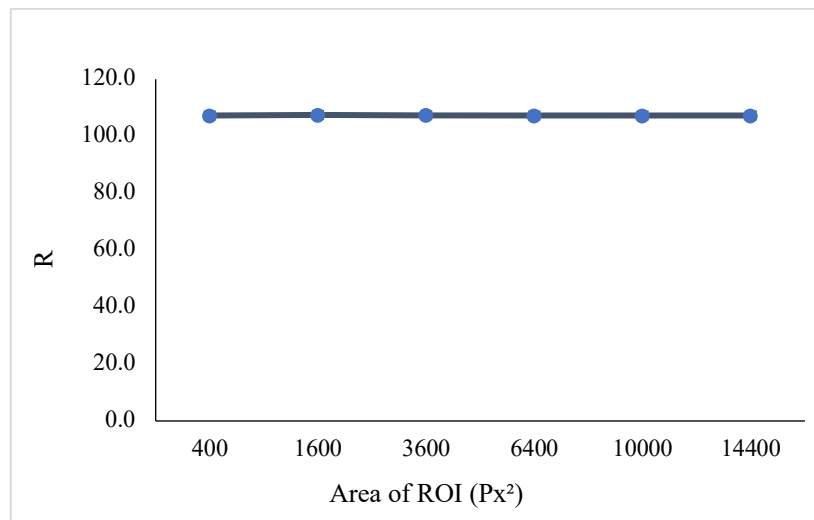
Position of the detection camera

The detection camera can be positioned in two ways: from above (top view) or from the side (side view). The effect of both views on the response was investigated; the higher response was observed with the side view, which was deemed optimal and used in subsequent studies (Figure 19).

Figure 19.

Position of detection camera.
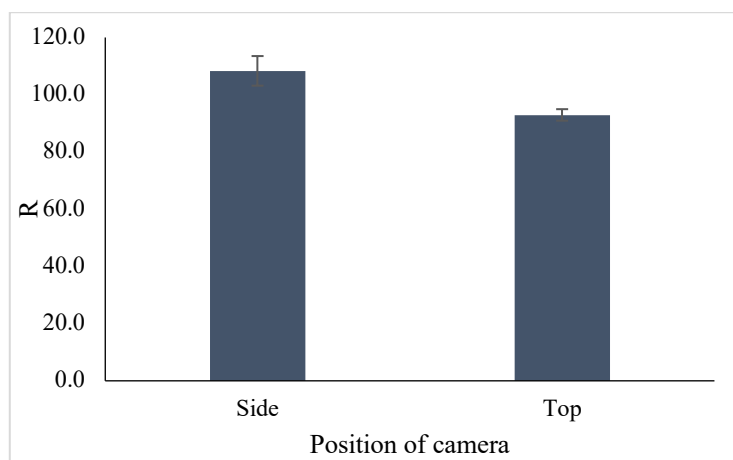
Distance between the camera and cuvette

The effect of the distance of the smartphone camera to the sample cuvette was studied by monitoring the distance between 5.0 to 9.0 cm. The camera's autofocus of the image of the sample cuvette was poor below 5.0 cm, resulting in a blurred image. A downtrend was observed in the response with increase in the distance between the camera and sample cuvette although the sharpness of the image increased which could improve the repeatability of the method (Figure 20.**Error! Reference source not found.**). A final decision was to take 7.0 cm as a compromise between repeatability and sensitivity.

Figure 20.

Distance between camera and sample cuvette.
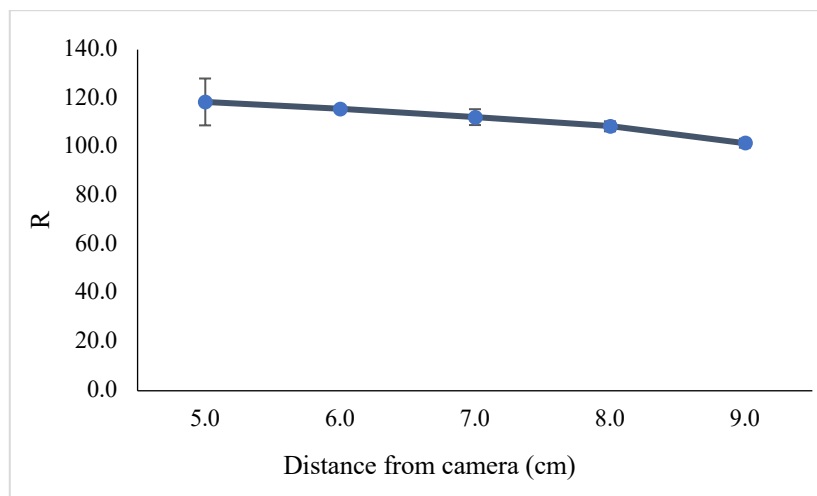
Optimization of the reaction time and solidification of floating organic drop-dispersive liquid-liquid microextraction conditions

The reaction time and SFOD-DLLME optimization studies were carried out using a standard solution containing 10.0 µmol L^{-1} of iodate ions. Preliminary conditions were decided as follows; For the redox reaction, 5.0 mL of the sample solution containing 10.0 µM of iodate ions was transferred into a 15 mL screw capped centrifuge tube, before addition of 0.5 mL of 1.0 mol L^{-1} HCl and 0.5 mL of 0.6 mol L^{-1} of KI. Before proceeding to the SFOD-DLLME step, the mixture was mechanically agitated for 10 s with a vortex before adding 300 µL of 1-UN as extraction solvent and 1.0 mL of ACN as disperser solvent. Vortex and centrifugation were performed for 1 min each before solidifying the upper phase in an ice bath for 5 min. The extract is collected in a UV/Vis microcuvette and the image was captured in the colorimetric box. Optimizations were performed based on these preliminary conditions, one variable at a time, while keeping other conditions constant. The best conditions were used in subsequent experiments.

Reaction time

It is critical to investigate the effect of the reaction time required for the complete conversion of iodate to iodine in order to achieve equilibrium for maximum extraction recovery and repeatability. The preliminary conditions were used in this study, and the solution was allowed to stand for 0 to 4 min after the redox reaction before proceeding to the SFOD-DLLME step. A constant response was observed, indicating that time has no effect on reaction kinetics because equilibrium is reached instantaneously (Figure 21). As a result, the microextraction step follows immediately after the reaction.

Figure 21.

Reaction time.
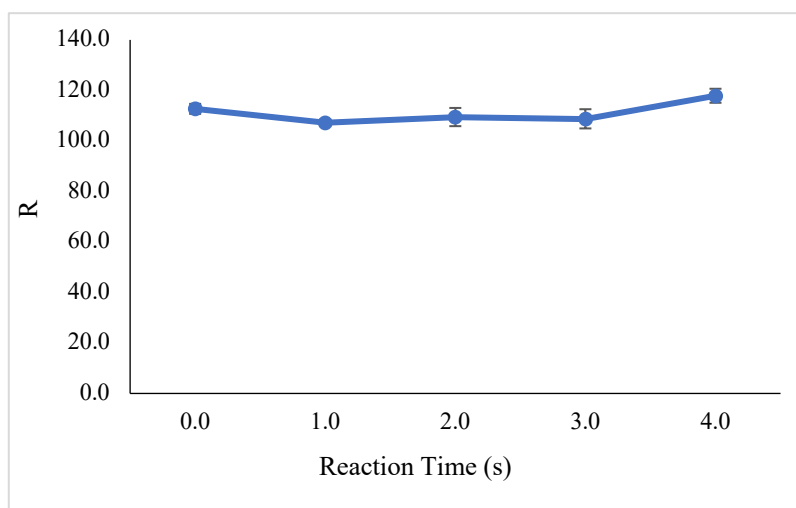
Type and volume of the extraction solvent

To ensure maximum analyte extraction recovery in SFOD-DLLME, it is critical to investigate the effect of different types of extraction solvent on the response. In this study, equal volumes (300 µL) of two low density solvents with room temperature melting points 1-UN, 1-DO, and two high density solvents CF and DPE were used. Following extraction, a 100 µL portion of each solvent was taken for analysis. The low-density solvents

performed better than the high-density solvents, with 1-UN providing the best response and was chosen as the optimum extraction solvent (Figure 22)

Figure 22.

Type of extraction solvent.
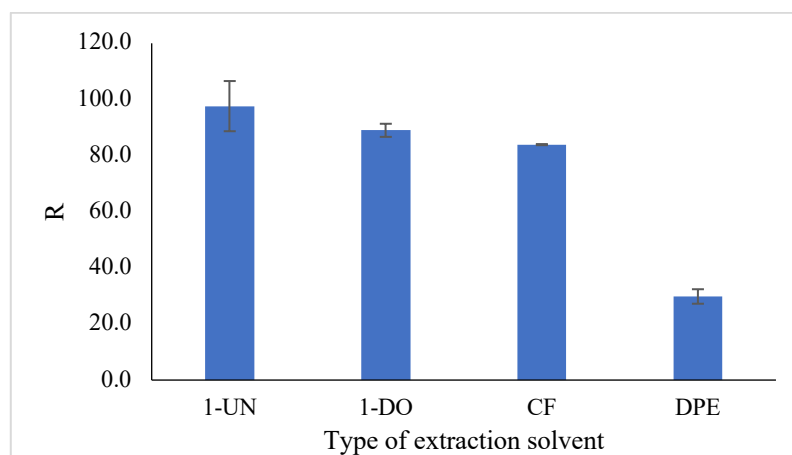
The effect of the volume of 1-UN on the response was studied within the range of 200 to 700 µL. An initial uptrend in the response was observed with an increase in the volume of 1-UN until 500 µL indicating that maximum extraction of the analyte was achieved at that volume. A further increase in volume resulted in a downward trend in response due to analyte dilution (Figure 23). As a result, 500 µL was chosen as the optimal volume of extraction solvent.

Figure 23.

Volume of extraction solvent.
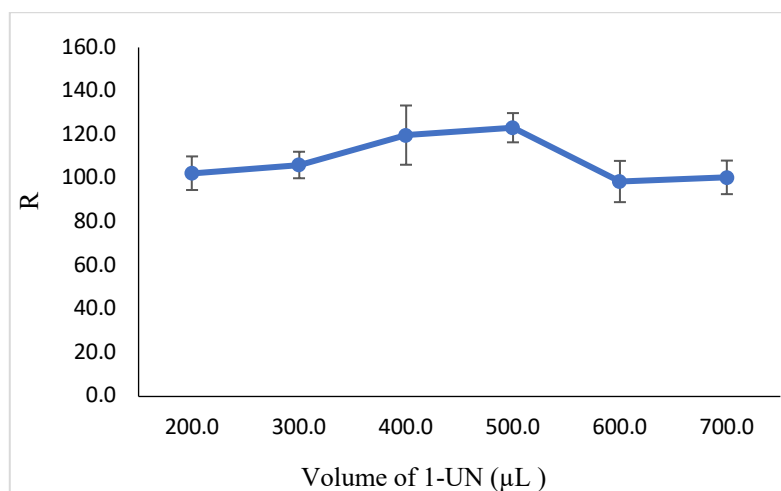
Type and volume of the disperser solvent

The disperser solvent in SFOD-DLLME serves to increase the area of contact between the extraction solvent and the aqueous sample solution, which are normally immiscible with each other, to improve extraction efficiency. The ideal disperser solvent should be miscible with both the extraction solvent and the aqueous sample solution. The effect of disperser solvent type on response was investigated using EtOH, MeOH, ACN, and ACT at a constant volume of 1.0 mL. Except for ACT, which had a lower response, all solvents showed a similar response (Figure 24). Because it is less toxic than the others, EtOH was chosen as the optimum disperser solvent.

Figure 24.

Type of disperser solvent.
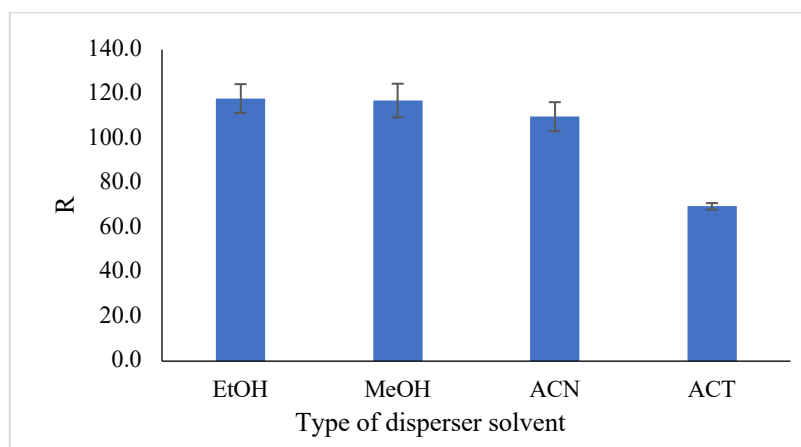
The effect of EtOH volume on response was investigated, with a range of 0.5 to 3.0 mL considered. An initial uptrend in the response was observed with an increase in the volume of EtOH until a volume of 1.5 mL was reached before a downtrend in the response was observed with subsequent increase in the volume of EtOH (Figure 25). The decrease in response could be attributed to an increase in iodine solubility in aqueous solution as EtOH concentration increases. The optimal volume of disperser solvent was determined to be 1.5 mL of EtOH.

Figure 25.

Volume of disperser solvent.
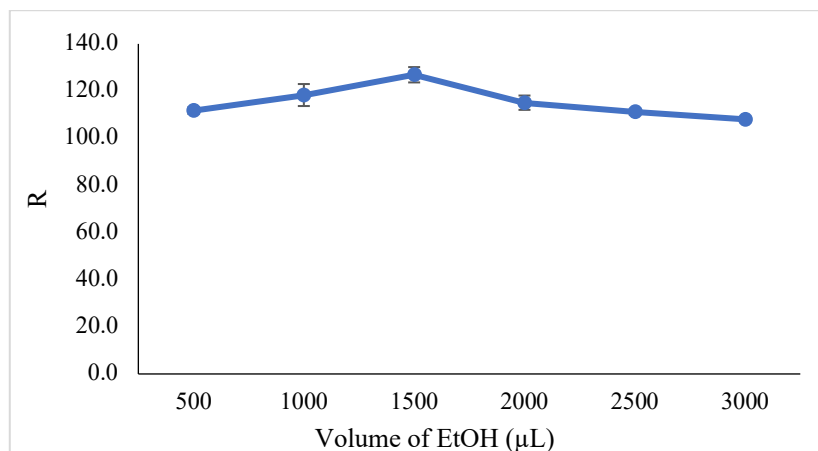
Extraction time

The effect of extraction time on the response, defined in SFOD-DLLME as the interval of time between the addition of the extraction and disperser solvent mixture prior to centrifugation, which is equivalent to the vortex time in this case, was investigated over a time range of 0 to 40 s. An uptrend in the response was observed until 20 s, when a constant trend was observed, indicating that maximum equilibrium had been reached at 20 s. (Figure 25). As a result, 20 s was chosen as the optimal extraction time.

Figure 26.

Extraction time.
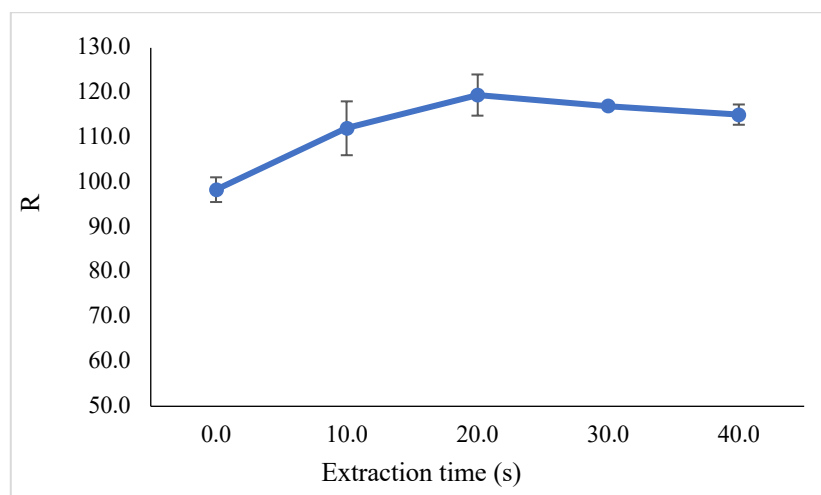
Analytical performance of solidification of floating organic drop-dispersive liquid-liquid microextraction

To evaluate the analytical performance of the proposed method, an external aqueous calibration graph was plotted using the standard of iodate ions in the concentration range of 10.0 to 300.0 µmol L^{-1} and applying the redox reaction alone prior to SDIC without microextraction. Furthermore, prior to using the SDIC-SFOD-DLLME method to plot standard addition calibration graphs, samples of iodized and non-iodized salt were spiked with iodate ions in the range of 0.5 to 20.0 µmol L^{-1}. Table 4 summarizes the data obtained, which shows acceptable performance highlighted by good linearity obtained for all calibration graphs with coefficients of determination (R^2) ranging from 0.9954 to 0.9997. The precision of the method is shown as a percentage relative standard deviation (%RSD) with intra- and interday precision between 1.2 to 3.8 and 2.4 to 5.6 respectively. The limit of detection (LOD) calculated using the equation $3S_b/m$, where S_b represents the standard deviation of the signal of the blank and m represents the slope of the calibration graph was 0.1 µmol L^{-1} (0.2 µg g^{-1}), while the limit of quantitation (LOQ) calculated using the equation $10S_b/m$ was between 0.2 to 0.4 µmol L^{-1}. A linear response was obtained from

the LOQ to 20.0 µmol L^{-1}. The calculated EFs ranged from 17.4 to 25.0 based on the ratio of the slope of the calibration graph with SFOD-DLLME-SDIC to the slope of the calibration graph with SDIC alone.

Table 4.

Figures of merit for SFOD-DLLME-SDIC for iodate in table salt samples.

Method	Sample[a]	Regression equation[b]	R^2	%RSD[c] Intraday	%RSD[c] Interday	LOD[d]	LOQ[e]	LDR[f]	EF[g]
SDIC	Aq.	$y = 0.44\,(\pm0.01)\,x + 0.54\,(\pm0.44)$	0.9997	1.3	2.6	2.0	6.7	6.7-300.0	-
SFOD-DLLME-SDIC	TS1	$y = 7.67\,(\pm0.10)\,x + 107.9\,(\pm1.20)$	0.9981	2.4	3.8	0.1 (0.2 µg g^{-1})	0.3	0.3-20.0	17.4
	TS2	$y = 8.18\,(\pm0.15)\,x + 108.7\,(\pm2.00)$	0.9954	3.8	5.6	0.1	0.4	0.4-20.0	18.6
	TS3	$y = 11.02\,(\pm0.10)\,x + 1.8\,(\pm1.20)$	0.9990	1.2	2.4	0.1	0.2	0.2-20.0	25.0
	TS4	$y = 7.67\,(\pm0.11)\,x + 2.0\,(\pm1.33)$	0.9976	3.0	4.5	0.1	0.3	0.3-20.0	17.4
	TS5	$y = 8.79\,(\pm0.13)\,x + 3.5\,(\pm1.65)$	0.9972	2.6	4.1	0.1	0.3	0.3-20.0	20.0
	TS6	$y = 10.82\,(\pm0.20)\,x - 1.9\,(\pm2.44)$	0.9959	3.4	5.0	0.1	0.4	0.4-20.0	24.6
	TS7	$y = 8.67\,(0.16)\,x + 87.7\,(\pm2.00)$	0.9957	2.9	4.5	0.1	0.4	0.4-20.0	19.7

[a] Aq.: Aqueous, TS: Table salt.

[b] $R = \text{slope}(\pm SD) \times [\text{iodate concentration (µM)}] + \text{intercept}(\pm SD)$.

[c] Percentage relative standard deviation, $n = 3$.

[d] Limit of detection (µmol L^{-1}).

[e] Limit of quantitation (µmol L^{-1}).

[f] Linear dynamic range (µmol L^{-1}).

[g] Enrichment factor: Ratio of calibration slope with SFOD-DLLME-SDIC to that with SDIC.

Recovery studies and determination of iodate in table salt

To investigate the possibility of a matrix effect, addition-recovery tests were carried out by spiking samples of table salt with iodate at three concentrations (7.5, 15.0, and 20.0

µmol L^{-1}) and using the SFOD-DLLME-SDIC method. The percentage relative recovery (% RR) shown in Table 4.2 was between 89.3 and 109.3. ANOVA test was used to evaluate the matrix effect by comparison of the slopes of the standard addition calibration graphs presented in Table 4 with $P < 0.05$ indicating statistically significant difference between them and revealing that there is indeed matrix effect, necessitation the need for using standard-addition calibration method in order to eliminate the matrix effect. Iodate was detected in two of the table salts samples with a concentration of 30.0 and 28.0 $\mu g\ g^{-1}$ (Table 5).

Table 5.

Percentage relative recovery of iodate from table salt.

Sample[a]	Added (µmol L^{-1})	Found (µM)	%RR[b]
TS1	-	0.4 (30.0 µg g^{-1})	-
	7.5	7.1	89.3
	15.0	15.1	98.0
	20.0	20.3	99.5
TS2	-	0.4 (29.1 µg g^{-1})	-
	7.5	8.1	108.0
	15.0	14.8	98.7
	20.0	19.6	98.0
TS3	-	<LOD	-
	7.5	7.5	100.0
	15.0	15.0	100.1
	20.0	19.8	99.0
TS4	-	<LOD	-
	7.5	8.1	108.0
	15.0	14.7	98.0
	20.0	20.0	100.0
TS5	-	<LOD	-
	7.5	8.2	109.3
	15.0	15.0	100.0
	20.0	19.8	99.0
TS6	-	<LOQ	-
	7.5	7.7	100.0
	15.0	14.4	94.7
	20.0	20.6	102.0
TS7	-	0.4 (28.0 µg g^{-1})	-
	7.5	7.7	97.3
	15.0	14.8	96.0
	20.0	21.0	103.0

[a] TS: Table salt.

[b] Percentage relative recovery, a value obtained considering extraction yields from standard-addition calibrations.

Comparison of the proposed SFOD-DLLME-SDIC method with other methods

The proposed method's accuracy was tested using an independent study with UV/Vis. The performance of both methods was comparable in terms of LODs, LOQs, R^2, and %RSD (Table 6). Nonetheless, the proposed SFOD-DLLME-SDIC method is significantly less expensive than the UV/Vis method. Furthermore, the iodate concentrations obtained by both techniques were statistically compared, revealing good agreement ($p>0.05$). Furthermore, the proposed SFOD-DLLME-SDIC was compared to those found in the literature for determining iodate in table salt by taking variables such as analysis time, sensitivity, linearity, and repeatability into account. The proposed method's major advantages over others include its speed, ease of use, and low cost. In terms of speed, the analysis took 12 min total, including dissolution, redox reaction, microextraction, and detection, which is much faster than most methods in the literature (Table 6). comparable sensitivity was obtained with conductivity detection (Kumar et al., 2001), gas chromatography-thermal conductivity detection (GC-TCD) (Xie et al., 2019), and ion chromatography with ultra-violet detection (IC-UV) (Huang et al., 2013), nonetheless, less sensitivity compared with fluorescence probes with cadmium sulphide quantum dots (CdS-QDs) (Tan et al., 2010), and capillary zone electrophoresis (CZE) (Wang et al., 2009). However, these methods require much more capital investment, tedious procedures, and sophisticated experience.

Table 6.

Comparison of SDIC-SFOD-DLLME with other methods for the determination of iodate in table salt.

Extraction method/ technique[a]	Analysis time (min)	LOD[b] ($\mu g\ mL^{-1}$)	LOQ[c] ($\mu g\ mL^{-1}$)	R^2	%RSD[d]	Ref.
GC-TCD	40	0.014	0.047	0.9990	1.09-2.69	(Xie et al., 2019)
CdS-QDs	30	0.00105	0.0035	0.9987	-	(Tan et al., 2010)
IC-UV	25	0.046	0.152	0.9996	<2.1	(Huang et al., 2013)
Conductivity	16	0.5	1.667	-	-	(Kumar et al., 2001)
Amperometry	10	-	-	0.9994	5.23	(Jakmunee & Grudpan, 2001)
CZE	7	0.0035	0.012	0.9993	1.08-2.25	(Wang et al., 2009)
UV-Vis	7	0.10	0.2	0.9970	3.2	This study
SFOD-DLLME-SDIC	12	0.10	0.3	0.9970	3.6	

[a] GC-TCD: gas chromatography-thermal conductivity detection; CdS-QDs: Cadmium sulphide quantum dots as fluorescence probes; IC-UV: Ion chromatography with ultraviolet detection; CZE: Capillary zone electrophoresis; UV/Vis: Ultraviolet-visible spectrophotometry.

[b] Limit of detection.

[c] Limit of quantitation.

[d] Percentage relative standard deviation.

Supramolecular Solvent Liquid-Liquid Microextraction Combined with Smartphone Digital Image Colorimetry for The Determination of Curcumin in Food Samples

The following section discusses the various optimizations that were performed for the optimization of the SMS-LLME-SDIC conditions for the determination of curcumin in food samples.

Optimization of smartphone digital image colorimetry conditions

Construction of the colorimetric box

A few modifications were made in the construction of the colorimetric box from the previous study. This was necessary because unlike in the previous study where a specific reaction was possible for derivatizing the analyte in the form of a specific redox reaction for iodate thereby eliminating possible interferences, in this study there was no such reaction the consequence of which spectral interference was observed from preliminary experiments when the previous design and setup of the colorimetric box was used and compared with two independent studies using UV/Vis and HPLC. When the proposed SMS-LLME-SDIC method was compared to the two independent studies, a positive error was observed, and statistical analysis revealed a significant difference ($P <$ 0.05). This necessitated the modification of the colorimetric box in order to eliminate spectral interference.

The same aluminum box with the same dimensions was used as the previous study however, the interior was painted black to further reduce scattering and reflections. In addition, the battery-powered LED lamp which is a continuum source was replaced with a unicolored backlight of another smartphone screen illuminating light that is equivalent to the λ_{max} of curcumin (428 nm) serving as a monochromatic source (Figure 27.). This

modification improved the detection method's sensitivity and selectivity while also extending its linear dynamic range.

Other improvements that were observed included an increase in the blank value (253±2), which is close to the ideal value of 255 in comparison to the previous study, which obtained a blank value of 180±2. Furthermore, sample throughput was increased because up to three cuvettes could be captured at the same time due to the monochromatic light source placed directly behind the cuvettes, resulting in uniform illumination of the cuvettes. This also ensures that the blank and sample are captured at the same time, which helps to eliminate spectral interferences. Furthermore, smartphone batteries are of higher quality than LED batteries, which prevents the light intensity from fluctuating as it did in the case of the LED lamp as the batteries aged. Furthermore, unlike most lamps, the brightness of the smartphone backlight can be controlled as needed by the method, as opposed to the LED lamp, which has a fixed brightness.

Figure 27.

The colorimetric box with monochromatic light source.
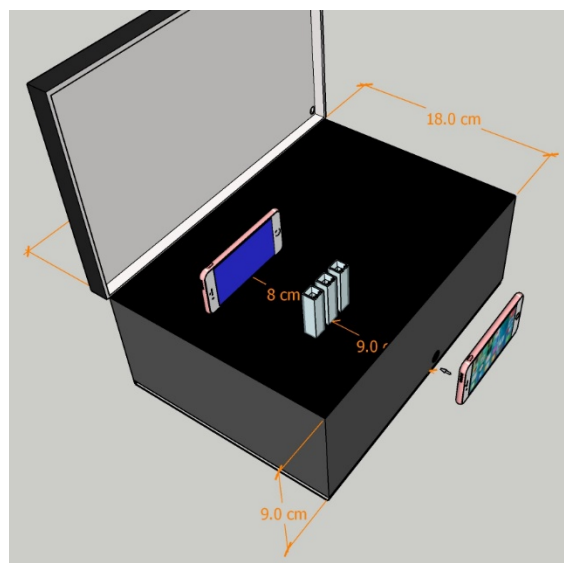
RBG channel selection and data processing method

By splitting the RBG channels, the most intense channel as revealed by the mean values of the histogram of each channel can be chosen for the entire experiment, making this step one of the first and most important. The B channel provided the highest intensity for this study and was used throughout.

The use of minus absorbance for quantitation distinguishes SDIC from other absorption techniques because in the RGB model, the mean histogram values assigned to colors range from 0 to 255, with white having a value of 255 and absolute black having a value of 0. As a result, as the analyte concentration increases linearly with the analyte's color intensity, the mean value of a specific RGB channel decrease. Consequently, the blank has a higher value than the analyte. Thus, minus absorbance is used to obtain a positive slope in the calibration curve.

Position of the sample holder and distance between the sample holder and camera

The absorbance can be measured from two angles: the top or the side of the colorimetric box. If the top position is chosen, the sample cuvette must be placed directly on top of the monochromatic light source. This is only possible if the bottom of the cuvette is completely transparent to visible light, which most cuvettes are not. This means that the most practical option is to measure the sample from the side, in which case the sample cuvette can be placed between two smart phones, one serving as the monochromatic light source and the other for photographing.

The camera's autofocus plays a significant role in photo quality. The model of the camera, focus settings, lenses, light intensity, the target image (sample in this case), contrast, size, and movement of the camera are all factors that can affect autofocus (Zhang et al., 2018). These variables are interdependent; in a situation where they are constant, the

distance between the camera and the sample will be the most important factor influencing autofocus. The sample cuvette's distance from the detection camera was optimized between 4.0 and 12.0 cm. The response showed an uptrend from 4.0 to 9.0 cm before becoming constant (Figure 29), indicating that there is a minimum distance required for autofocus. As a result, 9.0 cm was determined to be the optimal distance between the sample and the detection camera and was used for subsequent analysis.

Figure 28.

Distance between sample holder and camera.
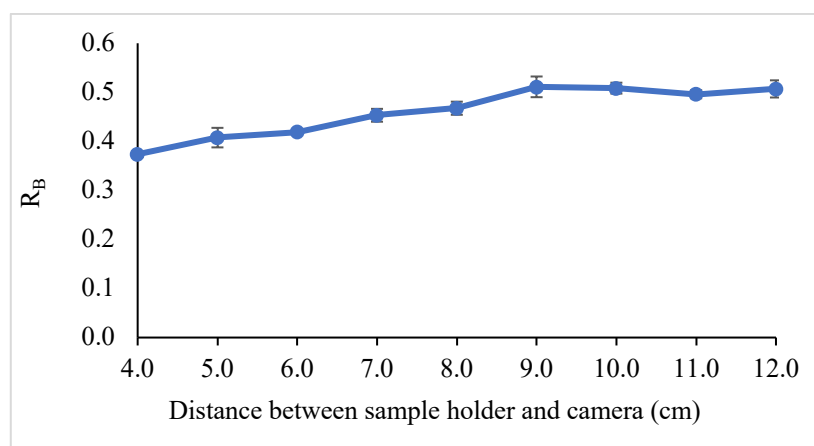
The region of interest

The cropped area selected by the ImageJ program for measurement while ignoring other parts of the image is the region of interest (ROI) measured in px^2. If the solution is homogeneous, the standard deviation of the mean of the histogram will be low, resulting in better repeatability. To optimize the ROI, the cropped area was varied between 900 and 6400 px^2 within the image's sample zone, as expected. Because of the homogeneity of the sample solution, which resulted in uniform color, a consistent trend in the response was observed (Figure 29). This means that any ROI can be used without influencing the response. For subsequent experiments, the optimal ROI was determined to be 1600 px^2.

Figure 29.

Selection of region of interest.
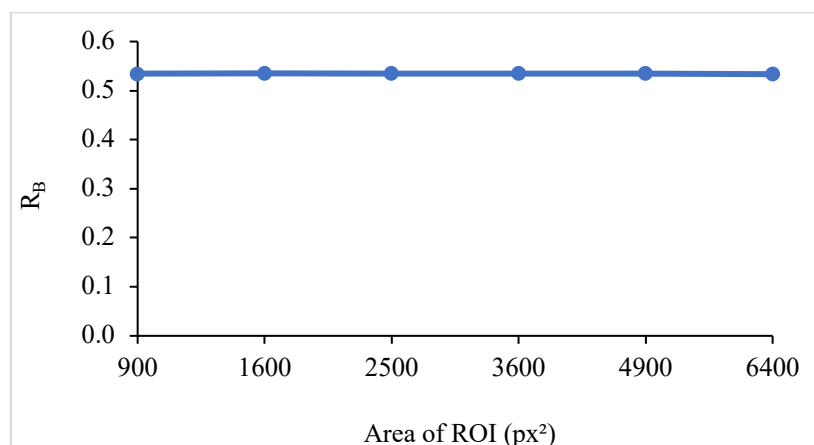
Brightness of the monochromatic light source

The brightness of the monochromatic light source plays a major role in the response because it affects absorption, saturation of the detection camera and autofocus. To carry out the optimization, the intensity of bright colors was reduced in the iOS smartphone by going to settings, accessibility, display and text size, and checking the option "reduce white point" as well as selecting 100% to eliminate bright colors. Furthermore, because no such scale exists in the device, a scale was designed on the screen to divide the brightness into percentages. A negative response trend was observed as the brightness of the monochromatic light source increased (Figure 30), which could be attributed to the detection camera's specifications. However, below 15% brightness, a dark image was captured, making quantitation impractical. As a result, the optimum brightness of the monochromatic light source was determined to be 15%.

Figure 30.

Brightness of the monochromatic light source.
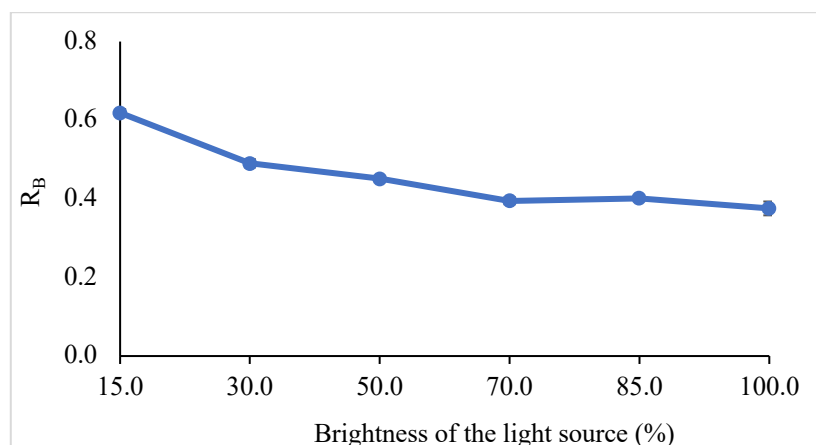
Optimization of supramolecular solvent liquid-liquid microextraction conditions

The microextraction conditions were optimized using a tea sample void of the analyte by spiking the sample at 25.0 µg mL^{-1} of curcumin standard to match the matrix.

Type of extraction solvent

The number of amphiphiles present in the aqueous solution influences SMS extraction efficiency. The greater the concentration of amphiphiles, the greater the extraction efficiency. (Ballesteros-Gomez et al., 2010). To study the effect of the type of SMS on extraction efficiency, a combination of THF with 1-UN, 1-DO and a mixture of 1-UN:1-DO; 1:1 (v/v). Maximum response was observed with THF/1-UN SMS followed by THF/1-UN/1-DO and finally, THF/1-DO (Figure 31.). This behavior is consistent with the general rule of SMS involving reversed micelles, which states that amphiphile concentration is inversely proportional to the length of the alcohol's alkyl chain (Ballesteros-Gomez et al., 2010). Because 1-UN has a shorter alkyl chain than 1-DO, the concentration of amphiphile in THF/1-UN is the highest among the SMS combinations studied. As a result, THF/1-UN was chosen as the optimal SMS.

Figure 31.

Type of supramolecular solvent.
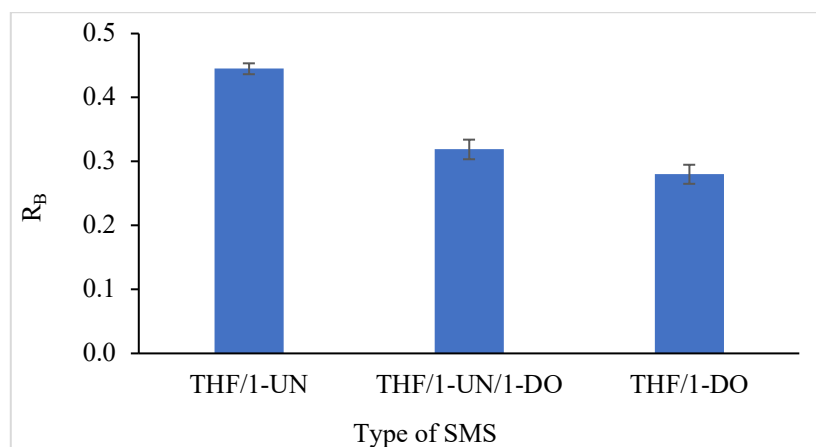
Composition of supramolecular solvent

SMS can tune their physiochemical properties such as polarity by varying the volume ratio of the two solvents until the desired polarity is achieved. The effect of the SMS volume ratio on extraction efficiency was investigated by varying the volume ratio of THF:1-UN from 2.0 to 5.5. The response initially showed an uptrend as the volume ratio was increased up to point 4.0 before becoming relatively constant at point 4.5 and finally showing a downtrend beyond that point (Figure 32). Consequently, the optimum volume ratio of THF:1-UN was determined to be 4.0.

Figure 32.

Composition of supramolecular solvent.
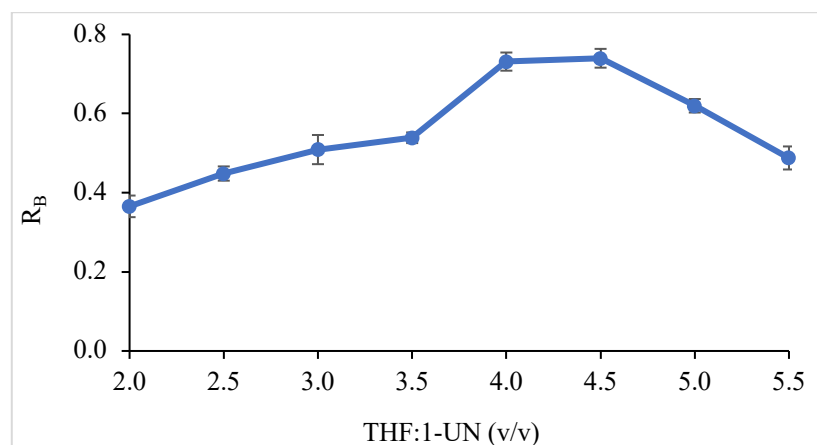
Sample pH

The pH of the solution influences both the formation of SMS and the chemical structure of the analyte. The neutral form of curcumin will exist in aqueous solution at a pH level below its pK_{a1} (8.8) whereas its ionized form will be present at higher pH. The effect of sample pH on extraction efficiency was investigated from pH 2.5 to 9.5. The response showed an initial uptrend as the pH was raised to pH 7.0, followed by a gradual decrease (Figure 33). This could be because the neutral form of curcumin has a higher affinity for the extraction solvent than the ionized form, which has a stronger affinity for the aqueous phase. Consequently, pH 7.0 was chosen as the optimal pH for further investigation.

Figure 33.

Sample pH.
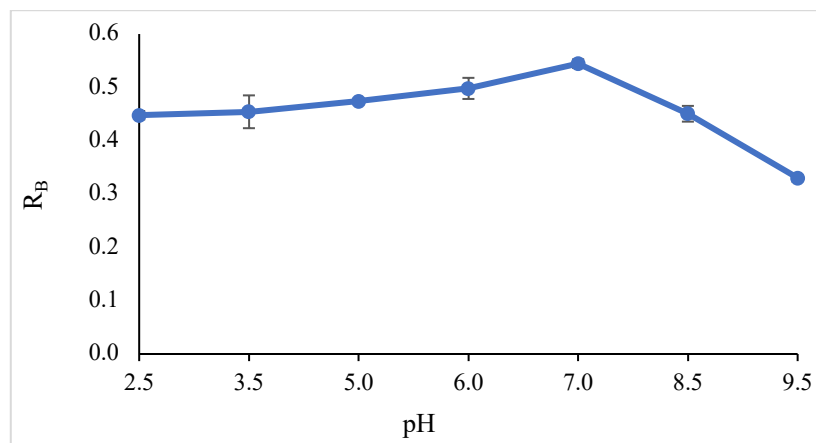
Ionic strength

The addition of salt in the sample solution can affect extraction efficiency by the salting-out effect, which could lead to elevation in polarity of the aqueous solution, thereby increasing the affinity of the analyte towards the hydrophobic extraction solvent. Nevertheless, higher concentration of salt could decrease miscibility of the two phases thereby decreasing the interaction of the analyte with the extraction solvent leading to lower extraction efficiency, therefore, the proper concentration of salt is required to avoid both extremes. The effect of ionic strength was studied by varying the concentration of NaCl between 0.0 to 4.0 %w/v. An initial uptrend was observed in the response with increase in the concentration of NaCl until 2.0% (w/v), where a constant response was observed (Figure 34.). Therefore, 2.0%w/v of NaCl was taken as the optimum extraction solvent.

Figure 34.

Ionic strength.
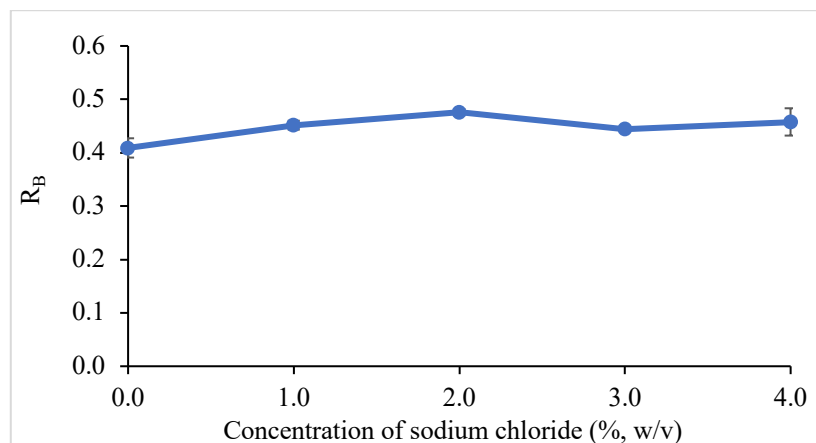
Extraction time

Mechanical agitation of the analyte in the form of a vortex can help with analyte extraction by shortening the equilibrium time for the analyte to be extracted into the extraction phase. By varying the vortex time from 0 to 120 s in 30 s increments, the effect of extraction time was investigated. An uptrend in the response was observed with increasing vortex time until 60 s, when the trend became constant, indicating that equilibrium has been reached and increasing the time has no significant effect on extraction (Figure 35). As a result, 60 s were chosen as the optimal extraction time.

Figure 35.

Extraction time.
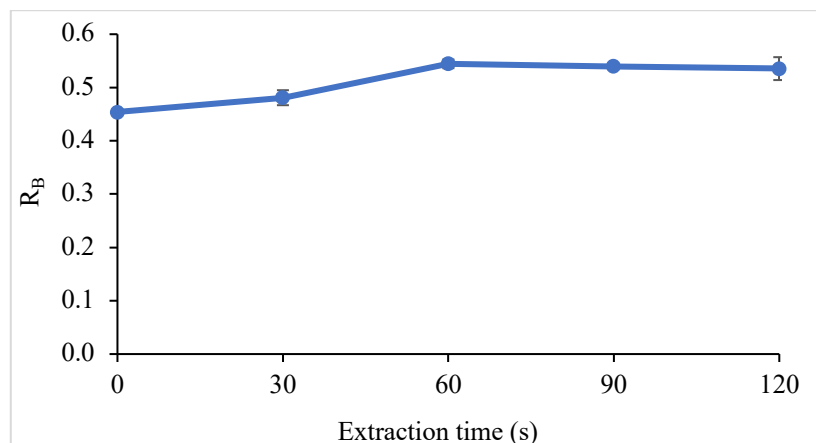
Figures of merit for SMS-LLME-SDIC

Standard addition calibration graphs were plotted by spiking the samples with standard of curcumin between the range of 3.0 to 25.0 $\mu g\ mL^{-1}$ and applying the SMS-LLME-SDIC procedure to evaluate the analytical performance of the method. The summary of the result shown in Table 7 shows good linearity with R^2 between 0.9965 to 0.9995, the method's precision based on %RSD for intra- and interday precision were in the range of 1.8 to 4.3 and 2.2 to 8.5% respectively. The LOD calculated using the equation $3S_b/m$, where S_b is the standard deviation of the intercept and m is the slope of the regression equation was between 0.2 to 0.9 $\mu g\ mL^{-1}$, whereas the LOQ calculated using the equation $10S_b/m$, was between 0.8 to 3.0 $\mu g\ mL^{-1}$. The linearity started from the LOQ to 25.0 $\mu g\ mL^{-1}$.

Table 7.

Figures of merit for SMS-LLME-SDIC for turmeric and tea samples.

Method	Sample	Regression equation[a]	R^2	LOD[b]	LOQ[c]	LDR[d]	%RSD[e] Intraday	Interday
UV/Vis	Aqueous standards	$y = 0.13\ (\pm 1.0 \times 10^{-3})x + 0.01\ (\pm 1.0 \times 10^{-2})$	0.9986	0.2	0.8	0.8-15.0	1.8	2.2
SMS-LLME-SDIC	Aqueous standards	$y = 0.03\ (\pm 2.0 \times 10^{-4})x - 0.01\ (\pm 2.0 \times 10^{-3})$	0.9989	0.2	0.6	0.6-25.0	1.9	3.5
	Tumeric 1	$y = 0.01\ (\pm 2.0 \times 10^{-4})\ x + 0.15\ (\pm 2.0 \times 10^{-3})$	0.9974	0.6	2.0	2.0-25.0	2.6	4.6
	Tumeric 2	$y = 0.01\ (\pm 2.0 \times 10^{-4})\ x + 0.3\ (\pm 3.0 \times 10^{-3})$	0.9965	0.9	3.0	3.0-25.0	3.9	8.4
	Tea 1	$y = 0.02\ (\pm 2.0 \times 10^{-4})\ x + 0.1\ (\pm 3.0 \times 10^{-3})$	0.9966	0.5	1.5	1.5-25.0	4.3	8.5
	Tea 2	$y = 0.02\ (\pm 3.0 \times 10^{-4})\ x + 0.01\ (\pm 4.0 \times 10^{-3})$	0.9976	0.6	2.0	2.0-25.0	2.1	5.8
	Tea 3	$y = 0.02\ (\pm 1.0 \times 10^{-4})\ x + 0.01\ (\pm 1.6 \times 10^{-3})$	0.9995	0.2	0.8	0.8-25.0	2.0	4.6

[a] $R_B = \text{Slope}(\pm SD) \times [\text{Curcumin concentration } (\mu g\ mL^{-1})] + \text{intercept}(\pm SD)$.

[b] Limit of detection ($\mu g\ mL^{-1}$).

[c] Limit of quantitation ($\mu g\ mL^{-1}$).

[d] Linear dynamic range ($\mu g\ mL^{-1}$).

[e] Percentage relative standard deviation, $n = 3$.

Recovery studies and determination of curcumin in turmeric and tea samples

To assess the possibility of matrix effect, addition-recovery tests were carried out by spiking the samples with curcumin standard at three concentration levels (5.0, 15.0 and 25.0 $\mu g\ mL^{-1}$) prior to applying the proposed SMS-LLME-SDIC procedure. The %RR were between 94.0 to 104.0% (Table 8). The ANOVA test was used to compare the slopes of the standard addition calibration curves to evaluate the matrix effect. The result revealed a statistically significant difference ($P < 0.05$) necessitating the use of the standard addition method to eliminate it. Curcumin was found in two turmeric samples at concentrations of

2.3 and 4.1 % (w/w), as well as one tea sample at 1.8 % (w/w). Curcumin could not be detected in the other samples because their levels were lower than the method's LOD. To assess the accuracy of the proposed method, an independent study was conducted using UV/Vis and statistically comparing the concentration of curcumin obtained by both methods. Both methods produced good statistical agreement ($P > 0.05$).

Table 8.

Percentage relative recovery of curcumin in turmeric and tea samples.

Sample	Added (μg mL^{-1})	Found (μg mL^{-1})	%RR[a]
Tumeric 1	-	11.5 (2.3%, w/w)	-
	5.0	5.0	100.0
	15.0	15.1	100.7
Tumeric 2	-	20.3 (4.1%, w/w)	-
	5.0	5.1	102.0
	15.0	15.0	100.0
Tea 1	-	9.1 (1.8%, w/w)	-
	5.0	5.2	104.0
	15.0	14.5	96.7
Tea 2	-	<LOD	-
	5.0	5.0	100.0
	15.0	15.0	100.0
	25.0	25.2	100.8
Tea 3	-	<LOD	-
	5.0	4.7	94.0
	15.0	14.8	98.7
	25.0	25.0	100.0

[a] Percentage relative recovery, a value obtained considering extraction yields from standard-addition calibrations.

Comparison of the proposed SMS-LLME-SDIC with other methods

The method's performance was first compared to that of the UV/Vis method. Both methods performed similarly in terms of analysis time, total volume of organic solvent used per sample, sensitivity, precision, and linearity (Table 9). The proposed method, on

the other hand, requires far less capital investment, portability, and reliance on electricity than UV-Vis. When compared to other methods found in the literature for determining curcumin in food samples, the proposed method demonstrated comparable and, in some cases, superior performance, such as having the shortest analysis time and the least volume of organic solvent used per sample, in addition to simplicity and low cost, which is especially important for laboratories located in low-income countries. Other methods provided better sensitivity (Table 9) with the disadvantage of longer analysis time, larger volumes of organic solvent, and much higher acquisition and maintenance costs, demonstrating that the proposed method is a much faster, greener, and more affordable alternative.

Table 9.

Comparison of the proposed SMS-LLME-SDIC method with other methods for the determination of curcumin in food samples.

Extraction method/ Technique[a]	Sample	Analysis time (min)	Vorg.[b] (µL)	LOD[c] (µg mL^{-1})	R^{2d}	%RSD[e]	Ref.
SPE-CE-AD	Turmeric	1210	250000	0.01	0.9986	6.3	(Sun et al., 2002)
SE-VA-DES-ME-UV/Vis	Spice, tea, cinnamon, sesame	>30	~100000	0.0015	0.9967	4.3	(Altunay et al., 2020)
UA-IL-DLLME-UV/Vis	Different foods	23	4575	0.0005	0.9995	4.3	(Unsal et al., 2019)
VA-DES-ELLME-UV/Vis	Turmeric, tea	8	1800	2	0.9994	1.8	(Aydin et al., 2018)
SLE-DIC	Turmeric	~3	6000	0.48	0.9926	1.35	(Wongthanyakram et al., 2019)
SLE-UV/Vis	Turmeric, tea	3	1000	0.2	0.9986	2.2	This study
SMS-LLME-SDIC				0.6	0.9975	2.0-8.5	

[a] SPE-CE-AD: Solid-phase extraction-capillary electrophoresis-amperometric detection.

SE-VA-DES-ME-UV/Vis: Soxhlet extraction-vortex assisted-deep eutectic solvent microextraction-ultraviolet/visible spectrophotometry.

UA-IL-DLLME-UV/Vis: Ultrasound assisted-ionic liquid-dispersive liquid–liquid microextraction-ultraviolet/visible spectrophotometry.

VA-DES-ELLME-UV/Vis: Vortex assisted-deep eutectic solvent-emulsification liquid–liquid microextraction-ultraviolet/visible spectrophotometry.

SLE-DIC: Solid-liquid extraction-digital image colorimetry.

SLE-UV/Vis: Solid-liquid extraction-ultraviolet/visible spectrophotometry.

SMS-LLME-SDIC: Supramolecular solvent-liquid–liquid microextraction-smartphone digital image colorimetry.

[b] Total volume of organic solvents consumed per sample.

[c] Limit of detection.

[d] Coefficient of determination.

[e] Percentage relative standard deviation.

Dispersive Solid-Phase Microextraction Combined With Smartphone Digital Image Colorimetry for the Determination of Boron in Nuts

Optimization of smartphone digital image colorimetry conditions

Selection of the RGB channel

The intensity of the mean of the histogram of the channels in the RGB model varies depending on the color of the solution. When the image of the solutions was split into its RGB channels, the G channel had the highest intensity and was used for all analysis.

Selection of the wavelength of the monochromatic light source

The effect of the wavelength of the monochromatic light source was studied by generating the color equivalent of the wavelengths within the visible region of 500-600 nm, which is within the complementary color range of the red complex of the analyte. The maximum response was obtained at 575.0 nm, which was used as the wavelength of the monochromatic light source. (Figure 36).

Figure 36.

Scanning the wavelength of the monochromatic light source.
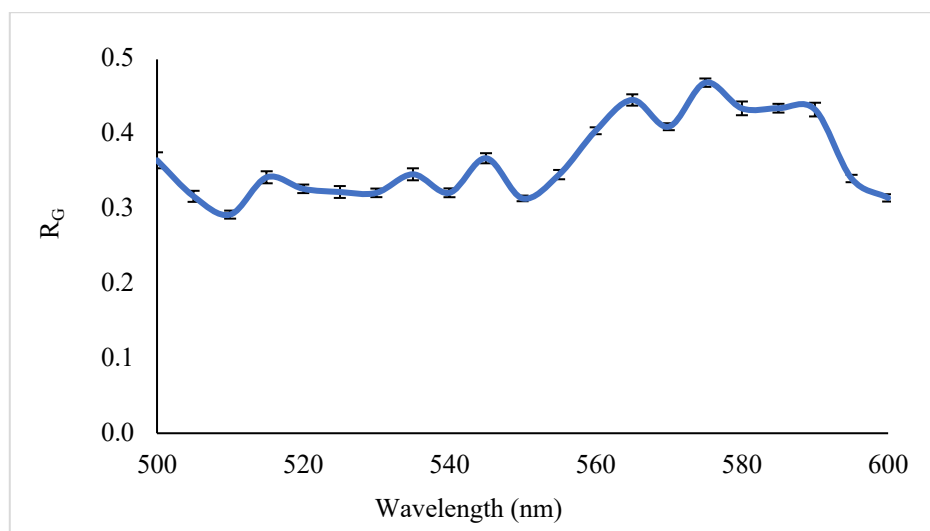
Region of interest and distance between the sample and detection camera

The effect of the ROI was studied within 900-6400 px^2. A constant response was obtained indication the homogeneity of the solution (Figure 37). Therefore, any ROI can be use, however, 1600 px^2 was selected for all analysis.

Figure 37.

Effect of ROI.
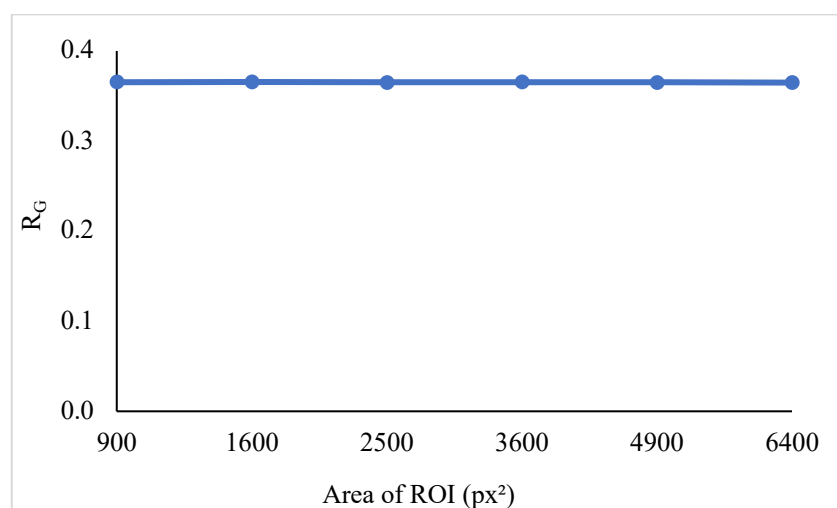
The distance between the sample holder and detection camera will have a significant effect on the autofocus performance of the camera if other variables such as lenses, light intensity, focus settings, size, contrast and motion of the camera are kept constant (Zhang et al., 2018). Hence, the effect of the distance between the sample holder and detection camera was studied between 7.0 to 12.0 cm (Figure 38). The highest response was obtained at 10.0 cm and was used for all analysis.

Figure 38.

Effect of the distance between the detection camera and sample.
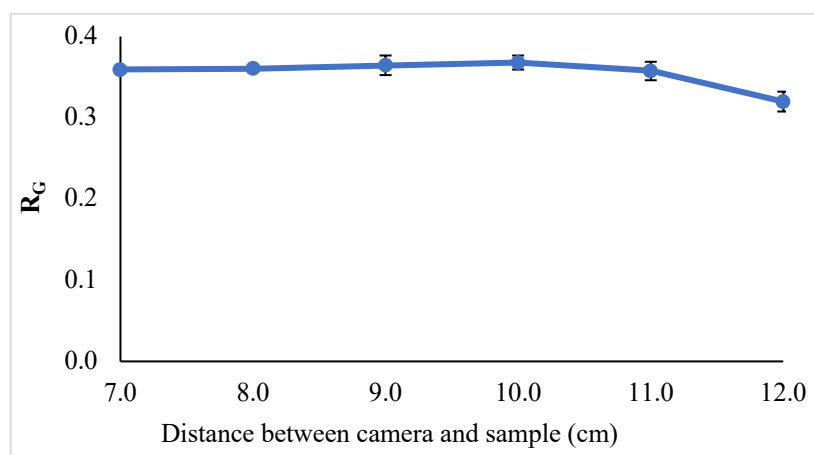
Optimization of complexation and dispersive solid-phase microextraction conditions

A standard solution of 2.0 µg mL^{-1} of boron was used for optimization using the one parameter at a time approach.

Complexation

The starting conditions for complexation were decided based on a previous study (Qin, 2013) by scaling down the amount of solvents used by a factor to minimize chemical waste and also reduce the evaporation time which will consequently reduce analysis time to abide to green analytical chemistry practices (Armenta et al., 2008). A, 100 µL of the

2.0 µg mL^{-1} of boron standard solution was collected into a porcelain evaporation dish and 400 µL of the curcumin reagent was added and evaporated to dryness at 55 °C. The solvent used for dissolution of the complex was optimized after cooling by taking 1.0 mL each of ACN, ACT, EtOH and MeOH prior to DSPME-SDIC. The highest response was obtained with MeOH (Figure 39) probably due to the high polarity of MeOH which is less selective towards the hydrophobic complex of the analyte causing the analyte to partition more strongly to the adsorbent during DSPME leading to higher recovery. Thus, MeOH was selected for all analysis.

Figure 39.

Effect of dissolution solvent.
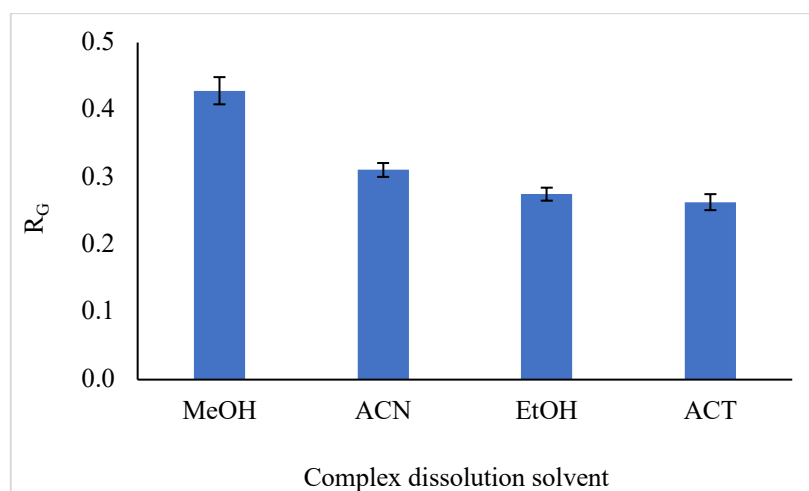
Thereafter, the volume of MeOH was optimized from 0.5 to 1.5 mL. The response had an initial increase from 0.5 mL up to 1.0 mL before decreasing probably due to the presence of excess organic solvent than necessary which will decrease the adsorption of the analyte during DSPME (Figure 40). Therefore, 1 mL of MeOH was selected and used for all analysis.

Figure 40.

Effect of the volume of MeOH dissolution of complex.
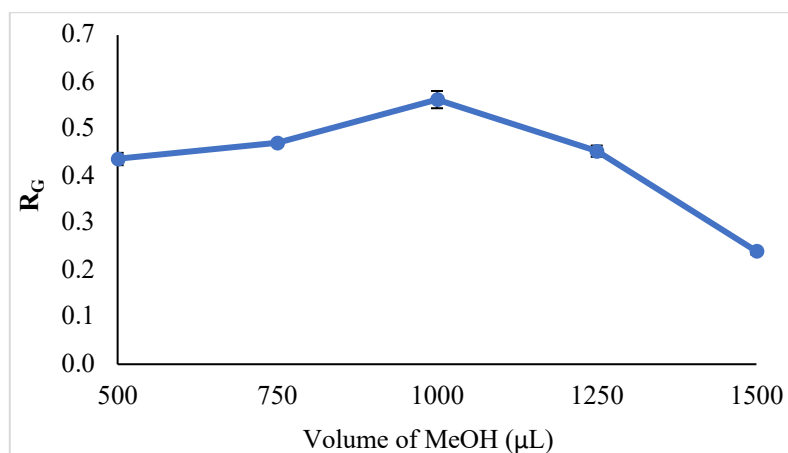
Sample pH and concentration of buffer

The pH of the sample has a significant effect on the extraction efficiency due to its effect on adsorption kinetic between the analyte and the adsorbent (Karlidag, Kocoglu, et al., 2020). The optimization study was carried out with 20 mg of ZrNPs as the adsorbent, and the elution solvent was ACN (100 µL). The pH of the solution was varied from pH 1.5 to 11.5. However, from pH 8.5 onwards, the solution became colorless and unquantifiable by SDIC probably due to instability of the complex at basic pH. The highest response was observed at pH 2.5 with phosphate buffer (Figure 41). Thus, pH 2.5 was selected as the optimum pH.

Figure 41.

Effect of the pH of the sample solution.
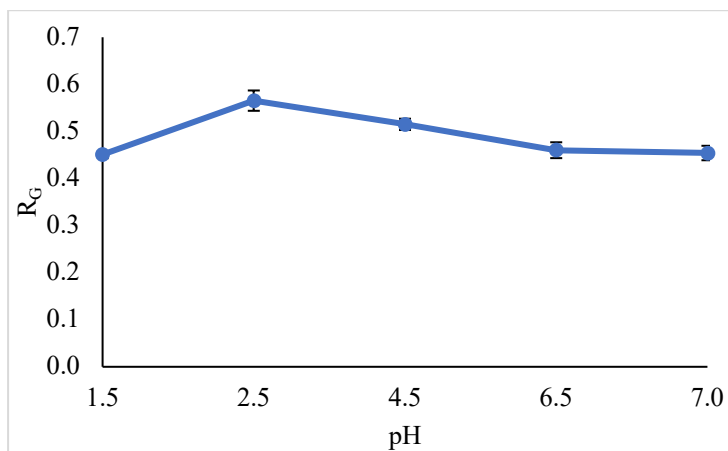
The concentration of the buffer was optimized from 10.0 to 100.0 mmol L^{-1}. The response increased up to 25.0 mmol L^{-1} concentration of the buffer before becoming constant (Figure 42). Therefore, 25.0 mmol L^{-1} of phosphate buffer (pH 2.5) was used for subsequent analysis.

Figure 42.

Effect of the concentration of the buffer.
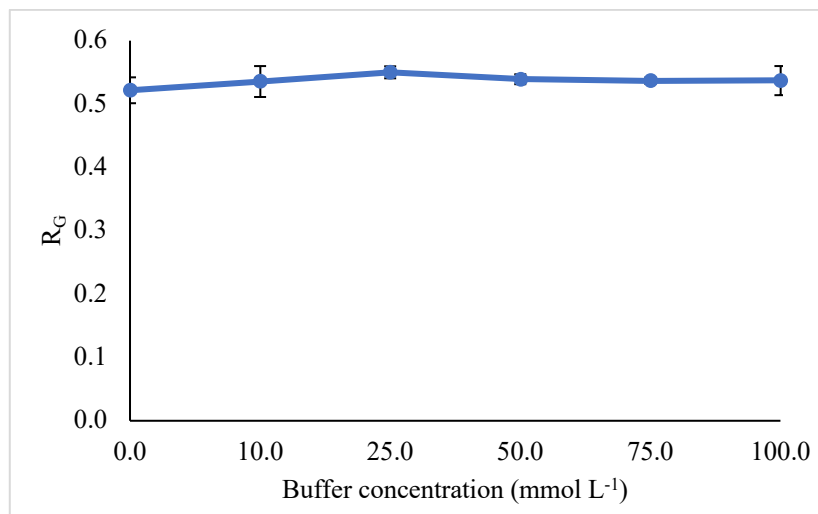
Amount of the adsorbent

The amount of adsorbent influences extraction efficiency because, depending on the adsorption capacity of the adsorbent, a minimum amount of adsorbent is required to adsorb the analyte present in the sample solution. Below this amount, the analyte recovery will be lower, whereas above the amount, a larger volume of eluent will be required to desorb the analyte, resulting in not only waste but also a decrease in the enrichment factor. The mass of ZrNPs was varied from 10.0 to 50.0 mg. The response increased with increase of adsorbent up to 30 mg before decreasing probably due to insufficient amount of the eluent for complete desorption of the analyte (Figure 43). Therefore, 30.0 mg of ZrNPs was used for subsequent analysis.

Figure 43.

Effect of the amount of adsorbent.
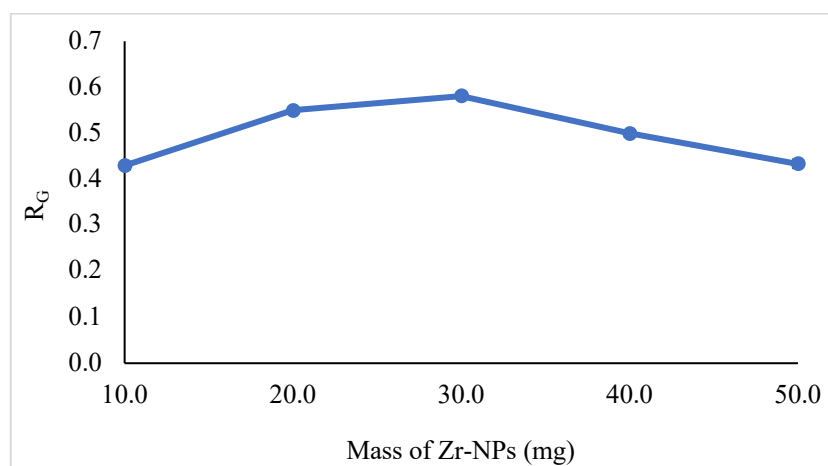
Type and volume of eluent.

The selectivity of the eluent towards the analyte will influence the desorption of the analyte from the surface of the adsorbent. The effect of the type of eluent was studied using 100 μL of the eluents (ACN, ACT, EtOH, MeOH, and THF). The highest response was observed with ACT and was selected as the optimum eluent (Figure 44).

Figure 44.

Effect of the type of eluent.
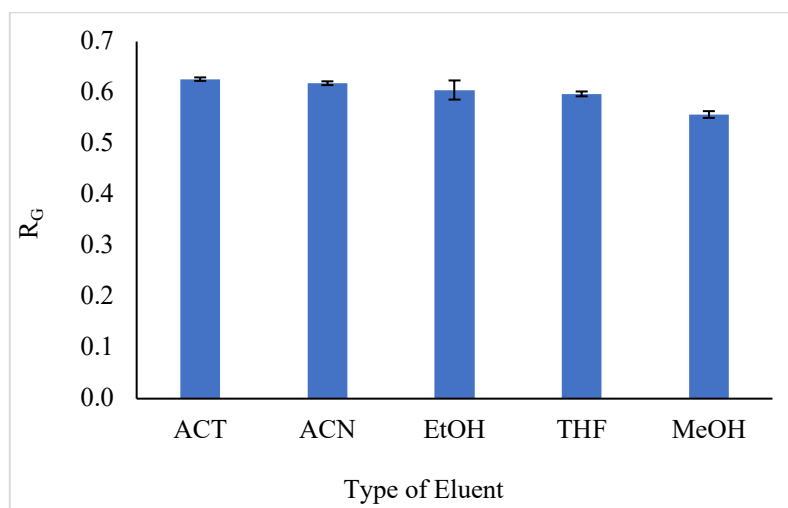
The effect of the volume of ACT was studied from 50 to 250 µL. The response increased with increase in volume of ACT up to 100 µL before decreasing probably due to the dilution of the analyte afterwards (Figure 45). Therefore, 100 µL of ACT was used for subsequent analysis.

Figure 45.

Effect of the volume of eluent.
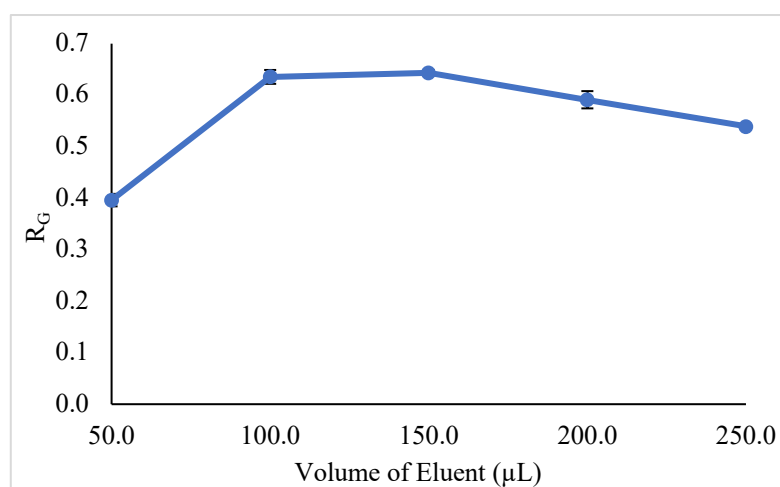
Adsorption and desorption time

The adsorption and desorption were evaluated as the period the solution is exposed to mechanical agitation by means of vortex. The effect of the adsorption time was studied within a vortex time of 0.5 to 4.0 min. The response increased with increase in vortex time up to 2.0 min when the response became constant indicating that adsorption equilibrium was achieved in 2.0 min (Figure 46).

Figure 46.

Effect of adsorption time.
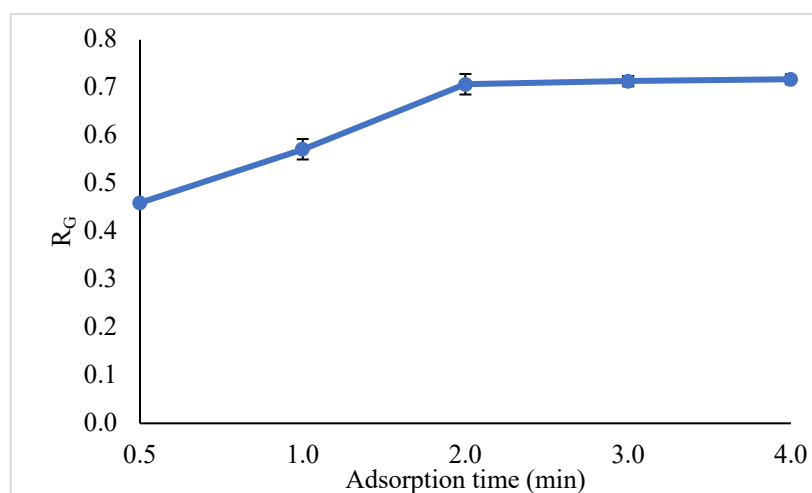
The desorption time was studied within 0.5 to 2.0 min. Maximum response was achieved at 1.0 min thereafter, the response was constant indicting that equilibrium amount of the analyte has been eluted from the surface of the adsorbent (Figure 47). Hence 1.0 min of desorption was used throughout the study.

Figure 47.

Effect of desorption time.
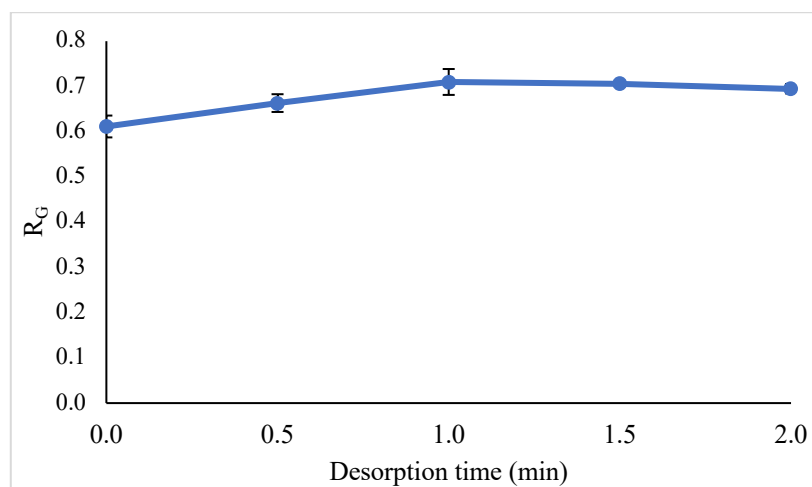
Analytical performance of DSPME-SDIC

Analytical performance of the method was assessed by plotting external aqueous calibration graphs by preparing standard concentration of boron between 0.3 to 2.5 µg mL^{-1} and complexing with the curcumin reagent prior to SDIC alone (Table 10). Furthermore, standard addition calibrations were plotted by spiking the samples with standard solutions of boron at concentrations of 0.2 to 4.0 µg mL^{-1} and applying the proposed DSPME-SDIC method (Table 1). The calibration graphs were linear with coefficient of determination (R^2) between 0.9954 to 0.9991. The method's precision was evaluated as percentage relative standard deviation (%RSD) with intra- and inter-day precision ranging from 0.83 to 4.92 and 2.68 to 6.77 respectively. The limits of detection (LOD) calculated using $3S_b/m$, where S_b is the standard deviation of the intercept and m is the slope of the regression equation, and limits of quantitation (LOQ), calculated as $10S_b/m$ were 0.08 and 0.26 µg mL^{-1} respectively. A linear response was obtained from LOQ to 4.0 µg mL^{-1}. The study conducted with UV/Vis spectrophotometry validated the accuracy of the method as concentrations of boron found in all samples with both techniques were in a good statistical agreement ($P > 0.05$) (Table 11).

Table 10.

Figures of merit of DSPME-SDIC for nuts.

Method	Sample	Regression equation[a]	R^2	LOD[b]	LOQ[c]	LDR[d]	%RSD[e] Intraday	%RSD[e] Interday
UV/Vis	Aqueous standards	$y = 0.22\ (\pm3.5 \times 10^{-3})x + 0.01\ (\pm4.3 \times 10^{-3})$	0.9966	0.06	0.20	0.2-2.0	3.90	5.75
SDIC	Aqueous standards	$y = 0.25\ (\pm4.2 \times 10^{-3})x - 0.02\ (\pm6.3 \times 10^{-3})$	0.9954	0.08	0.26	0.3-2.5	2.18	4.02
DSPME-SDIC	Almond	$y = 0.10\ (\pm1.7 \times 10^{-3})x + 0.10(\pm3.8 \times 10^{-3})$	0.9956	0.11	0.37	0.4-4.0	4.92	6.77
DSPME-SDIC	Hazelnut	$y = 0.11\ (\pm8.4 \times 10^{-4})\ x + 0.10\ (\pm1.9 \times 10^{-3})$	0.9991	0.05	0.17	0.2-4.0	1.53	3.37
DSPME-SDIC	Ivory	$y = 0.13\ (\pm2.1 \times 10^{-3})\ x + 0.13\ (\pm4.7 \times 10^{-3})$	0.9955	0.11	0.38	0.4-4.0	2.44	4.29
DSPME-SDIC	Peanut	$y = 0.13\ (\pm1.4 \times 10^{-3})\ x + 0.15\ (\pm3.1 \times 10^{-3})$	0.9981	0.07	0.24	0.2-4.0	2.28	4.12
DSPME-SDIC	Walnut	$y = 0.12\ (\pm2.0 \times 10^{-3})\ x + 0.05\ (\pm4.5 \times 10^{-3})$	0.9956	0.11	0.37	0.4-4.0	0.83	2.68

[a] Absorbance (mAu) $=$ Slope($\pm$SD) $\times$ [Boron concentration ($\mu g\ mL^{-1}$)] $+$ intercept($\pm$SD).

[b] Limit of detection (μg mL^{-1}).

[c] Limit of quantitation (μg mL^{-1}).

[d] Linear dynamic range (μg mL^{-1}).

[e] Percentage relative standard deviation, $n = 3$.

Recovery studies and determination of boron in nuts

The effect of matrix was evaluated using addition-recovery test by spiking samples of the nuts with known concentrations of boron (i.e., 0.5, 1.0 and 3.0 µg mL^{-1}) and applying the DSPME-SDIC method. The percent relative recoveries (%RR) calculated based on the extraction yields from standard addition calibrations were between the range of 91.04 to 105.56 (Table 11). The analysis of variance (ANOVA) test was used to evaluate the matrix effect by comparing the slopes of the standard-addition calibration graphs and aqueous calibration graphs (Table 10). A statistical significance difference was found between the slopes (P<0.05) indication matrix effect. Thus, standard addition calibration method was

employed to eradicate the effect. All samples of the nuts were found to contain boron between 10.67 to 28.05 µg g^{-1} of nut.

Table 11.

Percentage relative recoveries of boron from nut samples.

Sample	Added (µg mL^{-1})	Found (µg mL^{-1})	%RR[a]	Found (UV/Vis) (µg g^{-1})
Almond	-	0.96 (24.10 (±1.88)µg g^{-1})	-	25.03 (±0.75)
	0.50	0.51	101.3	
	1.00	1.04	104.4	
	3.00	2.90	96.6	
Hazelnut	-	0.86 (21.46(±0.83) µg g^{-1})	-	19.96 (±0.52)
	0.50	0.48	95.2	
	1.00	1.02	101.6	
	3.00	3.04	101.5	
Ivory	-	1.02 (25.62 (±1.94)µg g^{-1})	-	24.50 (±0.88)
	0.50	0.46	91.0	
	1.00	0.96	96.8	
	3.00	3.04	101.0	
Peanut	-	1.12 (28.05 (±1.29)µg g^{-1})	-	28.28 (±1.16)
	0.50	0.53	105.6	
	1.00	1.02	102.2	
	3.00	2.95	98.4	
Walnut	-	0.43 (10.10 (±0.77)µg g^{-1})	-	9.62 (±0.36)
	0.50	0.47	93.3	
	1.00	0.92	91.6	
	3.00	3.00	100.0	

[a] Percentage relative recovery, a value obtained considering extraction yields from standard-addition calibrations.

Comparison of the proposed DSPME-SDIC method with other methods

The proposed DSPME-SDIC method was first compared with an independent study with UV/Vis. Comparable analytical performance was observed in terms of volume of acid, organic solvent, LOD and %RSD (Table 12). However, the negligible cost, portability, and

limited reliance on electricity of SDIC compared to UV/Vis gives it an advantage. Comparison of the proposed method was also made with other methods in the literature reported for the determination of boron. Comparable LODs were obtained except for a method proposed with ICP-MS (Simsek & Aykut, 2007), and DLLME-ICP-MS (Chandrasekaran et al., 2013) that obtained superior LODs due to sophisticated instrumentation that comes at a substantial cost. The proposed method used comparable or lower volumes of organic solvent and acids combined as compared with the other methods making it generally environmentally friendly due to the absence of a digestion step that consumes large volumes of acids in addition to extending the overall analysis time. In general, the proposed DSPME-SDIC method offers a suitable alternative to other instrumental techniques at a substantial lower cost.

Table 12.

Comparison of DSPME-SDIC with other methods for the determination of boron.

Extraction method/technique	Sample	V_{acid}^b (μL)	V_{org}^c (μL)	LOD^d (μg mL^{-1})	%RSD^e	Ref.
MNP/CNT/GCE	Nuts	10000	0	0.08	-	(Liv & Nakiboglu, 2020)
UV/Vis	Water	168	29000	0.03	2.05-4.63	(Qin, 2013)
CURN-FILM-DIC	Wastewater	0	200	0.05	2.29-5.66	(Boonkanon et al., 2020)
ICP-MS	Hazelnut	10000	500	1.0×10^{-4}	-	(Simsek & Aykut, 2007)
DLLME-ICP-MS	Ground and seawater	0	800	3.0×10^{-4}	3.00	(Chandrasekaran et al., 2013)
UV/Vis	Nuts	17	1400	0.06	3.90-5.75	This study
DSPME-SDIC			1600	0.08	0.83-6.77	

MNP/CNT/GCE: Metal nanoparticles-carbon nanotube modified glassy carbon electrode

UV/Vis: Ultraviolet/visible spectrophotometry.

CURN-FILM-DIC: Curcumin nanoparticles-film-digital image colorimetry.

ICP-MS: Inductively coupled plasma-mass spectrometry

DLLME-ICP-MS: Dispersive liquid–liquid microextraction- inductively coupled plasma-quadrupole mass spectrometry

DSPME-SDIC: Dispersive solid-phase microextraction-smartphone digital image colorimetry.

[b] Total volume of acid consumed per sample

[c] Total volume of organic solvents consumed per sample.

[d] Limit of detection.

[e] Percentage relative standard deviation.

CHAPTER V
CONCLUSIONS AND RECOMMENDATIONS

LLME and DSPME were shown in this study to improve the sensitivity and selectivity of a relatively simple and novel SDIC detection technique that exhibited those two weaknesses. Three studies were conducted to demonstrate the applicability of the proposed combination to food samples.

In the first study, SFOD-DLLME was used to preconcentrate iodate in a table salt sample after performing the well-known iodate-specific redox reaction with iodide in an acidic medium and detecting it with SDIC. The proposed detection system entails building a simple homemade colorimetric box illuminated by a battery-powered LED lamp, using a smartphone camera to capture reproducible images of the sample solution placed in a UV/Vis microcuvette inside the colorimetric box, and converting the pixel intensity of the colored solution to a number using ImageJ image processing software. The proposed method produced EFs ranging from 17.4 to 25.0. allowing the detection of iodate in genuine table salt samples.

SMS-LLME was used in the second study to preconcentrate curcumin in tea and spices before detection with SDIC. The colorimetric box was significantly modified and improved by replacing the LED lamp; a continuum light source with a monochromatic light source by using a second smartphone illuminating a wavelength specific light equivalent to the λ_{max} of the analyte. The change resulted in a noticeable improvement in the method's selectivity, LDR of the calibration graph, better accuracy, higher sample throughput, and a more robust detection system because the brightness of the smartphone's backlight can be easily controlled and is unaffected by the battery's lifetime, which is not the case for a battery-powered LED lamp. Curcumin was found in genuine tea and spice samples.

In the third and final study, DSPME was combined with SDIC for the determination of boron in different nuts. The modified colorimetric box was used as the second study. A

monochromatic light source was used by scanning the wavelength of the monochromatic source to obtain the one that gives the highest response. The curcumin method was used by complexing boron with a curcumin reagent in acidic medium to form a colored solution suitable for detection by SDIC. DSPME was used for sample clean-up. Analytical satisfactory results were obtained, and boron could be detected in five different nut samples analyzed.

Some conclusions drawn from the three studies are that microextraction techniques do indeed improve the sensitivity and selectivity of a relatively simple detection system such as SDIC. Other advantages of microextraction techniques included quick analysis time, the use of microvolumes of relatively green solvents, simplicity, and high extraction efficiency. SDIC, on the other hand, has been shown to be a useful alternative to complicated high-tech instruments, with notable advantages such as portability, speed, ease of use, zero reliance on electricity, the potential for on-site analysis, and almost zero cost, which is especially important for low-income countries that cannot afford to acquire and maintain expensive instruments. SDIC could be hyphenated using a simple chromatographic technique such as Thin-layer chromatography (TLC) for quantitation, overcoming one of TLC's major limitations.

REFERENCES

Abadi, M. D. M., Chamsaz, M., Arbab-Zavar, M. H., & Shemirani, F. (2013). Supramolecular dispersive liquid-liquid microextraction based solidification of floating organic drops for speciation and spectrophotometric determination of chromium in real samples [Article]. *Analytical Methods*, *5*(12), 2971-2977. https://doi.org/10.1039/c3ay00036b

Adlnasab, L., Ezoddin, M., Shabanian, M., & Mahjoob, B. (2019). Development of ferrofluid mediated CLDH@Fe3O4@Tanic acid- based supramolecular solvent: Application in air-assisted dispersive micro solid phase extraction for preconcentration of diazinon and metalaxyl from various fruit juice samples [Article]. *Microchemical Journal*, *146*, 1-11. https://doi.org/10.1016/j.microc.2018.12.020

Afkhami, A., Pirdadeh-Beiranvand, M., & Madrakian, T. (2017). A Method Based on Ultrasound-assisted Solidification of Floating Drop Microextraction Technique for the Spectrophotometric Determination of Curcumin in Turmeric Powder. *Analytical and Bioanalytical Chemistry Research*, *4*(1), 1-10.

Aggarwal, B. B., Sundaram, C., Malani, N., & Ichikawa, H. (2007). Curcumin: the Indian solid gold. *The molecular targets and therapeutic uses of curcumin in health and disease*, 1-75.

Al-Nidawi, M., & Alshana, U. (2021). Reversed-phase switchable-hydrophilicity solvent liquid-liquid microextraction of copper prior to its determination by smartphone digital image colorimetry. *Journal of Food Composition and Analysis*, *104*, Article 104140. https://doi.org/10.1016/j.jfca.2021.104140

Al-Nidawi, M., Alshana, U., Caleb, J., Hassan, M., Rahman, Z. U., Hanoglu, D. Y., & Calis, I. Switchable-hydrophilicity solvent liquid-liquid microextraction versus dispersive liquid-liquid microextraction prior to HPLC-UV for the determination and isolation of piperine from Piper nigrum L. *Journal of Separation Science*. https://doi.org/10.1002/jssc.202000152

Alshana, U., Ertas, N., & Goger, N. G. (2015). Determination of parabens in human milk and other food samples by capillary electrophoresis after dispersive liquid-liquid microextraction with back-extraction. *Food Chemistry*, *181*, 1-8. https://doi.org/10.1016/j.foodchem.2015.02.074

Alshana, U., Hassan, M., Al-Nidawi, M., Yilmaz, E., & Soylak, M. (2020). Switchable-hydrophilicity solvent liquid-liquid microextraction. *Trac-Trends in Analytical Chemistry*, *131*, Article 116025. https://doi.org/10.1016/j.trac.2020.116025

Altunay, N., Elik, A., & Gurkan, R. (2020). Preparation and application of alcohol based deep eutectic solvents for extraction of curcumin in food samples prior to its spectrophotometric determination. *Food Chemistry*, *310*, Article 125933. https://doi.org/10.1016/j.foodchem.2019.125933

Arabi, M., Ostovan, A., Asfaram, A., & Ghaedi, M. (2018). Development of an eco-friendly approach based on dispersive liquid- liquid microextraction for the quantitative determination of quercetin in Nasturtium officinale, Apium

graveolens, Spinacia oleracea, Brassica oleracea var. sabellica, and food samples. *New Journal of Chemistry*, *42*(17), 14340-14348. https://doi.org/10.1039/c8nj02485e

Armenta, S., Garrigues, S., & de la Guardia, M. (2008). Green Analytical Chemistry. *Trac-Trends in Analytical Chemistry*, *27*(6), 497-511. https://doi.org/10.1016/j.trac.2008.05.003

Arthur, C. L., & Pawliszyn, J. (1990). SOLID-PHASE MICROEXTRACTION WITH THERMAL-DESORPTION USING FUSED-SILICA OPTICAL FIBERS. *Analytical Chemistry*, *62*(19), 2145-2148. https://doi.org/10.1021/ac00218a019

Ashouri, V., Adib, K., Fariman, G. A., Ganjali, M. R., & Rahimi-Nasrabadi, M. (2021). Determination of arsenic species using functionalized ionic liquid by in situ dispersive liquid-liquid microextraction followed by atomic absorption spectrometry. *Food Chemistry*, *349*, Article 129115. https://doi.org/10.1016/j.foodchem.2021.129115

Aydin, F., Yilmaz, E., & Soylak, M. (2018). Vortex assisted deep eutectic solvent (DES)-emulsification liquid-liquid microextraction of trace curcumin in food and herbal tea samples. *Food Chemistry*, *243*, 442-447. https://doi.org/10.1016/j.foodchem.2017.09.154

Ballesteros-Gomez, A., Rubio, S., & Perez-Bendito, D. (2009). Potential of supramolecular solvents for the extraction of contaminants in liquid foods [Article]. *Journal of Chromatography A*, *1216*(3), 530-539. https://doi.org/10.1016/j.chroma.2008.06.029

Ballesteros-Gomez, A., Sicilia, M. D., & Rubio, S. (2010). Supramolecular solvents in the extraction of organic compounds. A review. *Analytica Chimica Acta*, *677*(2), 108-130. https://doi.org/10.1016/j.aca.2010.07.027

Barreto, J. A., de Assis, R. D., Santos, L. B., Cassella, R. J., & Lemos, V. A. (2020). Pressure variation in-syringe dispersive liquid-liquid microextraction associated with digital image colorimetry: Determination of cobalt in food samples. *Microchemical Journal*, *157*, Article 105064. https://doi.org/10.1016/j.microc.2020.105064

Bezerra, M. A., Cerqueira, U., Ferreira, S. L. C., Novaes, C. G., Novais, F. C., Valasques, G. S., & da Silva, B. N. Recent developments in the application of cloud point extraction as procedure for speciation of trace elements. *Applied Spectroscopy Reviews*. https://doi.org/10.1080/05704928.2021.1916516

Bhagat, P. R., Acharya, R., Nair, A. G. C., Pandey, A. K., Rajurkar, N. S., & Reddy, A. V. R. (2009). Estimation of iodine in food, food products and salt using ENAA. *Food Chemistry*, *115*(2), 706-710. https://doi.org/10.1016/j.foodchem.2008.11.092

Boonkanon, C., Phatthanawiwat, K., Wongniramaikul, W., & Choodum, A. (2020). Curcumin nanoparticle doped starch thin film as a green colorimetric sensor for detection of boron. *Spectrochimica Acta Part a-Molecular and Biomolecular Spectroscopy*, *224*, Article 117351. https://doi.org/10.1016/j.saa.2019.117351

Bozorgzadeh, E., Pasdaran, A., & Ebrahimi-Najafabadi, H. (2021). Determination of toxic heavy metals in fish samples using dispersive micro solid phase extraction combined with inductively coupled plasma optical emission spectroscopy. *Food Chemistry*, *346*, Article 128916. https://doi.org/10.1016/j.foodchem.2020.128916

Burato, J. S. D., Medina, D. A. V., de Toffoli, A. L., Maciel, E. V. S., & Lancas, F. M. (2020). Recent advances and trends in miniaturized sample preparation techniques. *Journal of Separation Science*, *43*(1), 202-225. https://doi.org/10.1002/jssc.201900776

Burguera, M., Burguera, J. L., Rondon, C., & Carrero, P. (2001). Determination of boron in blood, urine and bone by electrothermal atomic absorption spectrometry using zirconium and citric acid as modifiers. *Spectrochimica Acta Part B-Atomic Spectroscopy*, *56*(10), 1845-1857. https://doi.org/10.1016/s0584-8547(01)00340-8

Cacciola, F., Dugo, P., & Mondello, L. (2017). Multidimensional liquid chromatography in food analysis [Review]. *Trac-Trends in Analytical Chemistry*, *96*, 116-123. https://doi.org/10.1016/j.trac.2017.06.009

Caleb, J., & Alshana, U. (2021). Supramolecular solvent-liquid-liquid microextraction followed by smartphone digital image colorimetry for the determination of curcumin in food samples. *Sustainable Chemistry and Pharmacy*, *21*, 100424.

Caleb, J., Alshana, U., Hanoglu, A., & Calis, I. (2021). Dispersive liquid-liquid microextraction for the isolation and HPLC-DAD determination of three major capsaicinoids in Capsicum annuum L. *Turkish Journal of Chemistry*, *45*(2), 420-+.

Campillo, N., Vinas, P., Sandrejova, J., & Andruch, V. (2017). Ten years of dispersive liquid-liquid microextraction and derived techniques. *Applied Spectroscopy Reviews*, *52*(4), 267-415. https://doi.org/10.1080/05704928.2016.1224240

Campmajo, G., Rodriguez-Javier, L. R., Saurina, J., & Nunez, O. (2021). Assessment of paprika geographical origin fraud by high-performance liquid chromatography with fluorescence detection (HPLC-FLD) fingerprinting. *Food Chemistry*, *352*, Article 129397. https://doi.org/10.1016/j.foodchem.2021.129397

Capitan-Vallvey, L. F., Lopez-Ruiz, N., Martinez-Olmos, A., Erenas, M. M., & Palma, A. J. (2015). Recent developments in computer vision-based analytical chemistry: A tutorial review. *Analytica Chimica Acta*, *899*, 23-56. https://doi.org/10.1016/j.aca.2015.10.009

Castro, R., Natera, R., Duran, E., & Garcia-Barroso, C. (2008). Application of solid phase extraction techniques to analyse volatile compounds in wines and other enological products. *European Food Research and Technology*, *228*(1), 1-18. https://doi.org/10.1007/s00217-008-0900-4

Chandra, A., Maata, M., & Prasad, S. (2019). Determination of iodine content in Fijian foods using spectrophotometric kinetic method. *Microchemical Journal*, *148*, 475-479. https://doi.org/10.1016/j.microc.2019.04.060

Chandrasekaran, K., Karunasagar, D., & Arunachalam, J. (2013). Dispersive liquid-liquid micro extraction of boron as tetrafluoroborate ion (BF4-) from natural waters, wastewater and seawater samples and determination using a micro-flow nebulizer in inductively coupled plasma-quadrupole mass spectrometry. *Journal of Analytical Atomic Spectrometry*, *28*(1), 142-149. https://doi.org/10.1039/c2ja30272a

Clydesdale, F. M., & Ahmed, E. M. (1978). Colorimetry—methodology and applications. *Critical Reviews in Food Science & Nutrition*, *10*(3), 243-301.

Coskun, A. F., Wong, J., Khodadadi, D., Nagi, R., Tey, A., & Ozcan, A. (2013). A personalized food allergen testing platform on a cellphone. *Lab on a Chip*, *13*(4), 636-640.

Daniel, D., Lopes, F. S., dos Santos, V. B., & do Lago, C. L. (2018). Detection of coffee adulteration with soybean and corn by capillary electrophoresis-tandem mass spectrometry. *Food Chemistry*, *243*, 305-310. https://doi.org/10.1016/j.foodchem.2017.09.140

Dmitrienko, S. G., Apyari, V. V., Tolmacheva, V. V., & Gorbunova, M. V. (2020). Dispersive Liquid-Liquid Microextraction of Organic Compounds: An Overview of Reviews. *Journal of Analytical Chemistry*, *75*(10), 1237-1251. https://doi.org/10.1134/s1061934820100056

Duan, C. F., Shen, Z., Wu, D. P., & Guan, Y. F. (2011). Recent developments in solid-phase microextraction for on-site sampling and sample preparation. *Trac-Trends in Analytical Chemistry*, *30*(10), 1568-1574. https://doi.org/10.1016/j.trac.2011.08.005

Dwamena, A. K. (2019). Recent Advances in Hydrophobic Deep Eutectic Solvents for Extraction. *Separations*, *6*(1), Article 9. https://doi.org/10.3390/separations6010009

Eckhoff, K. M., & Maage, A. (1997). Iodine content in fish and other food products from East Africa analyzed by ICP-MS. *Journal of Food Composition and Analysis*, *10*(3), 270-282.

Er, E. O., Bozyigit, G. D., Buyukpinar, C., & Bakirdere, S. Magnetic Nanoparticles Based Solid Phase Extraction Methods for the Determination of Trace Elements. *Critical Reviews in Analytical Chemistry*. https://doi.org/10.1080/10408347.2020.1797465

Ezoddin, M., Majidi, B., & Abdi, K. (2015). Ultrasound-assisted supramolecular dispersive liquid-liquid microextraction based on solidification of floating organic drops for preconcentration of palladium in water and road dust samples. *Journal of Molecular Liquids*, *209*, 515-519. https://doi.org/10.1016/j.molliq.2015.06.031

Fan, Y. J., Li, J. W., Guo, Y. P., Xie, L. W., & Zhang, G. (2021). Digital image colorimetry on smartphone for chemical analysis: A review. *Measurement*, *171*, Article 108829. https://doi.org/10.1016/j.measurement.2020.108829

Faraji, M., Noormohammadi, F., Jafarinejad, S., & Moradi, M. (2017). Supramolecular-based solvent microextraction of carbaryl in water samples followed by high performance liquid chromatography determination. *International Journal of Environmental Analytical Chemistry*, *97*(8), 730-742. https://doi.org/10.1080/03067319.2017.1353088

Firdaus, M. L., Alwi, W., Trinoveldi, F., Rahayu, I., Rahmidar, L., & Warsito, K. (2014). Determination of Chromium and Iron Using Digital Image-based Colorimetry. *4th International Conference on Sustainable Future for Human Security Sustain 2013*, *20*, 298-304. https://doi.org/10.1016/j.proenv.2014.03.037

Ghambarian, M., Yamini, Y., & Esrafili, A. (2013). Liquid-phase microextraction based on solidified floating drops of organic solvents. *Microchimica Acta*, *180*(7-8), 519-535. https://doi.org/10.1007/s00604-013-0969-8

Ghoraba, Z., Aibaghi, B., & Soleymanpour, A. (2018). Ultrasound-assisted dispersive liquid-liquid microextraction followed by ion mobility spectrometry for the

simultaneous determination of bendiocarb and azinphos-ethyl in water, soil, food and beverage samples. *Ecotoxicology and Environmental Safety*, *165*, 459-466. https://doi.org/10.1016/j.ecoenv.2018.09.021

Ghorbani, M., Aghamohammadhassan, M., Chamsaz, M., Akhlaghi, H., & Pedramrad, T. (2019). Dispersive solid phase microextraction. *Trac-Trends in Analytical Chemistry*, *118*, 793-809. https://doi.org/10.1016/j.trac.2019.07.012

Gjelstad, A. (2019). Three-phase hollow fiber liquid-phase microextraction and parallel artificial liquid membrane extraction. *Trac-Trends in Analytical Chemistry*, *113*, 25-31. https://doi.org/10.1016/j.trac.2019.01.007

Gouda, A. A., Elmasry, M. S., Hashem, H., & El-Sayed, H. M. (2018). Eco-friendly environmental trace analysis of thorium using a new supramolecular solvent-based liquid-liquid microextraction combined with spectrophotometry. *Microchemical Journal*, *142*, 102-107. https://doi.org/10.1016/j.microc.2018.06.024

Hassan, M., Erbas, Z., Alshana, U., & Soylak, M. (2020). Ligandless reversed-phase switchable-hydrophilicity solvent liquid-liquid microextraction combined with flame-atomic absorption spectrometry for the determination of copper in oil samples. *Microchemical Journal*, *156*, Article 104868. https://doi.org/10.1016/j.microc.2020.104868

Hassan, M., Uzcan, F., Alshana, U., & Soylak, M. (2021). Switchable-hydrophilicity solvent liquid-liquid microextraction prior to magnetic nanoparticle-based dispersive solid-phase microextraction for spectrophotometric determination of erythrosine in food and other samples. *Food Chemistry*, *348*, Article 129053. https://doi.org/10.1016/j.foodchem.2021.129053

Huang, Z. P., Subhani, Q., Zhu, Z. Y., Guo, W. Q., & Zhu, Y. (2013). A single pump cycling-column-switching technique coupled with homemade high exchange capacity columns for the determination of iodate in iodized edible salt by ion chromatography with UV detection. *Food Chemistry*, *139*(1-4), 144-148. https://doi.org/10.1016/j.foodchem.2013.01.070

Jain, R., Jha, R. R., Kumari, A., & Khatri, I. (2021). Dispersive liquid-liquid microextraction combined with digital image colorimetry for paracetamol analysis. *Microchemical Journal*, *162*, Article 105870. https://doi.org/10.1016/j.microc.2020.105870

Jakmunee, J., & Grudpan, K. (2001). Flow injection amperometry for the determination of iodate in iodized table salt [Article; Proceedings Paper]. *Analytica Chimica Acta*, *438*(1-2), 299-304. https://doi.org/10.1016/s0003-2670(01)00798-x

Jeannot, M. A., & Cantwell, F. F. (1996). Solvent microextraction into a single drop. *Analytical Chemistry*, *68*(13), 2236-2240. https://doi.org/10.1021/ac960042z

Ji, Y. H., Zhao, M., Li, A. W., & Zhao, L. S. (2021). Hydrophobic deep eutectic solvent-based ultrasonic-assisted dispersive liquid-liquid microextraction for preconcentration and determination of trace cadmium and arsenic in wine samples. *Microchemical Journal*, *164*, Article 105974. https://doi.org/10.1016/j.microc.2021.105974

Jing, X., Huang, X., Wang, H. H., Xue, H. Y., Wu, B. Q., Wang, X. W., & Jia, L. Y. (2021). Popping candy-assisted dispersive liquid-liquid microextraction for enantioselective determination of prothioconazole and its chiral metabolite in

water, beer, Baijiu, and vinegar samples by HPLC. *Food Chemistry*, *348*, Article 129147. https://doi.org/10.1016/j.foodchem.2021.129147

Jing, X., Wang, H., Huang, X., Chen, Z., Zhu, J., & Wang, X. (2021). Digital image colorimetry detection of carbaryl in food samples based on liquid phase microextraction coupled with a microfluidic thread-based analytical device. *Food Chemistry*, *337*, 127971.

John, J., Rugmini, S. D., & Nair, B. S. (2018). Kinetics and Mechanism of the Thermal and Hydrolytic Decomposition Reaction of Rosocyanin. *International Journal of Chemical Kinetics*, *50*(3), 164-177. https://doi.org/10.1002/kin.21148

Kailasa, S. K., Koduru, J. R., Park, T. J., Singhal, R. K., & Wu, H. F. (2021). Applications of single-drop microextraction in analytical chemistry: A review. *Trends in Environmental Analytical Chemistry*, *29*, Article e00113. https://doi.org/10.1016/j.teac.2020.e00113

Karlidag, N. E., Kocoglu, E. S., Toprak, M., Yilmaz, O., & Bakirdere, S. (2020). Zirconium nanoparticles based dispersive solid phase extraction prior to slotted quartz tube-flame atomic absorption spectrophotometry for the determination of selenium in green tea samples. *Food Chemistry*, *329*, Article 127210. https://doi.org/10.1016/j.foodchem.2020.127210

Karlidag, N. E., Toprak, M., Tekin, Z., & Bakirdere, S. (2020). Zirconium nanoparticles based ligandless dispersive solid phase extraction for the determination of antimony in bergamot and mint tea samples by slotted quartz tube-flame atomic absorption spectrophotometry. *Journal of Food Composition and Analysis*, *92*, Article 103583. https://doi.org/10.1016/j.jfca.2020.103583

Kashanaki, R., Ebrahimzadeh, H., & Moradi, M. (2018). Metal-organic framework based micro solid phase extraction coupled with supramolecular solvent microextraction to determine copper in water and food samples. *New Journal of Chemistry*, *42*(8), 5806-5813. https://doi.org/10.1039/c8nj00340h

Khan, W. A., Arain, M. B., Yamini, Y., Shah, N., Kazi, T. G., Pedersen-Bjergaard, S., & Tajik, M. (2020). Hollow fiber-based liquid phase microextraction followed by analytical instrumental techniques for quantitative analysis of heavy metal ions and pharmaceuticals. *Journal of Pharmaceutical Analysis*, *10*(2), 109-122. https://doi.org/10.1016/j.jpha.2019.12.003

Khezeli, T., & Daneshfar, A. (2017). Development of dispersive micro-solid phase extraction based on micro and nano sorbents. *Trac-Trends in Analytical Chemistry*, *89*, 99-118. https://doi.org/10.1016/j.trac.2017.01.004

Khorshidi, N., Rahimi, M., & Salimikia, I. (2020). Application of aeration-assisted homogeneous liquid–liquid microextraction procedure using Box–Behnken design for determination of curcumin by HPLC. *Journal of separation science*, *43*(13), 2513-2520.

Klampfl, C. W., & Katzmayr, M. U. (1998). Determination of low-molecular-mass anionic compounds in beverage samples using capillary zone electrophoresis with simultaneous indirect ultraviolet and conductivity detection. *Journal of Chromatography A*, *822*(1), 117-123. https://doi.org/10.1016/s0021-9673(98)00563-9

Kori, S. (2021). Cloud point extraction coupled with back extraction: a green methodology in analytical chemistry. *Forensic Sciences Research*, *6*(1), 19-33. https://doi.org/10.1080/20961790.2019.1643567

Kulkarni, P. S., Dhar, S. D., & Kulkarni, S. D. (2013). A rapid assessment method for determination of iodate in table salt samples. *Journal of Analytical Science and Technology*, *4*(1), 1-6.

Kumar, S. D., Maiti, B., & Mathur, P. K. (2001). Determination of iodate and sulphate in iodized common salt by ion chromatography with conductivity detection [Article]. *Talanta*, *53*(4), 701-705. https://doi.org/10.1016/s0039-9140(00)00504-x

Leong, M. I., & Huang, S. D. (2009). Dispersive liquid-liquid microextraction method based on solidification of floating organic drop for extraction of organochlorine pesticides in water samples. *Journal of Chromatography A*, *1216*(45), 7645-7650. https://doi.org/10.1016/j.chroma.2009.09.004

Leung, A. M., & Braverman, L. E. (2014). Consequences of excess iodine. *Nature Reviews Endocrinology*, *10*(3), 136-142. https://doi.org/10.1038/nrendo.2013.251

Li, J., Wang, Y. B., Li, K. Y., Cao, Y. Q., Wu, S., & Wu, L. (2015). Advances in different configurations of solid-phase microextraction and their applications in food and environmental analysis. *Trac-Trends in Analytical Chemistry*, *72*, 141-152. https://doi.org/10.1016/j.trac.2015.04.023

Liang, P., Yang, E. J., Yu, J., & Wen, L. J. (2014). Supramolecular solvent dispersive liquid-liquid microextraction based on solidification of floating drop and graphite furnace atomic absorption spectrometry for the determination of trace lead in food and water samples. *Analytical Methods*, *6*(11), 3729-3734. https://doi.org/10.1039/c4ay00019f

Liu, H. L., Meng, Q., Zhao, X., Ye, Y. L., & Tong, H. R. (2021). Inductively coupled plasma mass spectrometry (ICP-MS) and inductively coupled plasma optical emission spectrometer (ICP-OES)-based discrimination for the authentication of tea. *Food Control*, *123*, Article 107735. https://doi.org/10.1016/j.foodcont.2020.107735

Liv, L., & Nakiboglu, N. (2020). Cost-effective voltammetric determination of boron in dried fruits and nuts using modified electrodes. *Food Chemistry*, *311*, Article 126013. https://doi.org/10.1016/j.foodchem.2019.126013

Lopez-Molinero, A., Cubero, V. T., Irigoyen, R. D., & Piazuelo, D. S. (2013). Feasibility of digital image colorimetry-Application for water calcium hardness determination. *Talanta*, *103*, 236-244. https://doi.org/10.1016/j.talanta.2012.10.038

Lord, H., & Pawliszyn, J. (2000). Microextraction of drugs. *Journal of Chromatography A*, *902*(1), 17-63. https://doi.org/10.1016/s0021-9673(00)00836-0

Luguera, M., Madrid, Y., & Camara, C. (1991). COMBINATION OF CHEMICAL MODIFIERS AND GRAPHITE TUBE PRETREATMENT TO DETERMINE BORON BY ELECTROTHERMAL ATOMIC-ABSORPTION SPECTROMETRY. *Journal of Analytical Atomic Spectrometry*, *6*(8), 669-672. https://doi.org/10.1039/ja9910600669

Maciel, E. V. S., de Toffoli, A. L., & Lancas, F. M. (2018). Recent trends in sorption-based sample preparation and liquid chromatography techniques for food analysis. *Electrophoresis*, *39*(13), 1582-1596. https://doi.org/10.1002/elps.201800009

MacMahon, S., Ridge, C. D., & Begley, T. H. (2014). Liquid Chromatography-Tandem Mass Spectrometry (LC-MS/MS) Method for the Direct Detection of 2-Monochloropropanediol (2-MCPD) Esters in Edible Oils. *Journal of Agricultural and Food Chemistry*, *62*(48), 11647-11656. https://doi.org/10.1021/jf503994m

Madikizela, L. M., Pakade, V. E., Ncube, S., Tutu, H., & Chimuka, L. (2020). Application of Hollow Fibre-Liquid Phase Microextraction Technique for Isolation and Pre-Concentration of Pharmaceuticals in Water. *Membranes*, *10*(11), Article 311. https://doi.org/10.3390/membranes10110311

Manful, C. F., Vidal, N. P., Pham, T. H., Nadeem, M., Wheeler, E., Hamilton, M. C., . . . Thomas, R. H. (2019). Rapid determination of heterocyclic amines in ruminant meats using accelerated solvent extraction and ultra-high performance liquid chromatograph-mass spectrometry. *Methodsx*, *6*, 2686-2697. https://doi.org/10.1016/j.mex.2019.11.014

Masawat, P., Harfield, A., & Namwong, A. (2015). An iPhone-based digital image colorimeter for detecting tetracycline in milk. *Food Chemistry*, *184*, 23-29. https://doi.org/10.1016/j.foodchem.2015.03.089

Menghwar, P., Yilmaz, E., & Soylak, M. (2018). Development of an ultrasonic-assisted restricted access supramolecular solvent-based liquid phase microextraction (UA-RAS-LPME) method for separation-preconcentration and UV-VIS spectrophotometric detection of curcumin. *Separation Science and Technology*, *53*(16), 2612-2621. https://doi.org/10.1080/01496395.2018.1462389

Moghadamtousi, S. Z., Kadir, H. A., Hassandarvish, P., Tajik, H., Abubakar, S., & Zandi, K. A review on antibacterial, antiviral, and antifungal activity of curcumin. Biomed Research International. 2014; 2014: 186864. In.

Moradi, M., Yamini, Y., & Feizi, N. (2021). Development and challenges of supramolecular solvents in liquid-based microextraction methods. *Trac-Trends in Analytical Chemistry*, *138*, Article 116231. https://doi.org/10.1016/j.trac.2021.116231

Mortazavi, S. S., & Farmany, A. (2014). Catalytic-oxidation of Janus green in the presence of AgNPs: Application to the determination of iodate. *Journal of Industrial and Engineering Chemistry*, *20*(6), 4224-4226. https://doi.org/10.1016/j.jiec.2014.01.024

Musarurwa, H., & Tavengwa, N. T. (2021a). Deep eutectic solvent-based dispersive liquid-liquid micro-extraction of pesticides in food samples. *Food Chemistry*, *342*, Article 127943. https://doi.org/10.1016/j.foodchem.2020.127943

Musarurwa, H., & Tavengwa, N. T. (2021b). Supramolecular solvent-based micro-extraction of pesticides in food and environmental samples. *Talanta*, *223*, Article 121515. https://doi.org/10.1016/j.talanta.2020.121515

Musarurwa, H., & Tavengwa, N. T. (2021c). Switchable solvent-based micro-extraction of pesticides in food and environmental samples. *Talanta*, *224*, Article 121807. https://doi.org/10.1016/j.talanta.2020.121807

Naeemullah, Kazi, T. G., & Tuzen, M. (2015). Magnetic stirrer induced dispersive ionic-liquid microextraction for the determination of vanadium in water and food samples prior to graphite furnace atomic absorption spectrometry. *Food Chemistry*, *172*, 161-165. https://doi.org/10.1016/j.foodchem.2014.09.053

Noon, J., Mills, T. B., & Norton, I. T. (2020). The use of natural antioxidants to combat lipid oxidation in O/W emulsions [Article]. *Journal of Food Engineering*, *281*, 13, Article 110006. https://doi.org/10.1016/j.jfoodeng.2020.110006

Ozkantar, N., Soylak, M., & Tuzen, M. (2019). Determination of Copper Using Supramolecular Solvent-based Microextraction for Food, Spices, and Water Samples Prior to Analysis by Flame Atomic Absorption Spectrometry. *Atomic Spectroscopy*, *40*(1), 17-23. https://doi.org/10.46770/as.2019.01.003

Paiva, A. C., Crucello, J., Porto, N. D., & Hantao, L. W. (2021). Fundamentals of and recent advances in sorbent-based headspace extractions. *Trac-Trends in Analytical Chemistry*, *139*, Article 116252. https://doi.org/10.1016/j.trac.2021.116252

Pena-Pereira, F., Bendicho, C., Pavlovic, D. M., Martin-Esteban, A., Diaz-Alvarez, M., Pan, Y. W., . . . Psillakis, E. (2021). Miniaturized analytical methods for determination of environmental contaminants of emerging concern e A review. *Analytica Chimica Acta*, *1158*, Article 238108. https://doi.org/10.1016/j.aca.2020.11.040

Pena-Pereira, F., Senra-Ferreiro, S., Lavilla, I., & Bendicho, C. (2010). Determination of iodate in waters by cuvetteless UV-vis micro-spectrophotometry after liquid-phase microextraction. *Talanta*, *81*(1-2), 625-629. https://doi.org/10.1016/j.talanta.2009.12.053

Peng, B., Chen, G. R., Li, K., Zhou, M., Zhang, J., & Zhao, S. G. (2017). Dispersive liquid-liquid microextraction coupled with digital image colorimetric analysis for detection of total iron in water and food samples. *Food Chemistry*, *230*, 667-672. https://doi.org/10.1016/j.foodchem.2017.03.099

Pivari, F., Mingione, A., Brasacchio, C., & Soldati, L. (2019). Curcumin and Type 2 Diabetes Mellitus: Prevention and Treatment. *Nutrients*, *11*(8), Article 1837. https://doi.org/10.3390/nu11081837

Pizzorno, L. (2015). Nothing boring about boron. *Integrative Medicine: A Clinician's Journal*, *14*(4), 35.

Plotka-Wasylka, J., Szczepanska, N., de la Guardia, M., & Namiesnik, J. (2015). Miniaturized solid-phase extraction techniques. *Trac-Trends in Analytical Chemistry*, *73*, 19-38. https://doi.org/10.1016/j.trac.2015.04.026

Porto, I. S. A., Neto, J. H. S., dos Santos, L. O., Gomes, A. A., & Ferreira, S. L. C. (2019). Determination of ascorbic acid in natural fruit juices using digital image colorimetry. *Microchemical Journal*, *149*, Article 104031. https://doi.org/10.1016/j.microc.2019.104031

Prosen, H., & Zupancic-Kralj, L. (1999). Solid-phase microextraction. *Trac-Trends in Analytical Chemistry*, *18*(4), 272-282. https://doi.org/10.1016/s0165-9936(98)00109-5

Qin, Y. (2013). Determination of boron in water samples by the spectrophotometric curcumin method. *Environmental Protection and Resources Exploitation, Pts 1-3*, *807-809*, 323-326. https://doi.org/10.4028/www.scientific.net/AMR.807-809.323

Quesada-Gonzalez, D., & Merkoci, A. (2017). Mobile phone-based biosensing: An emerging "diagnostic and communication" technology. *Biosensors & Bioelectronics*, *92*, 549-562. https://doi.org/10.1016/j.bios.2016.10.062

Raril, C., Manjunatha, J. G., & Tigari, G. (2020). Low-cost voltammetric sensor based on an anionic surfactant modified carbon nanocomposite material for the rapid determination of curcumin in natural food supplement. *Instrumentation Science & Technology*, *48*(5), 561-582.

Rebary, B., Paul, P., & Ghosh, P. K. (2010). Determination of iodide and iodate in edible salt by ion chromatography with integrated amperometric detection. *Food Chemistry*, *123*(2), 529-534. https://doi.org/10.1016/j.foodchem.2010.04.046

Rezaee, M., Assadi, Y., Hosseinia, M. R. M., Aghaee, E., Ahmadi, F., & Berijani, S. (2006). Determination of organic compounds in water using dispersive liquid-liquid microextraction. *Journal of Chromatography A*, *1116*(1-2), 1-9. https://doi.org/10.1016/j.chroma.2006.03.007

Ritota, M., & Manzi, P. (2020). Rapid Determination of Total Tryptophan in Yoghurt by Ultra High Performance Liquid Chromatography with Fluorescence Detection. *Molecules*, *25*(21), Article 5025. https://doi.org/10.3390/molecules25215025

Rueden, C. T., Schindelin, J., Hiner, M. C., DeZonia, B. E., Walter, A. E., Arena, E. T., & Eliceiri, K. W. (2017). ImageJ2: ImageJ for the next generation of scientific image data. *Bmc Bioinformatics*, *18*, Article 529. https://doi.org/10.1186/s12859-017-1934-z

Sah, R. N., & Brown, P. H. (1997). Boron determination - A review of analytical methods. *Microchemical Journal*, *56*(3), 285-304. https://doi.org/10.1006/mchj.1997.1428

Salamat, Q., Yamini, Y., Moradi, M., Karimi, M., & Nazraz, M. (2018). Novel generation of nano-structured supramolecular solvents based on an ionic liquid as a green solvent for microextraction of some synthetic food dyes. *New Journal of Chemistry*, *42*(23), 19252-19259. https://doi.org/10.1039/c8nj03943g

Schiborr, C., Eckert, G. P., Rimbach, G., & Frank, J. (2010). A validated method for the quantification of curcumin in plasma and brain tissue by fast narrow-bore high-performance liquid chromatography with fluorescence detection. *Analytical and bioanalytical chemistry*, *397*(5), 1917-1925.

Seebunrueng, K., Phosiri, P., Apitanagotinon, R., & Srijaranai, S. (2020). A new environment-friendly supramolecular solvent-based liquid phase microextraction coupled to high performance liquid chromatography for simultaneous determination of six phenoxy acid herbicides in water and rice samples. *Microchemical Journal*, *152*, Article 104418. https://doi.org/10.1016/j.microc.2019.104418

Shrivas, K., & Jaiswal, N. K. (2013). Dispersive liquid-liquid microextraction for the determination of copper in cereals and vegetable food samples using flame atomic absorption spectrometry. *Food Chemistry*, *141*(3), 2263-2268. https://doi.org/10.1016/j.foodchem.2013.04.067

Simsek, A., & Aykut, O. (2007). Evaluation of the microelement profile of Turkish hazelnut (Corylus avellana L.) varieties for human nutrition and health. *International Journal of Food Sciences and Nutrition*, *58*(8), 677-688. https://doi.org/10.1080/09637480701403202

Skoog, D. A., Holler, F. J., & Crouch, S. R. (2017). *Principles of instrumental analysis*. Cengage learning.

Song, Y., Sun, H. J., Xiao, J., Wang, F., Ding, Y., Zhao, J. Y., . . . Wen, A. D. (2019). Development of a liquid chromatography-tandem mass spectrometric (LC-MS/MS) method for simultaneous determination of epigallocatechin-3-gallate, silibinin, and curcumin in plasma and different tissues after oral dosing of Protandim in rats and its application in pharmacokinetic and tissue distribution studies. *Journal of Pharmaceutical and Biomedical Analysis*, *170*, 54-62. https://doi.org/10.1016/j.jpba.2019.03.024

Sun, X. H., Gao, C. L., Cao, W. D., Yang, X. R., & Wang, E. K. (2002). Capillary electrophoresis with amperometric detection of curcumin in Chinese herbal medicine pretreated by solid-phase extraction. *Journal of Chromatography A*, *962*(1-2), 117-125, Article Pii s0021-9673(02)00509-5. https://doi.org/10.1016/s0021-9673(02)00509-5

Tamddoni, A., Mohammadi, E., Sedaghat, F., Qujeq, D., & As'Habi, A. (2020). The anticancer effects of curcumin via targeting the mammalian target of rapamycin complex 1 (mTORC1) signaling pathway. *Pharmacological research*, 104798.

Tan, C. R., Su, Z. H., Lin, B. G., Huang, H. W., Zeng, Y. L., Li, S. A., . . . Yu, R. Q. (2010). A novel method for iodate determination using cadmium sulfide quantum dots as fluorescence probes. *Analytica Chimica Acta*, *678*(2), 203-207. https://doi.org/10.1016/j.aca.2010.08.034

Tegladza, I. D., Qi, T., Chen, T. Y., Alorku, K., Tang, S., Shen, W., . . . Lee, H. K. (2020). Direct immersion single-drop microextraction of semi-volatile organic compounds in environmental samples: A review. *Journal of Hazardous Materials*, *393*, Article 122403. https://doi.org/10.1016/j.jhazmat.2020.122403

Tezcan, F., & Erim, F. B. (2018). Determination of Vitamin B2 Content in Black, Green, Sage, and Rosemary Tea Infusions by Capillary Electrophoresis with Laser-Induced Fluorescence Detection. *Beverages*, *4*(4), Article 86. https://doi.org/10.3390/beverages4040086

Toida, Y., & Watanabe, K. (1993). SPECTROPHOTOMETRIC DETERMINATION OF TRACE AMOUNTS OF BORON IN HIGH-PURITY GRAPHITE WITH CURCUMIN. *Bunseki Kagaku*, *42*(5), T65-T69.

Tsai, W. H., Huang, T. C., Huang, J. J., Hsue, Y. H., & Chuang, H. Y. (2009). Dispersive solid-phase microextraction method for sample extraction in the analysis of four tetracyclines in water and milk samples by high-performance liquid chromatography with diode-array detection. *Journal of Chromatography A*, *1216*(12), 2263-2269. https://doi.org/10.1016/j.chroma.2009.01.034

Tuzen, M., Elik, A., & Altunay, N. (2021). Ultrasound-assisted supramolecular solvent dispersive liquid-liquid microextraction for preconcentration and determination of Cr(VI) in waters and total chromium in beverages and vegetables [Article]. *Journal of Molecular Liquids*, *329*, 7, Article 115556. https://doi.org/10.1016/j.molliq.2021.115556

Unsal, Y. E., Tuzen, M., & Soylak, M. (2019). Ultrasound-Assisted Ionic Liquid-Dispersive Liquid-Liquid of Curcumin in Food Samples Microextraction and Its Spectrophotometric Determination. *Journal of Aoac International*, *102*(1), 217-221. https://doi.org/10.5740/jaoacint.18-0095

Urapen, R., & Masawat, P. (2015). Novel method for the determination of tetracycline antibiotics in bovine milk based on digital-image-based colorimetry. *International Dairy Journal*, *44*, 1-5. https://doi.org/10.1016/j.idairyj.2014.12.002

Vincenti, F., Montesano, C., Babino, P., Carboni, S., Napoletano, S., De Sangro, G., . . . Sergi, M. (2021). Finding evidence at a crime scene: Sensitive determination of benzodiazepine residues in drink and food paraphernalia by HPLC-HRMS/ MS [Article]. *Forensic Chemistry*, *23*, 7, Article 100327. https://doi.org/10.1016/j.forc.2021.100327

Wang, T. L., Zhao, S. Z., Shen, C. H., Tang, J., & Wang, D. (2009). Determination of iodate in table salt by transient isotachophoresis-capillary zone electrophoresis [Article]. *Food Chemistry*, *112*(1), 215-220. https://doi.org/10.1016/j.foodchem.2008.03.090

Wang, Y. Y., Zhao, G. Y., Chang, Q. Y., Zang, X. H., Wang, C., & Wang, Z. (2010). Developments in Solidification of Floating Organic Drop Liquid Phase Microextraction. *Chinese Journal of Analytical Chemistry*, *38*(10), 1517-1522. https://doi.org/10.1016/s1872-2040(09)60073-6

Wimmer, M. A., & Goldbach, H. E. (1999). A miniaturized curcumin method for the determination of boron in solutions and biological samples. *Journal of Plant Nutrition and Soil Science*, *162*(1), 15-18. https://doi.org/10.1002/(sici)1522-2624(199901)162:1<15::aid-jpln15>3.0.co;2-p

Wongthanyakram, J., Harfield, A., & Masawat, P. (2019). A smart device-based digital image colorimetry for immediate and simultaneous determination of curcumin in turmeric. *Computers and Electronics in Agriculture*, *166*, Article 104981. https://doi.org/10.1016/j.compag.2019.104981

Xie, J. Z., Zou, L. H., Xie, Y. F., Wu, X. D., & Wang, L. S. Analysis of the Monosaccharide Composition of Water-Soluble Coriolus versicolor Polysaccharides by Ultra-Performance Liquid Chromatography/Photodiode Array Detector. *Chromatographia*. https://doi.org/10.1007/s10337-021-04040-z

Xie, W. Q., Yu, K. X., & Gong, Y. X. (2019). Determination of iodate in iodized edible salt based on a headspace gas chromatographic technique. *Journal of Chromatography A*, *1584*, 187-191. https://doi.org/10.1016/j.chroma.2018.12.009

Xing, P. Z., Li, X., Feng, L., & Mao, X. F. (2021). Novel solid sampling electrothermal vaporization atomic absorption spectrometry for fast detection of cadmium in grain samples. *Journal of Analytical Atomic Spectrometry*, *36*(2), 285-293. https://doi.org/10.1039/d0ja00387e

Xu, C. H., Chen, G. S., Xiong, Z. H., Fan, Y. X., Wang, X. C., & Liu, Y. (2016). Applications of solid-phase microextraction in food analysis. *Trac-Trends in Analytical Chemistry*, *80*, 12-29. https://doi.org/10.1016/j.trac.2016.02.022

Xu, Y. D., Wei, L. L., Chen, X. M., Zhao, J. C., & Wang, Y. (2021). Application of the liquid-liquid dispersed microextraction based on phase transition behavior of temperature sensitive polymer to rapidly detect 5 BPs in food packaging. *Food Chemistry*, *347*, Article 128960. https://doi.org/10.1016/j.foodchem.2020.128960

Yu, W. L., Wen, D. S., Cai, D. K., Zheng, J. T., Gan, H. N., Jiang, F. L., . . . Zhong, G. P. (2019). Simultaneous determination of curcumin, tetrahydrocurcumin, quercetin, and paeoniflorin by UHPLC-MS/MS in rat plasma and its application to a

pharmacokinetic study. *Journal of Pharmaceutical and Biomedical Analysis*, *172*, 58-66. https://doi.org/10.1016/j.jpba.2019.04.033

Zarghampour, F., Yamini, Y., Baharfar, M., Javadian, G., & Faraji, M. (2020). On-chip electromembrane extraction followed by sensitive digital image-based colorimetry for determination of trace amounts of Cr(vi) [Article]. *Analytical Methods*, *12*(4), 483-490. https://doi.org/10.1039/c9ay02328c

Zgola-Grzeskowiak, A., & Grzeskowiak, T. (2011). Dispersive liquid-liquid microextraction. *Trac-Trends in Analytical Chemistry*, *30*(9), 1382-1399. https://doi.org/10.1016/j.trac.2011.04.014

Zhang, Y. P., Liu, L. Y., Gong, W. T., Yu, H. H., Wang, W., Zhao, C. Y., . . . Ueda, T. (2018). Autofocus System and Evaluation Methodologies: A Literature Review. *Sensors and Materials*, *30*(5), 1165-1174. https://doi.org/10.18494/sam.2018.1785

Zhao, R. Y., An, J., Sun, Y. M., He, L. J., Jiang, X. M., & Zhang, S. S. (2021). A simple and low-cost sample preparation for the effective extraction, purification and enrichment of aflatoxins in wheat by combining with ionic liquid-based dispersive liquid?liquid microextraction. *Microchemical Journal*, *164*, Article 106036. https://doi.org/10.1016/j.microc.2021.106036

Zheng, Y. T., Pan, C. X., Zhang, Z. J., Luo, W. Q., Liang, X. X., Shi, Y. H., . . . Du, Z. Y. (2020). Antiaging effect of Curcuma longa L. essential oil on ultraviolet-irradiated skin [Article]. *Microchemical Journal*, *154*, 6, Article 104608. https://doi.org/10.1016/j.microc.2020.104608

Zhou, W., Liu, Q., Zang, X., Hu, M., Yue, Y., Wang, Y., . . . Du, Z. (2020). Combination use of tolfenamic acid with curcumin improves anti-inflammatory activity and reduces toxicity in mice. *Journal of food biochemistry*, *44*(6), e13240.

Zohrabi, P., Shamsipur, M., Hashemi, M., & Hashemi, B. (2016). Liquid-phase microextraction of organophosphorus pesticides using supramolecular solvent as a carrier for ferrofluid. *Talanta*, *160*, 340-346. https://doi.org/10.1016/j.talanta.2016.07.036

Curriculum Vitae

Address: Department of Analytical Chemistry, Faculty of Pharmacy, Near East University, 99138, Nicosia, TRNC, Mersin 10, Turkey

Phone: +90 5338687771
E-mail: judejoshua.caleb@neu.edu.tr
Web page :
http://eczacilik.neu.edu.tr/people/academic-staff/jude-joshua-caleb/?lang=en

Teaching Assist. JUDE CALEB

December 1, 2021

PERSONAL INFORMATION	Marital status	Single
	Nationality	Nigerian
	Date of birth	March 27, 1990
	Place of birth	Saminaka, Kaduna State, Nigeria
EDUCATION	January 2009 – March 2013	BSc. in Industrial Chemistry (CGPA: 4.17/5.00) Department of Chemistry Kaduna State University (KASU), Kaduna, NIGERIA
	February 2016 – June 2017	MSc. in Analytical Chemistry (CGPA: 4.00/4.00) Department of Analytical Chemistry, Faculty of Pharmacy Near East University (NEU), T.R.N.C., Turkey Supervisor: Asst. Prof. Dr. Usama Alshana Co-supervisor: Prof. Dr. İhsan Çalış Thesis title: Dispersive liquid–liquid microextraction of some capsaicinoids from different cultivars of *Capsicum annum* prior to their determination by HPLC.
	September 2017 – Date	Ph.D. in Analytical Chemistry (CGPA: 3.93/4.00) Department of Analytical Chemistry, Faculty of Pharmacy, Near East University, T.R.N.C., Turkey Supervisor: Asst. Prof. Dr. Usama Alshana Thesis title: Microextraction techniques combined with

smartphone digital image colorimetry in the analysis of food samples.

LANGUAGES English (Fluent)
Hausa (Fluent)
Turkish (Beginner)

WORK EXPERIENCE

2018 – Present Teaching Assistant

Faculty of Pharmacy, Near East University, Nicosia, TRNC, Turkey

2013 – 2014 Mathematics Teacher

National Youth Service Corps (NYSC) Government Junior Secondary School Odu, Udege Development Area, Nasarawa State

March – May, 2012 Students Industrial Attachment (IT) Programme
Kaduna Refining and Petrochemical Company limited (KRPC) a Subsidiary of NNPC KM 16 Kachia Road, P.M.B. 2252, Kaduna

ADMINISTRATIVE TASKS

0ctober 2020- Date Member of students right and advisor committee, Faculty of Pharmacy, Near East University, T.R.N.C., Turkey

September 2011 – September 2012 President, Student Chemical society of Nigeria (SCSN) Kaduna State University Chapter 2011/ 2012 Session

September 2010 – September 2011 Vice President, Student Chemical Society of Nigeria (SCSN)Kaduna state University Chapter 2010/ 2011 Session

COURSES RECENTLY

| Year | Semester | Course | h/week | | Number of students |
| | | | Theoretical | Practical | |

TAUGHT

2020–2021	Spring	Analytical Chemistry Lab. I (BSc.)	-	1	251
	Fall	Analytical Chemistry Lab. II (BSc.)	-	1	279
2019–2020	Spring	Analytical Chemistry Lab. I (BSc.)	-	1	285
	Fall	Analytical Chemistry Lab. II (BSc.)	-	1	267

RESEARCH INTERESTS

Chromatographic Separation
Digital Image Colorimetry
Elemental Analysis
Microextractions
Green Analytical Chemistry

TECHNICAL EXPERIENCE

High-Performance Liquid Chromatography (HPLC)
Atomic Absorption and Emission Spectrometry (AAS and AES)
Ultraviolet/Visible Spectrophotometry (UV/VIS)

PUBLICATIONS

JOURNAL PAPERS

1. **J. Caleb**, U. Alshana, A. Hanoğlu, İ. Çalış, Dispersive liquid–liquid microextraction for the isolation and HPLC-DAD determination of three major capsaicinoids in *Capsicum annuum* L. Turkish Journal of Chemistry, 2021 Published. [Impact Factor: 1.239]

2. **J. Caleb**, U. Alshana, Supramolecular solvent-liquid–liquid microextraction followed by smartphone digital image colorimetry for the determination of curcumin in food samples. Sustainable Chemistry and Pharmacy, 2021 Published. [Impact Factor: 4.508]

3. **J. Caleb**, U. Alshana, N. Ertaş, Smartphone digital image colorimetry combined with solidification of floating organic drop-dispersive liquid–liquid microextraction for the determination of iodate in table salt. Food Chemistry, 2020 Published. [Impact Factor: 7.514]

4. M. Al-Nidawi, U. Alshana, **J. Caleb**, M. Hassan, Z. U. Rahman, D. Y. Hanoğlu, İ. Çalış, Switchable-hydrophilicity solvent liquid–liquid microextraction versus dispersive liquid–liquid microextraction (DLLME) prior to HPLC-UV for the determination and isolation of piperine from *Piper nigrum* L. Journal of Separation Science, 2020 Published. [Impact Factor: 3.645]

5. S. Abughrin, U. Alshana, **J. Caleb**, Smartphone digital image colorimetry for the determination of aluminum in antiperspirant products. Turkish Journal of Pharmaceutical Sciences, 2021 Published. [Impact Factor: 0.950]

6. N. Agiel, **J. Caleb,** H. Meriçli1, U. Alshana, F. Meriçli, Comparison and Validation of Bioactive flavonoids by RP-HPLC in *Crataegus* species related to pharmaceutical *Crataegus* product, Indian Journal of Pharmaceutical Sciences, Submitted. [Impact Factor: 0.975]

CONFERENCE PRESENTATIONS

➢ **INTERNATIONAL**

1. **J. Caleb**, Smartphone digital image colorimetry combined with dispersive solid phase microextraction for the determination of boron in environmental water samples in N. Cyprus 5th *International Congress on Natural Resources and Sustainable Environmental Management (NRSEM-2021)* (Online/ Nicosia/ TRNC: 08–12 November 2021).

2. **J. Caleb**, U. Alshana, Smartphone digital image colorimetry combined with supramolecular solvent-liquid–liquid microextraction for the determination of curcumin in food samples 3rd *International Congress on Analytical and Bioanalytical Chemistry* (Online/ Turkey: 22–26 March 2021).

3. N. Agiel, **J. Caleb**, A. H. Meriçli, U. Alshana, F. Meriçli, Prospective Crataegus species from Libya and Northern Cyprus for production of herbal medicine *6th International Mediterranean Symposium on Medicinal and Aromatic Plant (MESMAP – 6)* (İzmir/ Turkey: 15-17 October 2020).

4. **J. Caleb**, U. Alshana, N Ertaş, Dispersive liquid–liquid microextraction followed by smartphone digital image colorimetry for the determination of iodate in table salt *2nd International Congress on Analytical and Bioanalytical Chemistry* (Antalya/ Turkey: 11–14 March 2020).

5. N. Agiel, **J. Caleb**, A. H. Meriçli, U. Alshana, F. Meriçli, Reversed-dispersive liquid–liquid microextraction (RDLLME) prior to HPLC-DAD for quantitation of bioactive flavonoids in *Crataegus azarolus* and *Crataegus pallasii, 6th World Congress on Medıcınal and Aromatic Plants (WOCMAP VI)* (Famagusta/ North Cyprus: 13–17 November 2019).

6. A. G. Usman, U. Alshana, **J. Caleb**, Determination of total hardness of water from six municipalities of North Cyprus tap water by complexometric titration. *2nd International Conference on the Environment Survival and Sustainability (ESS2019)* (Nicosia/ TRNC: 07–11 October 2019).

7. M. Al-Nidawi, U. Alshana, **J. Caleb**, Z. U. Rahman, D. Yiğit, Hanoğlu, İ. Çalış, Scaling-up of dispersive liquid–liquid microextraction for the isolation of piperine from black pepper. *1st International Congress on Analytical and Bioanalytical Chemistry* (Antalya/ Turkey: 27–30 March 2019).

8. **J. Caleb**, U. Alshana, A. Hanoğlu, İ. Çalış, Scaled-up dispersive liquid–liquid microextraction for the isolation of three major capsaicinoids from cultivars of capsicum annuum L. *1st International Congress on Analytical and Bioanalytical Chemistry* (Antalya/ Turkey: 27–30 March 2019).

9. **J. Caleb**, H. Tabur, U. Alshana, Dispersive liquid–liquid microextraction of caffeine from Turkish coffee prior to its determination by HPLC. *1st International Congress on Analytical and Bioanalytical Chemistry* (Antalya/ Turkey: 27–30 March 2019).

10. **J. Caleb**, U. Alshana, A. Hanoğlu, İ. Çalış, Dispersive liquid–liquid microextraction of some capsaicinoids from different cultivars of capsicum annuum prior to their determination by HPLC. *2nd International Gazi*

Pharma symposium series (GPSS 2017) (Ankara, Turkey: 11–13 October 2017).

11. Y. Mohamed, **J. Caleb**, Assessment of some air pollutants and their corresponding air quality index at selected activity areas in Kaduna Metropolis. *Chemical Society of Nigeria 37th International conference, Workshop and Exhibition* (Uyo, Nigeria: 2014).

> **NATIONAL**

1. M. Al-Nidawi, U. Alshana, **J. Caleb**, Z. U. Rahman, D. Yiğit, Hanoğlu, İ. Çalış, Isolating piperine for black pepper by scaled-up dispersive liquid–liquid microextraction. *31st National Chemistry Congress* (Istanbul/ Turkey: 10–13 September 2019).

2. Z. U. Rahman, **J. Caleb**, M. Al-Nidawi, U. Alshana, Solidification of floating organic drop microextraction of piperine from black and white pepper prior to its determination by HPLC. *30th National Chemistry Congress* (Famagusta, North Cyprus: 05–08 November 2018).

REFEREE ACTIVITIES	Contribution to peer review activities for: 1. Food Chemistry 2. Journal of Separation Science 3. Analytical Methods
FELLOWSHIPS AND AWARDS	1. Dr. Suat Günsel Lecturing Training Scholarship for Ph.D. Students, Near East University, TRNC, Turkey, 2018. 2. Near East University Postgraduate Scholarship for Ph.D. study in Analytical Chemistry, 2017. 3. Kaduna State Overseas Scholarship for Master Degree, 2016.

REFERENCES

1. Assist. Prof. Dr. Usama Alshana

   MSc. and Ph.D. Supervisor
   Department of Analytical Chemistry
   Faculty of Pharmacy
   Near East University, TRNC, Turkey
   E-mail: usama.alshana@neu.edu.tr
   (or u.alshana@squ.edu.om)

2. Prof. Dr. İhsan Çalış

   MSc. Co-supervisor
   Department of Pharmacognosy
   Dean, Faculty of Pharmacy
   Near East University, TRNC, Turkey
   E-mail: ihsan.calis@neu.edu.tr

3. Prof. Dr. Mustafa Soylak

   Department of Analytical Chemistry
   Faculty of Science
   Erciyes University, Kayseri, Turkey

E-mail: soylak@erciyes.edu.tr